Université de Montréal

Aneuploidy and Cell Cycle Control in the Mouse Preimplantation Embryo.

Par

Henry Brennan-Craddock

Programme de biologie moléculaire, Faculté de médecine

Mémoire présenté en vue de l'obtention du grade de Maîtrise en biologie moléculaire, option Générale

April 2023

Université de Montréal

Unité académique : Programmes de biologie moléculaire, Faculté de médecine

Ce mémoire (ou cette thèse) intitulé(e)

Aneuploidy and Cell Cycle Control in the Mouse Preimplantation Embryo.

Présenté par

Brennan-Craddock, Henry

A été évalué(e) par un jury composé des personnes suivantes

Dr. Gilles Hickson

Président-rapporteur

Dr. Greg FitzHarris

Directeur de recherche

Dr. Julie Brind'Amour

Membre du jury

Résumé

Durant la division cellulaire, la ségrégation des chromosomes et le partage du cytoplasme sont essentiels pour maintenir l'intégrité génomique. Cependant, les erreurs de ségrégation sont fréquentes chez l'embryon préimplantatoire de mammifère et entraînent un gain ou une perte de chromosomes, appelé aneuploïdie. L'aneuploïdie est préjudiciable au développement et est la principale cause de pertes de grossesse.

La mitose est coordonnée par cycle cellulaire, notamment la Cycline-B. Comprendre comment la destruction de la Cycline-B contrôle la sortie de la mitose des embryons pourrait expliquer pourquoi l'aneuploïdie est courante en clinique de fertilité. Nous avons étudié la destruction de la Cycline-B en fonction du stade de développement et de l'aneuploïdie. La littérature suggère que l'aneuploïdie perturbe le cycle cellulaire conduisant les cliniques de fertilité à utiliser la durée du cycle cellulaire et la morphologie (morphocinétique) pour prédire la santé de l'embryon. Cependant, la prédiction de la ploïdie par morphocinétique reste à démontrer. Notre objectif était de savoir comment l'aneuploïdie affecte le cycle cellulaire et le développement de l'embryon.

Après une micro-injection de CyclineB1:GFP (Cycline-B) et H2B:RFP (chromosomes), les embryons de souris furent imagés par microscopie confocale. Des cellules aneuploïdes furent générées chimiquement pour évaluer leurs morphocinétiques. Curieusement, l'apparition de la Cycline-B après nuclear envelope breakdown a été devancée avec la progression du développement indépendamment de la taille des cellules. De plus, les erreurs de ségrégation ont peu impacté le développement et la destruction de la Cycline-B. Nous concluons que la morphocinétique est un outil prédictif peu fiable pour identifier les embryons aneuploïdes.

Mots-clés : Cycline-B, Cycle cellulaire, Mitose, Aneuploïdie, Embryon, Morphocinétique

Abstract

During cell division, it is essential that chromosome segregation during mitosis, and the partitioning of the cytoplasm at cytokinesis occur in successive timing to maintain genomic integrity. However, segregation errors are frequently observed in the early mammalian embryo, causing daughter cells to inherit whole chromosome gains and losses, termed aneuploidy. Aneuploidy is detrimental to development, being the leading cause of pregnancy loss and developmental disorders.

The timing of mitosis is coordinated by the cell cycle component, Cyclin B. Understanding how Cyclin B destruction temporally controls mitotic exit in embryos could help elucidate why aneuploidy is common in IVF clinics. We investigate how Cyclin B destruction changes in different developmental stages and the presence of aneuploidy. Literature suggests aneuploidy disrupts the cell cycle, leading IVF clinics to use cell cycle timings and morphology (morphokinetics) to predict embryo health. However, whether morphokinetics predicts embryo ploidy is uncertain. We seek to investigate how aneuploidy affects the cell cycle and embryo development.

We used live-cell confocal imaging and microinjection of CyclinB1:GFP and H2B:RFP mRNA to visualise Cyclin B and chromosomes during mitosis in the 2-, 4- and 8-cell stage mouse embryo. Secondly, we pharmacologically-induced aneuploidy to assess aneuploid morphokinetics. Interestingly, we observe a developmental trend, independent of cell size, where Cyclin B onset begins progressively sooner after NEBD at the 2-, 4- and 8-cell stage. Additionally, chromosome segregation errors had little impact on Cyclin B destruction and development. Finally, we find morphokinetics to be a poor predictive tool in identifying aneuploid embryos.

Keywords: Cyclin B, Cell Cycle, Mitosis, Aneuploidy, Embryo, Morphokinetics

Table of Contents

List of Figures

List of Supplementary Figures

Acronyms and Abbreviations

APC/C	Anaphase Promoting Complex/Cyclosome
BSA	Bovine Serum Albumin
CDC20	Cell division cycle protein 20
CDK1	Cyclin Dependent Kinase 1
CENP-C	Centromere Protein C
CENP-E	Centromere Protein E
CO2	Carbon Dioxide
CREST	Calcinosis, Raynaud's Phenomenon, Esophageal Dysmotility, Sclerodactyly, and Telangiectasia.
DMSO	Dimethyl Sulfoxide
DNA	Deoxyribonucleic Acid
FISH	Fluorescence in Situ Hybridisation
GFP	Green Fluorescent Protein
H2B	Histone H2B
HyD	Hybrid Detector
ICM	Inner Cell Mass
Kif2b	Kinesin-like protein KIF2B
kMT	Kinetochore-Microtubule
KSOM	Potassium-supplemented Simplex Optimised Medium
LED	Light Emitting Diode
MCC	Mitotic Checkpoint Complex
MEFs	Mouse Embryonic Fibroblasts
MN	Micronucleus
M-phase	Mitosis
MPF	Maturation Promoting Factor
mRNA	Messenger Ribonucleic Acid
MT	Microtubule

MTOC	Microtubule Organising Center
NEBD	Nuclear Envelope Breakdown
OCT-4	Octamer-binding Transcription Factor 4
PBS	Phosphate-Buffered Saline
PFA	Paraformaldehyde
PGT-A	Preimplantation Genetic Testing for Aneuploidy
PLK1	Polo-like Kinase 1
RFP	Red Fluorescent Protein
RNA	Ribonucleic Acid
ROS	Reactive Oxygen Species
SAC	Spindle Assembly Checkpoint
SEM	Standard Error of Mean
S-Phase	Synthesis Phase
TE	Trophectoderm
ZGA	Zygotic Genome Activation

Dedicated to Mum, Dad, Anna, Robert and Phoebe

Remerciements

To have been given this opportunity starting at a time when the world was in lockdown was incredible. Greg, thank you for all of the opportunities you presented, for being generous with your time and guidance, and for pushing me to a higher standard of science.

To my colleagues at CRCHUM; Gaudeline, Karolina, Lia, Adelaide, Jeanine, Lin, Helia, Filip and Aleks. Thank you for your endless mentorship, coffee and chocolate to get me through.

Thank you to the FitzHarris Lab, McGill Centre for Research in Reproduction and Development, Research Centre de Recherche en Reproduction et Fertilité (Université de Montréal), and Université de Montréal for providing me with the equipment and funding necessary to complete my research.

Lastly, thank you to Mum & Dad, Rob, Anna and Phoebe. All of this would not have been possible without the confidence, support, and inspiration you all gave to me in one way or another.

Introduction

The work presented in this thesis aims to understand the cell cycle mechanisms which dictate the entry and exit from mitosis in the embryo, as well as the impact of chromosome segregation errors and aneuploidy on the cell cycle. How the cell cycle controls mitosis at different stages during development of the preimplantation embryo is not known. However, it is well documented that the mammalian embryo is frequently subject to segregation errors. Segregation errors cause chromosomal gains and losses in cells termed aneuploidy, which in somatic cells causes cell cycle arrest, apoptosis and oncogenesis. Aneuploidy is also detrimental to embryonic development. Therefore, understanding the fundamental cell cycle mechanisms regulating segregation is an important basis for understanding why segregation errors are so frequent in the mammalian embryo.

The second part of this thesis looks to simulate methods used in IVF clinics to observe if cell cycle timings are a good predictive tool for aneuploidy. Measuring aneuploidy is often used as a selective tool by IVF clinics to maximise the chances of successful implantation and pregnancy. Clinics are now using non-invasive measures, such as monitoring cell cycle timings, as a tool to select embryos with the greatest developmental potential. However, is it possible to predict the ploidy status of an embryo based on cell cycle alone? There have not been robust studies generating aneuploidy and assessing cell cycle timings to make this claim. Therefore we also set out to assess the impact of aneuploidy on the cell cycle timings in preimplantation embryos.

To set a basis for this introduction, I will first discuss cell division followed by the cell cycle control of M-phase. We will then detail how chromosome segregation errors can go wrong and the consequences of aneuploidy on cellular health. Because the embryo is a unique system with many idiosyncrasies, it is also necessary to provide a brief overview of the preimplantation embryo development, the consequences of aneuploidy in embryos and what is known about the cell cycle in embryos. Finally reaching how we arrived at the hypotheses that this thesis addresses.

Cell Division

During division, the cell must segregate its genetic material into two new daughter cells. Cell division can be distilled into two components; a nuclear division, where the genetic material is segregated to opposite poles of the cell, and a cytoplasmic division, where the membrane ingresses to divide the cytoplasm. These two types of division are termed mitosis and cytokinesis, and they must be tightly coupled to ensure the faithful inheritance of the chromosomes.

The cell cycle can be divided into 4 phases: G1, S, G2, and M-phase. G1, S, and G2 characterise the interphase, where the cell will grow and duplicate its genetic content. Interphase makes up most of the cell cycle, which is then followed by a relatively short M-phase, where the cell will divide to form two new daughter cells (Figure 1).

Growth phases, G1 and G2, allow for the synthesis of protein, organelles, and cellular growth. During S-phase the cell synthesises a duplicate copy of its DNA, doubling its genetic content, to become tetraploid. The arms of duplicate chromosomes then become bound together with a cohesin complex, which ensures that sister chromatids do not drift apart during cell division. Before entry into mitosis, the duplicated DNA is assessed in a DNA damage checkpoint and upon checkpoint satisfaction, the cell enters M-phase (Figure 1).

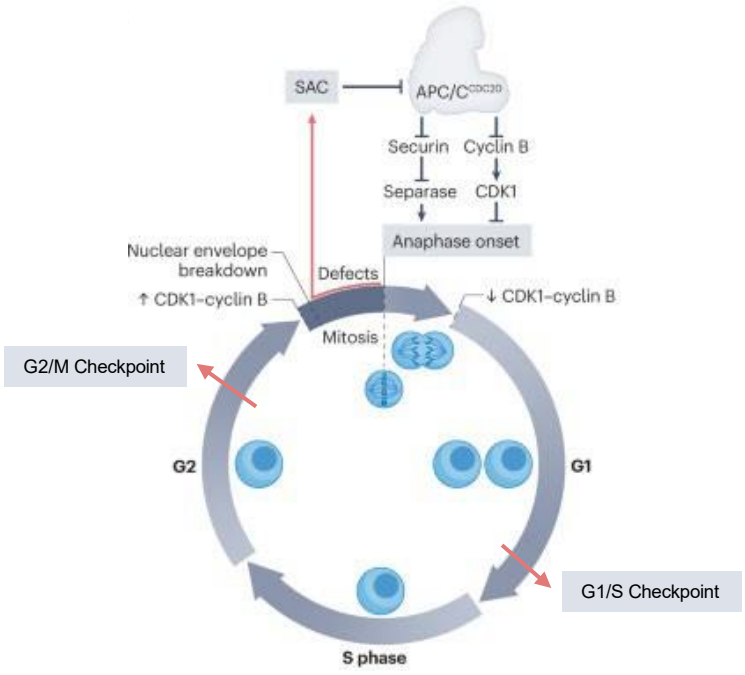

Figure 1 - Schematic of the eukaryotic cell cycle progression and checkpoints

The cell cycle has 4 main phases G1, S G2 and M-phase which can be subdivided into prophase, prometaphase, metaphase, anaphase and telophase. G1, S and G2 make up interphase and contain two major cell cycle checkpoints; the G1/S checkpoint which prevents cells from entering the S- phase in the presence of DNA damage and the G2/M checkpoint which ensures DNA synthesis is complete and without damage before mitosis. The Spindle Assembly Checkpoint (SAC) in M-phase ensures chromosomes are completely attached to the spindle before cell cycle progression. High CDK1-Cyclin B activity triggers entry into M-phase, APC/C mediated destruction is inhibited until complete attachment of kinetochore to the spindle before the destruction of Cyclin B and Securin to allow the cell to exit mitosis (Figure adapted from R. Li and Zhu 2022).

Mitosis

The cell cycle promotes entry into mitosis through an increase in activity of Cyclin-dependent kinase 1 (CDK1) which will induce entry to M-phase upon reaching a certain threshold, as in Figure 1 (Gautier et al. 1990; Gavet and Pines 2010). Mitosis consists of 5 phases: prophase, prometaphase, metaphase, anaphase and telophase (Figure 2).

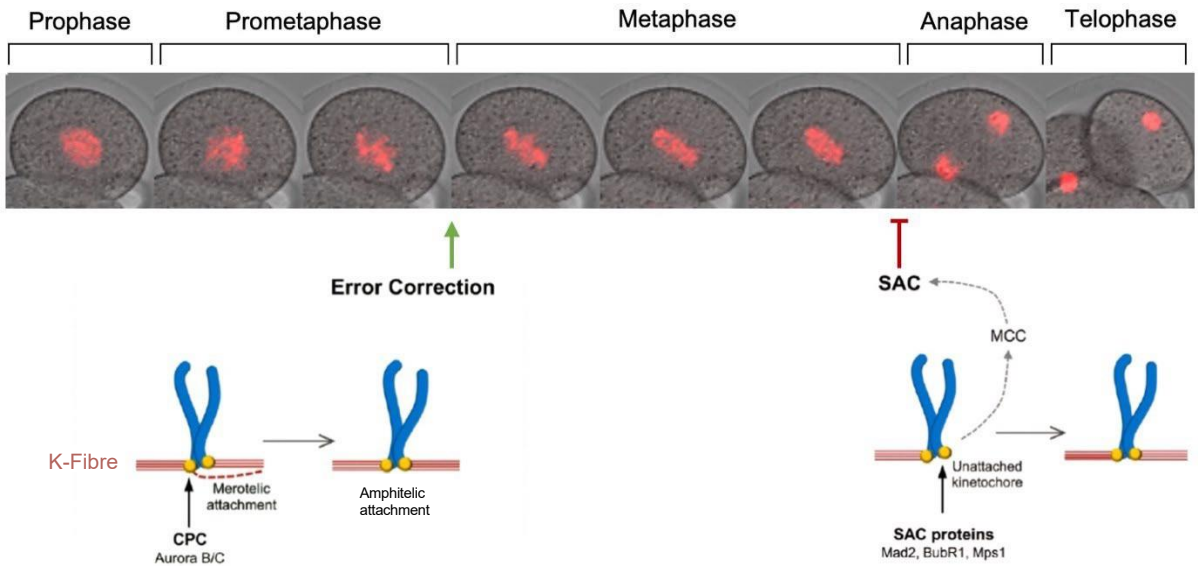

Figure 2 - The 5 phases of mitosis and kinetochore-microtubule attachment

2-cell stage embryo enters mitosis at prophase where chromosomes condense (red) and the nuclear envelope breaks down. Chromosomes then begin to be aligned to the centre of the cell (prometaphase) while error-correction mechanisms correct non-disjunction attachments such as merotelic attachments. Upon complete "error-free" amphitelic attachment (metaphase) chromosome pairs are bioriented forming a metaphase plate and the SAC is inactivated. SAC silencing through Mitotic Checkpoint Complex (MCC) release from the kinetochore allows chromosomes then segregate to opposite poles in anaphase, followed by nuclear envelope reformation at telophase to form two distinct nuclei. Imaged using live-cell confocal imaging and microinjection of H2B:RFP mRNA. (Figure adapted from Vázquez-Diez and FitzHarris 2018)

Prophase and prometaphase

In prophase, chromatin is condensed and packaged into sister chromatids. Long strands of DNA supercoil around histones to form densely packed pairs of chromosomes. Previously in S-phase, the sister chromatids became bound together by a multi-protein complex known as cohesin. This forms a ring-like structure around the chromosome arms of the paired chromosomes to prevent the sisters from drifting apart during mitosis (Brooker and Berkowitz 2014).

Concomitantly with chromosome condensation, a bipolar spindle begins to assemble. Mammalian somatic cells possess two organelles known as centrosomes, which during prophase migrate toward the poles and begin to nucleate a microtubule network known as the mitotic spindle. The spindle is a self-organising structure where dynamic growth and depolymerisation of microtubules leads to eventual capture of the chromosomes. Microtubules attach to a specific region of each chromosome known as the centromere. This region assembles kinetochores, a protein complex that transduces forces of the spindle to the chromosome. The kinetochore bundles microtubules together to form k-fibres which exert the forces needed for the orientation of the chromosome during prometaphase. Another population of spindle microtubules does not attach to kinetochores and instead run antiparallel to microtubules emanating from the opposite pole, forming the spindle midzone, which I will describe in further detail when discussing mitotic exit. A third population of microtubules, astral microtubules, maintain the spindle in position by anchoring the spindle to the plasma membrane.

By metaphase, the spindle has adopted a fusiform bipolar shape and the chromosomes progressively become centred to the middle of this structure, forming a metaphase plate. Correct kinetochore attachment requires two k-fibres from opposing poles to bind to each sister chromatid to produce a bioriented pair (amphitelic attachment). Error correction mechanisms in metaphase exist to ensure the biorientation of all sister chromatids before chromosome segregation. Inappropriate attachments can be classified as syntelic or merotelic. Syntelic attachments form when both sister kinetochores are bound to k-fibres emanating from the same

pole; whereas merotelic attachments occur when a single kinetochore is attached to opposing k-fibres (Figure 2).

Error-correction mechanisms: two rights can make a wrong

The mechanisms by which k-fibres correct their attachment to microtubules are not fully understood. One model proposed is a tension-dependent mechanism. Here, microtubules will continue to detach and reattach until both poles of the spindle exert the required tension on the sister chromatids, where they become stable. This was first shown by Nicklas in grasshopper spermatocytes, where mechanically applied tension from the opposite pole of syntelic attachments stabilised their attachment (Reviewed in Nicklas 1997). Syntelic attachments have a significant loss in tension, therefore a tension-dependent model is likely to be efficient in correcting syntelic attachments. However, merotelic attachments may be more susceptible to evading tension- dependent error correction, as tension is exerted from both poles (Cimini 2008). When fluorescence ratios of opposing k-fibres are equal to ~1, the merotelic sister chromosomes, remained aligned because the forces are equal but generate lagging chromosomes. Conversely, when fluorescence ratios of merotelic opposing k-fibres reach ~3, the disparity in tension is enough to cause misalignment from the metaphase plate. Despite the force disparity these chromosomes segregate normally, suggesting a tension-correction mechanism (Cimini, Cameron, and Salmon 2004). Therefore it requires a threshold of tension loss for destabilisation and reattachment for proper segregation.

It is thought that other correction mechanisms may play a role in correcting merotelic attachments. One proposed model is that Aurora B phosphorylates misattached kinetochores to promote unstable attachment and depolymerisation of k-fibres, as shown in Figure 2 (Kallio et al. 2002; Hauf et al. 2003; Lampson and Grishchuk 2017). To prevent premature segregation of the chromosomes before complete kinetochore-microtubule errors have been corrected, a critical cell cycle checkpoint is activated.

The spindle assembly checkpoint

The spindle assembly checkpoint (SAC) delays anaphase to ensure that microtubule-kinetochore attachment for each chromatid is established (Figure 2) (Rieder et al. 1994). To activate the SAC, unattached kinetochores catalyse the formation of the mitotic checkpoint complex (MCC), which is comprised of Mad2, Bub3, BubR1, and CDC20, as shown in Figure 2. The MCC inhibits the anaphase-promoting complex/cyclosome (APC/C). The APC/C is required for progression into anaphase as it targets Cyclin B and Securin for proteolytic destruction (Figure 2). Destruction of these substrates is necessary for mitotic exit and physical separation of the sister chromatids. The MCC inhibits the APC/C by sequestering its cofactor, CDC20. Without CDC20 the APC/C remains in an inactive form, preventing the metaphase-anaphase transition. In addition, other MCC components have been shown to act directly on the APC/C to reduce APC/C affinity to its substrates (Lara-Gonzalez, Pines, and Desai 2021).

Previous studies showed that the SAC is an all-or-nothing switch that will be activated in the presence of a single unattached kinetochore. For example, studies in experiments in Female Rat Kangaroo Kidney Epithelial Cells (Ptk1) cells identified the SAC to be a very robust checkpoint, where the presence of one unattached kinetochore delays anaphase until attachment (Rieder et al. 1994). However, more recent literature points towards the SAC signalling functioning as a gradient, proportional to the number of attached and unattached kinetochores (Collin et al. 2013). Elegant studies in HeLa cells which performed laser ablation to cut kinetochore microtubule (kMT) attachment to the spindle, found a proportional relationship between the number of unattached kinetochores and the rate of Securin destruction. This suggests that the SAC is more efficient in the presence of more unattached chromosomes (Dick and Gerlich 2013). Importantly, Dick and Gerlich observed a realignment of unattached chromosomes and a significantly delayed anaphase in the majority of cells, showing HeLa cells do possess a functional SAC. Clute and Pines also illustrated that the SAC remains functional after anaphase has been initiated. The addition of spindle poison during chromosome segregation reactivated the SAC and arrested HeLa in an anaphase-like state. This further shows that the SAC is not an all-or-nothing mechanism (Clute and Pines 1999). In most cells, the SAC can delay anaphase onset until

complete attachment of all kinetochores to the spindle (Lara-Gonzalez, Westhorpe, and Taylor 2012). Once kinetochores have attached to the spindle the MCC is released from the kinetochore, contributing to the eventual silencing of the SAC.

SAC silencing

After end-on microtubule kinetochore attachments are complete, SAC components Mad1 and Mad2 are stripped from the kinetochore in a dynein-mediated process (Kuhn and Dumont 2017; Lara-Gonzalez, Pines, and Desai 2021). Dynein is a minus-end directed motor protein which transports Mad1 and Mad2 to the spindle poles, preventing further catalysis of the MCC complex at the attached kinetochore (Lara-Gonzalez, Pines, and Desai 2021). Phosphatase activity is also essential in silencing the SAC and allowing mitotic exit. Unattached kinetochores recruit the phosphatase PP2A which is replaced by PP1 upon successful end-on attachment (Dan Liu et al. 2010). Inhibiting phosphatase recruitment to the kinetochore in HeLa cells has been shown to cause a permeant SAC activated phenotype, illustrating that phosphatase activity is also implicated in SAC silencing (Lara-Gonzalez, Pines, and Desai 2021). Finally, another proposed model is that the tension created from two end-on attachments increases the interkinetochore distance. Although this model is not fully understood, Aravmudhan et al. hypothesise that the increased opposing tension causes kinetochore components Ndc80 and Knl1 to move away from each other, contributing to SAC silencing (Aravamudhan, Goldfarb, and Joglekar 2015). However, this tension mechanism requires further study. In summary the SAC is silenced once the mitotic checkpoint complex, composed of Mad2, Bub3, BubR1, and CDC20 has been displaced from all kinetochore complexes.

Cyclin destruction

After SAC silencing the APC/C is activated. This E3 ubiquitin ligase polyubiquitinates Securin and Cyclin B, which is then recognised by the 26S proteasome for destruction (Izawa and Pines 2011). APC/C specificity to each substrate during progression through mitosis is regulated by two WD-40 repeat-containing adaptor proteins CDC20 and CDH1 (Li and Zhang 2009). Following SAC silencing, the APC/C first associates with the activating cofactor CDC20, which primarily targets

Cyclin B and Securin for destruction (Hagting et al. 2002; Zhang et al. 2016). The destruction of these substrates is essential for mitotic exit (Chang, Xu, and Luo 2003). Phosphorylation of the APC/C by Cyclin B/CDK1 has been shown to promote the binding of the APC/C to CDC20 (Zhang et al. 2016). When bound to CDC20 the E3 ubiquitin ligase (APC/C^{CDC20}) is now able to specifically polyubiquitinate Securin and Cyclin B. These substrates are then recognised by the 26S proteasome for destruction (Izawa and Pines 2011).

During early mitosis the formation of APC/CCDH1 is inhibited through phosphorylation, however later in mitotic exit the APC/C exchanges CDC20 for CDH1, changing its substrate specificity. APC/CCDH1 is not essential or mitotic exit but is important for G1/S regulation.

But how does the APC/C target specific substrates for destruction? APC/C substrates possess conserved specific sequences which are recognised by the APC/C and targeted for destruction. These sequences are known as the destruction box (D Box), KEN box and the ABBA motif. This specific motifs allows the recognition of APC/CCDC20 to Cyclin B and Securin, which both possess destruction box motifs (Yamano et al. 2004; Hagting et al. 2002). These two substrates are tagged by the ubiquitin ligase with a multi-ubiquitin chain, where the ubiquitin-proteosome system degrades ubiquitinated proteins (Pines 2006). During an active spindle assembly checkpoint, APC/C mediated destruction of Cyclin B1 is inhibited, however Cyclin A2 is ubiquitinated and destroyed throughout active SAC signalling (Zhang, Tischer, and Barford 2019). Recent studies have suggests that it possesses a newly identified D2 destruction box, which allows destruction by the APC/C even when bound to the inhibitory MCC (Zhang, Tischer, and Barford 2019). In late mitosis the APC/C replaces CDC20 with a different cofactor CDH1. APC/CCDH1 can recognise both the D box as well as KEN box motifs of mitotic substrates, allowing a wider range of substrates to be destroyed during mitotic exit. The APC/CCDH1 targets different APC/C substrates specific to late mitosis and plays a functional role in the transition from G1 to S-phase (Li and Zhang 2009).

The degradation of Securin permits a downstream protease, separase, to hydrolyse cohesin allowing sister chromatids to physically separate. Concomitantly, the APC/C targets Cyclin B for

destruction. Cyclin B is bound to CDK1 and keeps the kinase in its active form (Figure 3). Consequently, Cyclin B destruction inactivates CDK1, which is essential for the cell cycle to exit mitosis (Clute and Pines 1999; Chang, Xu, and Luo 2003).

The degradation of Securin permits another protease, separase, to hydrolyse cohesin allowing sister chromatids to physically separate. Concomitantly, the APC/C targets Cyclin B for destruction. Cyclin B is bound to CDK1 and keeps the kinase in its active form (Figure 3). Consequently, Cyclin B destruction inactivates CDK1, which is essential for the cell cycle to exit mitosis (Clute and Pines 1999; Chang, Xu, and Luo 2003).

Mitotic exit

Mitotic exit, defined by the metaphase-anaphase transition and cytokinesis, is one of the most drastic events during the cell cycle where the cell undergoes huge cytoskeletal restructuring. During mitotic exit two major segregation events, anaphase and cytokinesis, occur in rapid temporal succession to form two new daughter cells.

Anaphase

Following cohesin destruction, the sister chromatids are separated to opposite poles of the cell through two mechanistically distinct forces, microtubule depolymerisation and spindle elongation (Anjur-Dietrich, Kelleher, and Needleman 2021). Chromosome segregation commences with anaphase A, where the k-fibres depolymerise and shorten to generate a pulling force on the chromatid (Mitchison et al. 1986). Secondly, spindle elongation in Anaphase B is generated by the spindle midzone. Microtubule sliding in the midzone generates pushing forces contributing to spindle elongation and further segregation of the poles. The spindle midzone also plays an important role in cytokinesis, which is initiated after chromatids are far enough apart.

Cytokinesis and Telophase

The spindle has been shown to dictate where the contractile ring will be assembled on the plasma membrane. Early experiments showed that micromanipulation of the spindle using glass needles

would move the plane of cleavage accordingly (Rappaport 1996). Later studies have identified this as a result of components required for activation of the RhoA GTPase are delivered by the spindle to the equatorial membrane, which leads to the assembly of an actin-myosin ring around the equator of the cell (Green, Paluch, and Oegema 2012). After the chromosomes have separated far enough, the ring will contract, folding the plasma membrane in on itself. The cytokinetic furrow continues to ingress until forming an intercellular bridge which remains open until abscission. The intercellular bridge is composed of a network of microtubules and a cytoskeletal structure known as the midbody. Cytokinesis is fully complete once abscission has taken place, which closes the intercellular bridge leaving only a remnant of the midbody (Rappaport 1996). The time of physical separation between sister cells at abscission varies between species, but in HeLa cells was shown to take place acutely in G1, approximately 60 mins after anaphase onset (Gershony et al. 2014). During cytokinesis, the chromosomes begin to reform nuclear membranes chromosomes will begin to decondense to form two distinct nuclei, finalising telophase and mitosis, as shown in Figure 2.

Cell cycle coordination of mitosis

Chromosome segregation and cytokinesis timing must be strictly coordinated by the cell cycle to prevent premature segregation or cytokinesis, resulting in chromosome missegregation and aneuploidy. Generally, the cell cycle is controlled by positive and negative feedback loops of phosphorylation and dephosphorylation. A family of kinases known as Cyclin-dependent kinases (CDKs) tips the balance toward phosphorylation and promotes the next phase of the cell cycle. Once CDK activity reaches a threshold it will then be inactivated through proteolysis of the associated Cyclin. This degradation then allows the balance to return in favour of dephosphorylation, where phosphatases reverse CDK targets to finalise the transition into the new cell cycle phase (Figure 3).

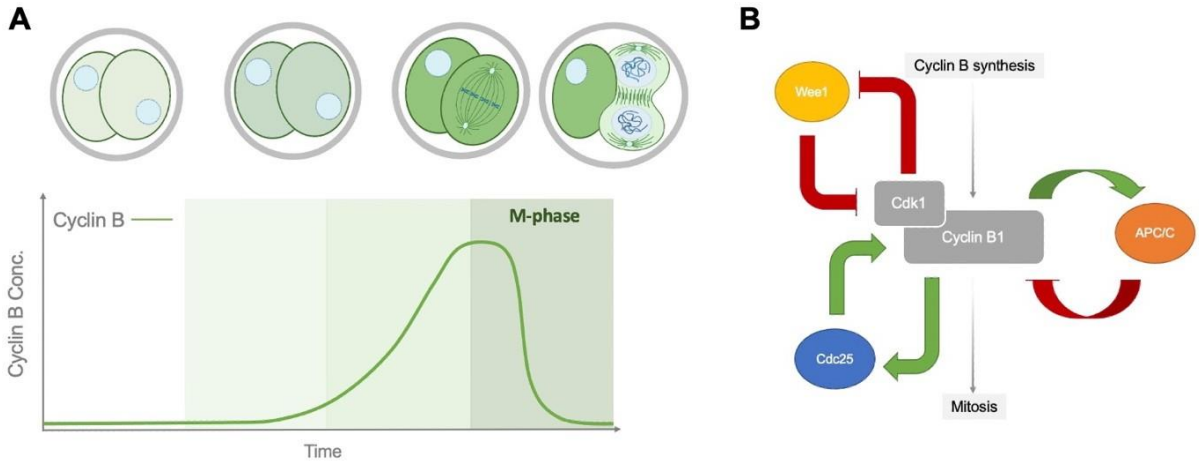

Figure 3 - Schematic of Cyclin B regulation of mitosis

(a) Cyclin B is synthesised during interphase until activation, which induces entry into M-phase. Upon SAC silencing Cyclin B is destroyed inactivating CDK1 and allowing progression into mitotic exit, characterised by a schematic of a 2-cell stage embryo entering anaphase and cytokinesis upon Cyclin B destruction. (b) Cyclin B is regulated by constant phosphorylation and dephosphorylation. Wee1 kinase phosphorylates CDK1 to inactivate the CDK1-Cyclin B complex during interphase, at the point of mitotic entry phosphatase CDC25 removes the Wee1 inhibitory phosphorylation activating CDK1 to induce mitotic entry. CDK1 is inactivated by the APC/C mediated destruction of Cyclin B (Figure 3b adapted from Tsai, Theriot, and Jr 2014)

The cyclins

Cyclins are proteins which act as cofactors for Cyclin dependent kinases (CDKs). These Cyclin/CDK complexes control the cell cycle through inducting major phosphorylation events, which are then subsequently removed by antagonistic phosphatases. To ensure a temporal and forward progression of the cell cycle, Cyclin/CDK complexes are sequentially activated and destroyed, with each class of Cyclin promoting entry into the following phase. There are many Cyclins involved throughout the whole cell cycle, however only two classes of Cyclins are involved in cell division: Cyclin A and Cyclin B.

A type Cyclins

In mammals, there are also two closely related A type Cyclins, Cyclin A1 (embryonic) and Cyclin A2 (somatic). The expression of Cyclin A1 is limited to the germ cell line and has been shown to play a major role in male meiosis, with disruption in mouse models leading to a meiotic block in spermatogenesis. Interestingly, Cyclin A1 appears to be redundant in female meiosis, with female mice displaying no phenotype (Liu et al. 1998). In contrast, Cyclin A2 is present in proliferating somatic tissues and is essential for embryonic development, with the deletion of Cyclin A2 causing embryonic lethality at day E5.5 (Murphy et al. 1997). Therefore, I will go on to explore the role of Cyclin A2 in mitosis. A type Cyclins can form complexes with two classes of CDKs, CDK1 and CDK2. This produces a dual functionality of A type Cyclins in the control of the cell cycle. After Cyclin A2 binds the corresponding CDK, the complex is activated through phosphorylation on specific threonine residues by Cyclin activating kinase (CAK) (Vermeulen, Van Bockstaele, and Berneman 2003; Merrick et al. 2008).

The first role of Cyclin A is during S-phase, where Cyclin A2 forms a complex with CDK2 (Cyclin A/CDK2) which is then activated by CAK. Early evidence for a role of Cyclin A2 in S-phase came from experiments where microinjection of Cyclin A anti-sense cDNA in human cells blocked DNA synthesis and G2 entry (Girard et al. 1991). Cyclin A2 was later shown to phosphorylate many components, such as CDC6, pre-replication complexes and subunits of DNA polymerase (Petersen et al. 1999; Katsuno et al. 2009; Frouin et al. 2005).

Secondly, Cyclin A has a role in the G2/M-phase transition. Similarly, to S-phase, a study in which microinjection of Cyclin A antibodies in G2 HeLa cells caused a pre-mitotic arrest. Following microinjection of Cyclin A in these arrested cells they would enter mitosis and resume the cell cycle. This suggested an essential role for the activity of Cyclin A2 in coordinating entry to M-phase (Pagano et al. 1992). Furthermore active Cyclin A2-CDK2 has been shown to promote mitotic entry through activation of CDC25, a phosphatase which removes the inhibitory phosphorylation of Wee1 from Cyclin B/CDK1 (Mitra and Enders 2004). This activation of Cyclin

B/CDK1 is then able to activate substrates required for entry into mitosis. The destruction of Cyclin A2 is also important for mitotic exit, as it was found to be necessary for the formation of stable microtubule-kinetochore attachment (Kabeche and Compton 2013).

B type Cyclins

B type Cyclins are essential in the transition into mitotic entry and their destruction is essential for mitotic exit. There are three main types of Cyclin B: Cyclin B1, B2 and B3. Cyclin B1 and its role in regulating the temporal events during mitotic entry and exit is well documented, however the roles of B2 and B3 are less well understood in mammals. Although there are three types of B class Cyclins, only Cyclin B1 is essential for early embryonic development. Knockout studies found Cyclin B2 -/- mice to have no phenotype aside from a small litter size, whereas as Cyclin B1 knockout mice will not develop past embryonic day 10 (Brandeis et al. 1998). Cyclin B1 and B2 are closely related but have idiosyncratic properties which result in different regulatory mechanisms during M-phase. Cyclin B2 localises specifically to the Golgi apparatus, whereas the B1 localises to microtubules. In addition, Cyclin B1 is imported to the nucleus prior to nuclear envelope breakdown, whereas B2 remains uniformly distributed and does not undergo translocation (Jackman, Firth, and Pines 1995). The different localisation of B type Cyclins is thought to result in specificity of each type of Cyclin B to reorganise different organelles in the cell during mitosis (Jackman, Firth, and Pines 1995).

Finally, Cyclin B3 is the last B type Cyclin involved in mitosis. This Cyclin has been understudied in mammalian models, but its function has been well documented in *Drosophila*. Studies in *Drosophila* identified that Cyclins are destroyed sequentially with the first being Cyclin A, followed by B1, B2 and finally Cyclin B3, which is initiated around the onset of anaphase (Yuan and O'Farrell 2015). Studies using RNAi knockdown and overexpression of Cyclin B3 would delay or advance the onset of anaphase respectively, suggesting a role in timing of anaphase in early evolutionary systems (Yuan and O'Farrell 2015). However, in the mammalian cell, Cyclin B3 expression is strictly limited to the germ line. Cyclin B3 plays an essential role in oogenesis, with female Cyclin B3 knockout mice being sterile and eggs arresting at metaphase of meiosis I (Karasu et al. 2019).

Moreover studies in human cell lines found Cyclin B3 is readily detected in the germ cells of testis but not in any other tissue (Nguyen et al. 2002), suggesting in mammals that Cyclin B3 is primarily a meiotic Cyclin. Therefore, I will go on to further discuss the mammalian B type Cyclins known to be involved in mitosis.

B type Cyclins specifically bind CDK1, a kinase which promotes entry into mitosis. The pool of Cyclin B1/CDK1 increases as Cyclin B1 is resynthesised during interphase. To prevent premature entry into mitosis, kinases Wee1 and Myt1 donate an inhibitory phosphorylation to the tyrosine (tyr) 15 and threonine 14 residues of CDK1. Prior to mitotic entry, phosphatases such as CDC25 act to remove inhibitory phosphorylation to activate Cyclin B-CDK1 and promote entry into mitosis.

Entry into mitosis is controlled by the mitotic Cyclin, Cyclin B. During interphase Cyclin B is synthesised, which binds Cyclin-dependent kinase 1 (CDK1). The Cyclin B-CDK1 complex becomes increasingly abundant, but remains inactive due to inhibitory phosphorylation by Wee1, delaying mitosis so the cell can complete the previous growth phase, G2 (Nurse 1975). At the point of mitotic entry, the inhibitory phosphorylation is removed by phosphatase CDC25, activating CDK1 (Figure 3b).

High CDK1 activity has been shown to have multiple regulatory effects in controlling entry into mitosis including coordinating NEBD, chromosome condensation and spindle assembly (Kimura et al. 1998; de Castro et al. 2017). Once the cell has entered mitosis, CDK1 activity must be reduced to exit mitosis, which is achieved through APC/C mediated destruction of Cyclin B (Chang, Xu, and Luo 2003; Izawa and Pines 2011). Cyclin B is ubiquitinylated by the APC/C and targeted for destruction. The destruction of Cyclin B inactivates CDK1 and allows for counteracting phosphatases such as PP1 and PP2A to dephosphorylate the targets of CDK1 (Nasa and Kettenbach 2018). CDK1 inactivation is necessary for the cell to exit mitosis, and is involved in a complex cascade of cell cycle protein regulation, well reviewed in (Enserink and Kolodner 2010). Although Securin destruction is necessary for the physical separation of sister chromatids, CDK1

inactivation plays an important role in the anaphase spindle to properly segregate chromosomes to spindle poles at anaphase (Wheatley et al. 1997; Potapova et al. 2006; Jones 2010).

Mechanisms preventing dephosphorylation during mitotic entry

The initial dephosphorylation event which occurs during mitosis is the dephosphorylation of Cyclin B1/CDK1. CDC25 removes the inhibitory phosphorylation's from pThr14 and pTyr15 donated by Wee1 and Myt1, to produce an active Cyclin B1/CDK1 complex (Moura and Conde 2019). Different isoforms of CDC25 are thought to activate different subcellular localisations of Cyclin b/CDK1 which is correlated with different events during mitotic entry. CDC25B has been shown to activate CDK1 at the centrosomes. CyclinB/CDK1 localised to the centrosomes will then translocate to the nucleus (Lindqvist et al. 2005), which will carry out phosphorylation on multiple targets to induce NEBD. CDC25A is responsible for CDK1 activation triggering chromosome condensation (Molinari et al. 2000; Moura and Conde 2019). Finally CDC25B and CDC25C is activated by Cyclin B/CDK1 in a positive feedback loop, which in turn dephosphorylates Wee1 and Myt1, to prevent any further inhibition of Cyclin B/CDK1 and an irreversible transition to m-phase (O'Farrell 2001; Moura and Conde 2019). This positive feedback loop is further contributed to by a stabilising phosphorylation which inhibits CDC25 degradation mechanisms allowing a stable pool of CDC25 (Moura and Conde 2019).

To delay dephosphorylation of CDK1 targets and ensure complete transition into M-phase, PP2A-B55 phosphatase must also be inhibited. This is because PP2A-B55 specifically dephosphorylates the sites of CDK1 phosphorylation (Keshri, Rajeevan, and Kotak 2020). To achieve this mitotic delay, rising CDK1 activity phosphorylates Greatwall (GWL), a serine/threonine kinase. GWL, which becomes active in late G2, phosphorylates substrates, Arpp19 and ENSA, which in turn allows Arpp19 and ENSA to bind and inhibit PP2A, protecting CDK1 phosphorylation during late G2 and early M-phase (Vigneron et al. 2009; Lorca and Castro 2013).

The control of rapid dephosphorylation during mitotic exit

The cell has committed to mitotic exit after spindle assembly checkpoint satisfaction and CDK1 substrates must be dephosphorylated by phosphatases in a mass dephosphorylation event. The events in late mitosis, such as chromosome segregation, decondensation and cytokinesis all require dephosphorylation of CDK1 targets. These dephosphorylations are coordinated by phosphatases PP1 and PP2A (Moura and Conde 2019). CDK1 prevents formation of microtubule bundling through phosphorylation of PRC1. PRC1 is an essential protein for microtubule bundling and midzone formation, which is important for contractile ring formation and cytokinesis. This inhibitory phosphorylation is removed by PP2A-B55 (Cundell et al. 2013; Zhu et al. 2006). Another important event in mitotic exit is the reformation of two new nuclei after genome segregation. Previously during NEBD, nuclear lamins were phosphorylated by Cyclin B1/CDK1 to promote their depolymerization. Nuclear envelope reformation requires dephosphorylation of nuclear lamins, which then facilitates the repolymerization of these cytoskeletal structures. PP1 localises to the nuclear lamina of reforming nuclei which accelerates its reassembly (Thompson, Bollen, and Fields 1997)

The switch that changes at M-phase from a mass phosphorylation to dephosphorylation event is triggered by the SAC, which begins Cyclin B destruction to initiate a swing in the scale towards the direction of dephosphorylation. The decrease in CDK1 activity after Cyclin destruction, causes a slight increase in PP1 activity, which is then able to remove the GWL induced phosphorylation of ENSA and Arrp19 (Heim, Konietzny, and Mayer 2015). CDK1 activity continues to fall and fails to re-establish inhibitory phosphorylation's of PP2A and PP1, ultimately leading to a cascade of activation of phosphatase activity (Lorca and Castro 2013).

The cell cycle control of cytokinesis

Cyclin B-CDK1 activity has also been shown to inhibit microtubule bundling proteins and motor proteins essential for midzone formation (Zhu et al. 2006). Therefore, the destruction of Cyclin B and CDK1 activity also has functionality in dictating the spatial positioning of furrowing. Furthermore, mammalian somatic cells have shown that the addition of CDK1 inhibitor to cells

arrested in metaphase triggers the onset of chromosome segregation and furrow ingression (Potapova et al. 2006). To ensure faithful chromosome segregation the timing of anaphase and cytokinesis must be well coordinated.

Contractile ring assembly is dependent upon RhoA, a small GTPase. Studies have shown that activation of RhoA is sufficient for triggering furrow ingression (Wagner and Glotzer 2016). RhoA requires the guanine exchange factor Ect2 in order to be activated. Upstream of RhoA activation, Ect2 is activated by centraspindilin. In mammals, centraspindilin is composed of a kinesin-6 motor protein (Kif23) dimer and a CYK-4 dimer, and localises to the spindle midzone during M-phase (Fededa and Gerlich 2012). Therefore, in order to initiate furrow ingression and cytokinesis is initiated by active RhoA which is activated by Ect2 associated with centraspindilin.

One direct effect of CDK1 upon cytokinesis is the ability of Ect2 to associate with the CYK-4 domain of centraspindilin. Yüce *et al.* elegantly display this interaction using Roscovitine, a potent CDK1 inhibitor. Nocodazole arrested cells were released and fixed at 40-, 60-, 90- and 120-minutes post release. Ect2 was then immunoprecipitated and western blot analysis revealed that in the presence of CDK1 inhibition, Ect2-CYK-4 association was significantly increased. Using partial deletion constructs, they later illustrate that this is dependent upon a phosphorylation of Ect2 T342 during metaphase which inhibits Ect2/Centraspindilin association (Yüce, Piekny, and Glotzer 2005). This illustrates that CDK1 has a negative upstream regulation of RhoA activation and inhibits the timing of cytokinesis onset until dephosphorylation of Ect2.

Genesis of chromosome segregation errors

Segregation errors during mitosis can lead to the daughter cells inheriting gains or losses of chromosomes termed aneuploidy, which has catastrophic consequences on cellular health. Chromosome segregation errors can arise from abnormal chromosome and spindle structure as well as errors in cell cycle regulation of mitosis.

Abnormal chromosome structure can result in kinetochores being entirely unattached or incorrectly attached to the spindle at the point of segregation onset, as described earlier. Unattached chromosomes are likely to be misaligned in the metaphase plate, resulting in the unilateral inheritance of a chromatid pair when cytokinesis divides the cell in two. In other cases the chromatid pair can be inappropriately attached to the spindle, resulting in uneven tension and abnormal separation. In somatic cells, SAC activation is maintained while the spindle is forming amphitelic attachments (Lara-Gonzalez, Pines, and Desai 2021), however about 1% of the time chromosomes can be missegregated (Compton 2011).

When the SAC is silenced in the presence of syntelic or merotelic attachment the chromosome is likely to be missegregated (Cimini et al. 2001). Syntelic attachments are rare, however merotelic attachments are susceptible to permit SAC silencing as both kinetochores are attached to opposite spindle poles (Figure 2) (Cimini et al. 2001). Initiation of anaphase when sister chromatids have merotelic attachments generates opposing forces on the chromatid, causing a decrease in the velocity of chromosomes moving poleward. This results in the chromosome lagging behind the main anaphase as shown in Figure 4 (Cimini et al. 2001). When the nuclear envelope reforms in telophase this laggard is prone to be excluded from the main nucleus and instead encapsulated in a separate small nucleus known as a micronucleus (Figure 4)(Gomes et al. 2022; Crasta et al. 2012). The DNA contained within these micronuclei is prone to DNA damage and chromothripsis, which can lead to oncogenesis (Kwon, Leibowitz, and Lee 2020). Chromothripsis is a genetic mutation, where the damaged chromosome is broken up and randomly reassembled (Zhang et al. 2015). Therefore, failure of error correction mechanisms and the SAC can result in lagging chromosomes, ultimately leading to severe DNA damage (Cimini et al. 2001)

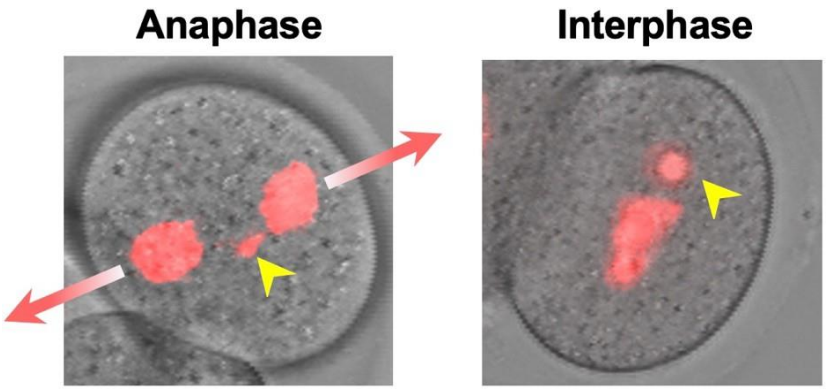

Figure 4 - Chromosome segregation errors leading to aneuploidy

2-cell stage embryo undergoing chromosome segregation in anaphase pane, anaphase direction indicated by red arrows. Yellow arrows indicate lagging chromosomes, excluded from the main anaphase. 2-cell stage embryo in the interphase panel with a yellow arrow indicating the formation of a micronucleus, a separate smaller body of condensed chromatin from the primary nucleus which is susceptible to DNA damage. Images taken using fluorescent live-cell confocal images and chromosomes are visible using H2B:RFP mRNA microinjection.

DNA damage leads to a state of chromosomal instability (CIN), exacerbating aneuploidy. Replication fork stalling during DNA damage repair can cause damaged DNA to persist into mitosis. The incomplete repair can form ultra-fine DNA bridges between sisters, which can cause chromosomes to lag in anaphase or even chromosome breakage, generating segmental and whole chromosome aneuploidy (R. Li and Zhu 2022). DNA damage responses can also further contribute to the over-stabilisation of kinetochore microtubules, risking stable mis-attachments and inaccurate segregation. Studies in human RPE1 cells, an immortalised human epithelial cell line, show DNA damage response proteins to signal through Aurora-A and PLK1 activity increasing k-MT stability. This generated an increase in lagging chromosomes, which was rescued by overexpression of kinetochore destabilising protein Kif2b (Bakhoum et al. 2014).

Premature cytokinesis, before complete segregation of the chromosomes, could lead to incompletely segregated chromosomes trapped in the furrow ingression. This can lead to furrow regression, cytokinesis failure and the formation of binucleated tetraploid cells (Shi and King 2005). Complete cytokinesis in the presence of missegregated chromosomes can also cause the formation of bulky chromosome bridges between daughter cells, again leading to DNA damage, chromosome breakage and chromothripsis (Maciejowski et al. 2015). Therefore, the cell cycle control of mitotic exit must be tightly controlled to prevent aneuploidy.

Consequences of aneuploidy in somatic cells

Immediate consequences of aneuploidy

Aneuploidy can lead to chromosomal instability (CIN). Often gains and losses of chromosomes have been shown to increase DNA damage and the number of missegregations persisting in following divisions (Passerini et al. 2016; Chunduri and Storchová 2019). After severe chromosome missegregation forms micronuclei and chromosome bridges, the cell mounts a DNA damage response (DDR). However, DNA repair mechanisms such as non- homologous end-joining are highly error-prone, resulting in replication fork stalling, mutations and reorganisation of damaged DNA. Not only does this cause dramatic reorganisation of the sequence, but also causes increased reactive oxygen species production (Maciejowski et al. 2015; Santaguida and Amon 2015). Oxidative stress can lead to impaired spindle formation, metabolic dysfunction and contribute to proteotoxic stress (Wang et al. 2017; R. Li and Zhu 2022).

Inheritance or loss of one or more chromosomes also causes large gene dosage differences from euploid cells and consequently changes the transcriptome, proteome and epigenome (Torres et al. 2007; R. Li and Zhu 2022). The imbalance of protein content can overwhelm mechanisms that regulate proteostasis, such as protein degradation and chaperone proteins, resulting in proteotoxic stress. Chaperone proteins assist protein folding to allow them to reach their soluble form, however imbalance in protein synthesis can lead to folding mechanisms becoming

overwhelmed. Chaperon proteins such as HSP90 have been shown in yeast and human cell lines to be a limiting factor in

aneuploid cells and overexpression can rescue the proteotoxic stress response exhibited in aneuploid cells (Donnelly et al. 2014; Ben-David and Amon 2020). Gene dosage imbalances of mitotic regulators such as FOXM1 have also been found in breast cancer cell lines and it is proposed these drive increased mitotic errors and genomic instability (Pfister et al. 2018).

Interestingly, aneuploidy can have both oncogenic and anti-proliferative properties, leading to the "Aneuploidy Paradox". Single chromosome gains in yeast, mouse and humans lead to slower development, and detrimental physiology (Williams et al. 2008; Torres et al. 2007; Segal and McCoy 1974). However, specific trisomies in human embryonic stem cells have also been shown to be tumour-promoting and increase proliferation (Ben-David et al. 2014). How can aneuploidy be both anti- and hyper-proliferative? Williams et al. argue that aneuploidy itself is not oncogenic but the cellular stress responses to aneuploidy might create an environment for aneuploidy to occur in a small number of cells (Williams et al. 2008). In the majority of cells, tumour suppressing mechanisms are effective, so I will now detail the antiproliferative mechanisms which are activated as a consequence of aneuploidy.

Long-term consequences of aneuploidy

Aneuploidy activates cell cycle arrest of apoptosis

The presence of an additional chromosome in yeast, mouse embryonic fibroblasts (MEFs) and human cells has been found to reduce proliferation (Torres et al. 2007; Williams et al. 2008; Segal and McCoy 1974). This slowed the rate of proliferation and is thought to be regulated by p53, a tumour suppressor protein, which limits aneuploidy-induced tumorigenesis. Knockdown of SAC components in HeLa cells to induce aneuploidy caused proteotoxic stress, double-stranded DNA breaks and cell death. Microarray analysis revealed upregulated expression of p53 and caspase-3/7, pathways involved in cell cycle suppression and apoptosis (Ohashi et al. 2015). Studies in

mice also revealed aneuploidy increased ROS to induce ATM-mediated p53 activation, which will cause the cell to enter an apoptotic or senescent cell pathway (M. Li et al. 2010).

DNA damage response induced by aneuploidy has also been shown to induce cells to enter an antiproliferative state known as senescence or G0, where the cell exits the cell cycle. Knockdown experiments of BubR1, a key SAC component, were shown to induce chromosome missegregation and profound growth inhibition in MEFs. Associated antiproliferative mechanism markers such as high β-galactosidase activity, p53, p21 and p16 were also shown to be upregulated (Baker et al. 2004). Aneuploidy induced in human fibroblasts was shown to result in telomere replication stress and cells enter a state of senescence. This study went on to show that overexpression of telomerase rescued the senescence phenotype observed (Meena et al. 2015). Therefore aneuploidy also induces a senescent state to prevent immortalisation of cells and potential tumorigenesis (Baker et al. 2004; Meena et al. 2015; Takahashi et al. 2006).

Effect of aneuploidy on mitosis

Aneuploidy has also been shown to impact the duration of the M-phase itself. Gene dosage imbalances of oncogenic genes can lead to oncogenic stress pathways which activate a DNA damage response (DDR) (Haigis and Sweet-Cordero 2011). Zhou et al. showed that DDR proteins target mitotic exit processes, for example, Mec1 kinase inhibits anaphase by stabilizing the yeast Securin (Clarke et al. 2001; C. Zhou et al. 2016). Human cells also demonstrate DDR to influence M-phase. DDR protein ATR has been shown to activate Aurora B to aid microtubule error correction during metaphase (Kabeche et al. 2018). Extension of mitosis can activate a mitotic clock checkpoint. When M-phase is extended and therefore likely to have been “stressful”, somatic cells will arrest in G1 (Dalton and Yang 2009)

Preimplantation embryo development

Because chromosome segregation fidelity is essential to cellular health, the first few cell divisions of the embryo must be faultless to ensure the successful replication of such few cells into an

entire organism. However, chromosome segregation errors are much more frequent in the mammalian embryo than in somatic cells (Vázquez-Diez and FitzHarris 2018). There are many idiosyncrasies of the mechanisms which control early embryonic divisions, which may make the embryo prone to increased segregation errors. To contextualise the impact of chromosome segregation errors in the early embryo, I will first detail preimplantation embryo development, shown in Figure 5, followed by what we know about aneuploidy in embryos.

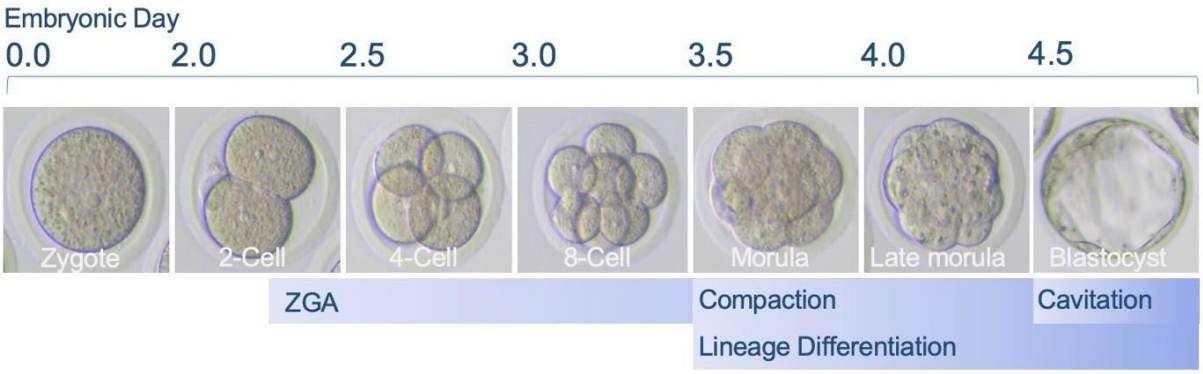

Figure 5 - Mouse embryo preimplantation development

After sperm-egg fusion, forming a zygote, the cell cycle of the egg resumes. The first cell cycles are the longest of preimplantation development with the first cell cycle finishing after 24 hours. The embryo then undergoes a series of reductive divisions, halving in volume each time. In the late 2-cell stage embryo the embryonic genome is activated and maternal mRNA products are degraded so the cell becomes entirely reliant on its own genome for transcription. Compaction takes place at the 8-cell stage, where tight junctions form between 8-cell stage blastomeres and are no longer individualised. This forms the apical-basal polarity associated with lineage differentiation, dictating the inner cell mass (ICM) and trophectoderm (TE). Cavitation occurs around day 4 of development, where a fluid-filled cavity forms in the centre of the embryo. The ICM will go on to develop the foetus while the TE will form the placenta. Images taken using Leica DM IL inverted microscope and schematics adapted from (Vázquez-Diez and FitzHarris 2018)

Fertilisation

After a single sperm has penetrated the zona pellucida, a glycoprotein shell protecting the egg from polyspermy, the sperm-egg membranes fuse. Each gamete contributes one pronucleus (PN), containing half of the paternal and maternal genome, forming a diploid cell (Georgadaki et al. 2016). Upon fertilisation, the cell is now totipotent and has the complete ability to differentiate into all cell types of the organism. The zygote is mostly transcriptionally inactive, except for a small wave of activation in the zygote, until zygotic genome activation (ZGA) which occurs at the 2-cell stage in mice and 4-8 cell transition in humans (Figure 5) (Lee, Bonneau, and Giraldez 2014). Therefore, until ZGA all protein synthesis is reliant upon residual maternal mRNAs contributed by the egg.

The first mitosis

The zygote undergoes its first cleavage approximately 24 hours after fertilisation to form a two-cell embryo. This is the longest of all cell divisions during preimplantation development in many organisms including Xenopus, mice and humans (Sikora-Polaczek et al. 2006a; Kubiak et al. 2008; Chavez et al. 2012). Uniquely, the duration is significantly prolonged by a delay in Cyclin B degradation, which is thought to be extended by Plk1 in the mouse embryo (Ajduk et al. 2017). The delay in Cyclin B destruction is thought to provide more time for the parental and maternal pronuclei to combine and form a single metaphase plate.

Morphological changes

Approximately every 12 hours from the 2nd mitosis, each blastomere will undergo another cleavage, doubling the total cell number. In addition, with each cleavage the blastomere will halve in size as the blastomeres omit a significant growth phase in the embryonic cell cycle, illustrated in Figure 5 (Tsichlaki and FitzHarris 2016).

After the 3rd mitosis, one of the first major morphological and developmental milestone begins in the morula embryo. Tight e-cadherin junctions form between neighbouring cells in a process called compaction. Tight junctions cause round and individualised blastomeres to become

flattened and cell boundaries become indistinguishable (Figure 5). This is the beginning of determining cell fate, as an apical and basal domain is formed (Johnson and Ziomek 1981; Korotkevich et al. 2017). Tight junctions designate distinct regions of the plasma membrane for the localisation of cell surface proteins. The apical domain remains on the outer surface of the morula, while the basal domain is contacting neighbouring cells only. Depending on the plane of cytokinesis in the next divisions, the daughter blastomeres will inherit different amounts of apical domain. Inheritance of the apical domain will direct the cell lineage, as the blastomeres begin to differentiate into inner cell mass (ICM) and trophectoderm (TE). The ICM will further differentiate into the epiblast and primitive endoderm contributing to the embryo proper. Whereas, the TE, which surrounds the inner ball of ICM, will form the placental tissues.

Following compaction, the next morphological landmark is cavitation, which begins around the late morula, shown in Figure 5. At cavitation, the blastocyst embryo will form a central fluid- filled cavity (blastocoel), formed by hydraulic pressure and the import of water due to an osmotic gradient generated by TE Na+/K+ ATPase pumps (Fleming et al. 1984; Chan et al. 2019). The blastocoel continues to expand and the cell number almost triples in size until the blastocyst is ready for implantation. Blastocyst expansion allows the embryo to hatch from the zona pellucida and the TE invades the uterine lining, leading to implantation.

Idiosyncrasies of mitosis in the preimplantation embryo

The mammalian embryo has many idiosyncrasies of cell division that somatic cells do not have, which may shed light on why they are prone to segregation errors. In this section, I will discuss the difference in the organisation of the spindle, transcription and cell cycle checkpoints of the embryo.

The embryonic spindle

The developing embryo experiences dramatic changes in cell size with each cleavage halving the cytoplasmic volume of daughter cells, visible in Figure 5 (Tsichlaki and FitzHarris 2016). This poses

challenges to regulating spindle size, to ensure that chromosomes are segregated sufficiently to opposite poles. In the zygote, the spindle is relatively short in comparison to the cell diameter and its length is intrinsically regulated. However, from the 2-cell stage onwards the spindle length becomes extrinsically regulated by the cell boundaries. Cytoplasmic removal experiments showed that this change in spindle size regulation was independent of cell size and more dependent upon the developmental stage of the embryo (Courtois et al. 2012). This illustrates that alongside changing cell size, there is a change in regulatory mechanisms influencing spindle size.

In addition, although the mouse model closely resembles human embryo development there are some additional differences which must be considered. Somatic cell mitosis requires two centrosomes for bipolar spindle formation, and the presence of more than two can result in the formation of multipolar spindles (Silkworth et al. 2009). To prevent multipolar spindle formation the egg degrades its centrioles and a single centrosome and centriole is donated by the sperm, to direct spindle assembly for the first mitotic division. Uniquely, the mouse embryo lacks centrioles until the late blastocyst stage, therefore the spindle poles nucleate from microtubule organising centres (MTOCs). Centrioles do appear in the mouse at the 64-cell stage, but even then it is not clear whether they are functional (Howe and FitzHarris 2013).

The zygote is also transcriptionally silent, therefore entirely reliant upon maternal transcripts and protein. There is an initial burst of transcription during the late zygote cell cycle (Bouniol, Nguyen, and Debey 1995), however full embryonic genome activation is not triggered until the late 2-cell stage embryo. It is at this point that maternal mRNA is degraded and the embryo becomes reliant on its own complement of DNA to transcribe mRNA (Lee, Bonneau, and Giraldez 2014).

The embryonic cell cycle

Somatic cells complete their full cell cycle approximately every 24h. Although comparable with the length of the zygote and 2-cell stage embryo, which takes 22-24h (Balakier, MacLusky, and Casper 1993); the duration of the cell cycle in the rest of preimplantation embryo averages development around 14 hours (Ciemerych and Sicinski 2005). The duration of the 4-cell stage and

8-cell stage interphase is much shorter than the previous two, taking around 12 hours to complete, displayed in Figure 5 (Smith and Johnson 1986).

Developmental changes in the embryo have been shown to influence the cell cycle timings. Macqueen and Johnson found that divisions generating smaller and larger cells during the 8- to 16-cell stage transition would result in larger cells having a shorter cell cycle (~12h) than their smaller sister cells (~14h) (MacQueen and Johnson 1983; Ciemerych and Sicinski 2005).

Furthermore, at the 8-cell stage, the mouse and human embryo begin to compact and establish cell polarity. The apical domain has been shown to establish spindle position and orientation, thereby directing complete or partial inheritance of the apical domain. Depending on the amount of apical domain inherited will determine the lineage of the daughter cell to form the ICM or trophectoderm (Korotkevich et al. 2017). Cell lineage and positioning are associated with different cell cycle dynamics. Cells nearer the ICM such as the mural trophectoderm proliferate faster than those in the polar trophectoderm (Copp 1978). Rat embryogenesis models also showed the ectoderm and mesoderm cell cycle duration to be ~7h whereas cells of the primitive streak would divide every ~3 hours (Auley, Werb, and Mirkes 1993).

The majority of cells possess Cyclin B1 and its knockout causes embryonic lethality (Brandeis et al. 1998). However, an interesting difference in the early preimplantation embryo is that Cyclin B1 knockout mice will undergo at least two cell divisions before arresting at the 4-cell stage embryo. This suggests that either residual Cyclin B protein or mRNA transcripts can maintain Cyclin B CDK1 activity, or that other Cyclins can compensate for incomplete Cyclin B function during the first few divisions (Strauss et al. 2018).

The embryo and its cell cycle checkpoints

Unlike somatic cells, the early embryo appears to lack functionality in many cell cycle checkpoints. Checkpoints that exist in somatic cells to prevent the propagation of aneuploid cells, such as tetraploidy-induced arrest and the mitotic clock checkpoint, have been shown to be absent in embryos (Paim and FitzHarris 2019; Allais and FitzHarris 2022; Bolton et al. 2016). In the mouse embryo, misaligned chromosomes have been shown to activate the SAC, through the recruitment of MCC components like Mad1, to misaligned chromosomes but fail to inhibit anaphase onset, resulting in chromosome segregation errors (Vázquez-Diez, Paim, and FitzHarris 2019). Because the SAC is essential in coordinating the timing of Cyclin B destruction, investigating the timing of mitotic exit without the presence of a functional SAC may elucidate other mechanisms dictating mitosis. Some of these peculiarities in the early embryo may contribute to the drastic increase in segregation observed in comparison to somatic cells. Aneuploid embryos are thought to have a poorer developmental potential as aneuploidy may lead to implantation failure, miscarriage and congenital defects (Hassold and Hunt 2001). Therefore, I will go on to detail the potential consequences of aneuploidy during preimplantation development.

Consequences of aneuploidy in embryos

Although mitotic missegregations are rare in somatic cells occurring at a rate of 1-6%, mitosis in human embryos is surprisingly error-prone with errors occurring during the first mitotic division 1/3rd of the time (Compton 2011; Currie et al. 2022). Chromosome segregation errors are infrequent in somatic cells due to the presence of the robust SAC. However, the mouse embryo SAC is not functional, resulting in misaligned chromosomes at anaphase (Vázquez-Diez, Paim, and FitzHarris 2019). The majority of full aneuploidies, which typically arise during meiosis, are fatal to embryonic development, with a few exceptions in trisomy 21, 18 and 13 (Hassold and Hunt 2001). Mitotic errors occurring during embryo development cause embryos to be made up of both aneuploid and euploid cells, termed mosaic embryos. Mosaicism is frequently observed in fertility clinics with as much as 60% of embryos containing chromosome imbalances originating from mitotic errors (Taylor et al. 2014).

Unlike most fully aneuploid embryos, mosaicism does have the potential to form healthy live births, however, studies suggest that the chances of a successful IVF cycle using mosaic embryos are reduced in comparison to euploid embryos (L. Zhang et al. 2019; Greco, Minasi, and Fiorentino 2015; Bolton et al. 2016). This is also reflected in the incidence of mosaicism found throughout preimplantation embryo development, with it being highest in early cleavage stage embryos and declining throughout gestation (Hook 1981). However, it is not clear if this is due to the elimination of aneuploid cells, altered cell cycle timings causing euploid cells to outcompete aneuploid, or the failure of mosaic embryos to develop post-implantation.

Bolton et al. 2016 used reversine, a Monopolar spindle 1-like 1 kinase inhibitor, to induce aneuploidy in early mouse preimplantation embryo. This was carried out at the 4 to 8-cell stage transition to study the impact of aneuploidy on embryonic development. Live-cell imaging of embryos cultured in reversine revealed lagging chromosomes and micronuclei formation in 50% of treated embryos. The aneuploidy generated was then assessed at the blastocyst stage using FISH for 3 randomly selected chromosomes, and it was found that the treatment increased the incidence of missegregation of these random chromosomes from 17% to 35%. They concluded that reversine generated sufficient aneuploidy to be able to assess its impact on embryonic development. They found reversine had no impact on the number of embryos reaching the blastocyst stage or the cell number at the early blastocyst stage. However, at the late blastocyst stage, the cell number was significantly reduced suggesting that aneuploid cells may be eliminated in late blastocyst development. Although reversine treatment did not impact morphological development the implantation rate was reduced, suggesting aneuploidy is only detrimental post-implantation. Next, they generated chimeras, combining reversine-treated and untreated cells to create a mixed embryo, emulating mosaicism. Cell cycle analysis of the reversine treated and untreated cells in the chimeric embryos revealed that aneuploid cells tend to develop slower, which was exacerbated when these aneuploid cells were in the trophectoderm. This is a possible reason for reduced cell number in late blastocyst aneuploid embryos. Later experiments suggest that the rate of apoptosis is also increased in these reversine-treated cells, specifically in the ICM (Bolton et al. 2016). However, the validity of these

experiments is contested as the level of aneuploidy in the chimeric embryos was never fully determined. Reversine treatment generated 50% aneuploidy, therefore it becomes difficult to tell the extent of aneuploidy generated in chimeric embryos. It would be worth repeating this style of experiment and tracking the development of aneuploid cells using a live- cell imaging technique and with robust methods of generating known levels of aneuploidy.

Aneuploidy in IVF clinics

Aneuploidy has been shown to have a detrimental impact on embryonic development. Bolton et. al show that embryos with a high number of aneuploid blastomeres have a lower chance of survival during post-implantation development (Bolton et al. 2016). Therefore IVF clinics aim to primarily transfer euploid embryos only, to maximise the chances of a successful pregnancy.

A common procedure clinics use to identify the ploidy status of an embryo is preimplantation genetic testing for aneuploidy (PGT-A), shown in Figure 6. At the blastocyst stage, a biopsy is taken from a thin layer of cells surrounding the embryo proper called the trophectoderm (TE). The TE biopsy uses the ploidy status of the sampled cells as a prediction tool for the ploidy across the whole embryo. However, the value of PGT-A is debated, as a robust randomised controlled study has not been performed. Although it has strong predictive value in identifying fully aneuploid embryos, the outcome of successful pregnancy becomes less clear if PGT-A identifies a mosaic embryo. In addition, PGT-A is an invasive procedure that requires micromanipulation of the embryos and cell removal. Finally, this is a complex and expensive process that requires skilled workers and increased costs to the patient. Therefore, clinics are in search of the “holy grail” of embryo selection, where it is possible to accurately predict the embryo ploidy status in a non-invasive and inexpensive procedure.

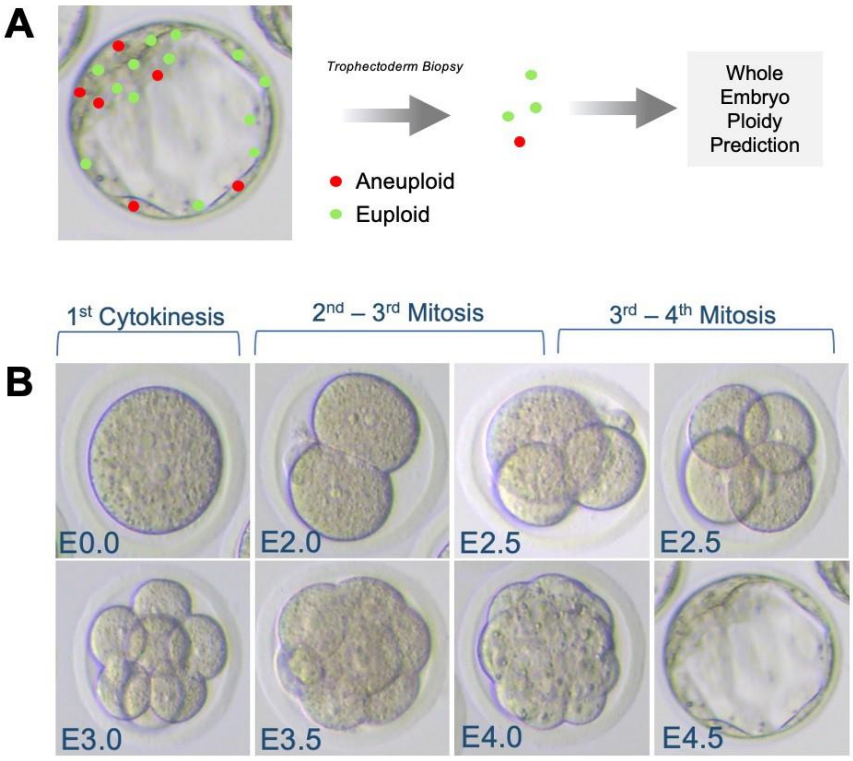

Figure 6 - Methods of embryo selection in IVF clinics

(a) The process of Pre-implantation genetic testing, where a small biopsy from the trophectoderm is taken. These cells are karyotyped for chromosomal gains and losses. This readout is then used as a prediction for the ploidy status of the whole embryo. (b) Morphokinetic movies, use brightfield imaging every 10 minutes to measure cell cycle timings such as the duration of the first cytokinesis as a measure of cellular health, the interval between the 2nd-3rd mitosis as a measure of interphase length and the interval between the 3rd and 4th mitosis as a measure of synchronicity. Images taken in (a and b) using Images taken using Leica DM IL inverted microscope.

One emerging approach IVF clinics use for embryo selection is time-lapse ('morphokinetic') movies, (Figure 6). Morphokinetics uses a brightfield microscope situated within the incubator to image embryos every 10 minutes, allowing clinicians to observe the morphology, duration of cell

divisions and timing between cleavages. Algorithms are then able to assist clinicians in selecting the embryo most likely to result in a successful pregnancy. Recent developments have even suggested that artificial intelligence software will be able to score and select embryos to transfer to future patients (Berntsen et al. 2022). However, it is unclear exactly what biological information is contained within these movies and what it can tell us about embryonic health. It has been proposed in the literature that atypical cell cycles may provide a means to detect aneuploid cells, but whether aneuploidy directly affects cell cycle timings is unclear (Reignier et al. 2018). Many studies retrospectively identify if the cells with atypical cell cycles were aneuploid, therefore it becomes difficult to disentangle the impact of aneuploidy upon the cell cycle from other upstream factors which may have led to the aneuploidy or atypical cell cycles (Chavez et al. 2012; Reignier et al. 2018). We aim to investigate how chromosome segregation errors and aneuploidy may impact the cell cycle timings of the mouse preimplantation embryo.

Aims and Objectives

Although well documented in the zygote and 2-cell stage embryo, how Cyclin B destruction changes throughout preimplantation is not well studied. The embryo undergoes many morphological and developmental transformations from the zygote to the 8-cell stage embryo, therefore we want to investigate how Cyclin B destruction corresponds to changing developmental and morphological milestones.

Secondly, the mammalian embryo is disposed to chromosome segregation error. One of the mechanisms predisposing embryos to mitotic errors is a non-functional SAC. Therefore we wanted to investigate how Cyclin B destruction is regulated in the mouse embryo and if it is dysregulated in the presence of segregation errors.

Finally, whether morphokinetics can predict the ploidy status of the embryo remains unclear. We seek to generate a robust method of generating aneuploidy followed by long-term live cell morphokinetic movies to investigate how aneuploidy affects the cell cycle.

Materials and Methods

Embryo Collection and Treatment

Embryo collection

Young (2-3 months) CD1 female mice were administered pregnant mare's serum gonadotrophin (PMSG) hormonal stimulation (5 IU of PMSG/mouse). 44-48 hours later these mice were administered human chorionic gonadotrophin (hCG) and individually mated with 3 to 12-month-old BDF1 males. PMSG and hCG were administered via subcutaneous injection in the lower abdomen. Food and water were available ad libitum and were kept in a 12-hour day/night cycle from 06:30 to 18:30. All animal experiments were authorized by the Comité Institutional de Protection des Animaux du CHUM (CIPA). When collecting 2-cell embryos, mouse sacrifice was performed 40 hours after mating. Collection of zygote required sacrifice 24-28 hours after mating. Mouse sacrifice was performed by cervical dislocation. The oviducts were dissected in homemade M2 media and embryos were released. After dissection, embryos were washed through KSOM media (003-026-XL, Wisent Bioproducts) and cultured in the incubator at 37°C and 5% CO2.

CENP-E inhibitor to induce aneuploidy

Zygotes were collected 24-26 hours post-HCG and immediately washed into pre-equilibrated 500nM GSK923295 (Cayman Chemical Company, 18389) or KSOM (Wisent Bioproducts, 003- 026-XL) supplemented with 1:1000 DMSO (Sigma Aldrich, D2650) as control and cultured in a 4-well plate without the presence of oil for 11 hours at 37°C and 5% CO2. To arrest the embryos in metaphase at the 2-cell stage for chromosome counting, embryos were washed into 100µM APCin (Tocris, 5747) + 200µM Monastrol (Calbiochem, 475879) and cultured for a further 16 hours. Metaphase-arrested embryos were then fixed and stained for chromosome counting. For measuring the proportion of treated embryos that developed to blastocyst, embryos were washed through 9 drops of 20µL KSOM 11 hours after introduction to the drug. Embryos were

scored for development every 24 hours until 120 hours post mating where they were then fixed and counted for the number of cells.

Embryos were collected at the 2-cell stage and microinjected with H2B:RFP mRNA, they were then washed through 9 drops of 20uL KSOM and cultured until they reached the 4-cell stage. 4-cell stage embryos were then washed and remained in 9 drops of 20uL 500nM GSK923295 under mineral oil. After the 4- to 8-cell transition, embryos were then washed back into KSOM and live-cell imaging was performed.

Micromanipulation Techniques

mRNA synthesis

pCMX/CyclinB1-GFP and H2B:RFP mRNA was synthesised in vitro using mMessage mMachine kit (ThermoFisher T7 and T3 respectively) and poly-adenylated using Poly(A)-tailing kit (Ambion) according to the manufacturer's protocol. pCMX/CyclinB1-GFP (27) was a gift from Jonathon Pines (Addgene plasmid #26061; http://n2t.net/addgene:26061; RRID:Addgene_26061). H2B:RFP was synthesised from plasmid pRN4 (gift from Alex McDougall, Observatoire Océanologique de Villefranche-sur-Mer, Villefranche Sur Mer, France). Clover:Geminin was synthesised PCR primers (Forward :5'-GACTATGGATCCAATTAACCCTCACTAAAGGGGCCACCATGGTGAGCAAGGGCGAG GAG-3'; Reverse: 5'- GACTATTCTAGATTACAGCGCCTTTCTCCGTTT -3' Integrated DNA Technologies). Clover:Geminin cDNA was then synthesised using a Polymerase Chain Reaction kit (New England Biolabs M0491S) using plasmid Clover-Geminin (Addgene #83915) as a template and subsequently mRNA was synthesised using T3 mMessage mMachine kit (ThermoFisher) and poly-adenylated using Poly(A)-tailing kit (Ambion).

Microinjection of mRNA

Embryos were microinjected at the Zygote, 2-, 4- and 8-cell stage in commercial M2 media (Sigma Aldrich, M7167) on Leica DM IL inverted microscope mounted with Narishige micromanipulators.

Holding pipette was used to create a suction to keep the embryo in place. Microinjection pipette containing dilute mRNA was used to deliver a precise amount of mRNA into the cytoplasm of the cell using a picopump (World Precision Instruments), as described in (FitzHarris, Carroll, and Swann 2018). After microinjection, embryos were washed in KSOM and left in the incubator for at least 2h after microinjection to establish fluorescent protein expression.

Cytoplasmic removal

Both blastomeres of 2-cell stage embryos were microinjected with CyclinB:GFP and H2B:RFP mRNA and left for 1 hour for the mRNA to diffuse throughout the cytoplasm. Injected embryos were then transferred to the Leica DM IL inverted microscope stage and placed in M2 media (Sigma Aldrich M7167) supplemented with Latrunculin A 5 µM (428021; EMD Millipore). Narishige micromanipulators were used for hydraulic control of glass pipettes during embryo micromanipulation. One glass pipette was attached to a piezo-electric drill to perforate the zona pellucida and aspirate the cytoplasm, while the embryo was held in position by the holding pipette. Following removal of the cytoplasm, the embryos were washed through 9 20uL drops of KSOM and placed in the incubator to recover before live-cell imaging.

Immunofluorescence

Fixation

Before fixation, a 96-well plate (TC-Platte 96; Sarstedt 83.3925) was prepared as follows. The embryos were put in the first drop which contained 20µL of 4% paraformaldehyde (PFA) + 0.25% Triton-X-100 in PHEM buffer for 30 minutes at room temperature. Next embryos were washed through 3 drops of 20µL 1% Bovine Serum Albumin (BSA) in PBS and left in the final drop to be blocked overnight or until staining was performed. All drops were covered in 2 drops of mineral oil to prevent evaporation.

Staining

To count chromosomes for assessing the amount of aneuploidy generated in 2-cell stage embryos after CENP-E inhibition, embryos were incubated in primary antibodies; CENP-C anti-rabbit (Covance Costum Antisera #PA5758, gift from Ben Black), CREST anti-human (gift from Marvin J. Fritzler) for 1.5 h at 37°C. Embryos were incubated in secondary antibodies; Alexa Fluor® 488 anti-rabbit (ThermoFisher A-11008) and 1:1000 Alexa Fluor® 546 anti-human (ThermoFisher A- 21089) for 1.5 h at 37°C. Finally stained for DNA using Hoescht (Invitrogen H1399) for 0.5 h at 37°C. To count the cell number for embryos cultured in CENP-E inhibitor which developed to blastocyst. Embryos were incubated in primary antibodies OCT-4 anti-mouse (Santa Cruz sc- 5279) for 1.5 h at 37°C. Embryos were incubated in secondary antibodies Alexa 488 Mouse

(ThermoFisher A-11029) and Alexa Phalloidin 555 (ThermoFisher A-34055) for 1.5 h at 37°C. Finally stained for DNA using Hoescht (Invitrogen H1399) for 0.5 h at 37°C.

Confocal Microscopy

Live-imaging of APC/C substrate destruction

Embryos were live-imaged on Leica SP8 confocal microscope to visualise H2B:RFP (chromosomes) and CyclinB1:GFP proteolysis during mitosis. Embryos were transferred to pre- equilibrated 2µL KSOM under oil in a 55mm glass-bottom dish and positioned on a heated confocal chamber (37C, 5% CO2). For all Cyclin B experiments, the following imaging parameters were used. 3-minute time interval with z-stack consisting of 8 slices, z-step size 1.4µm, pinhole
2.16 AU, optical section 3.961µm, frame averaging 2, zoom 1.28 (for 8-cell 8 1.9 zoom to adjust for cell size). All were acquired on 20x air objective with HyD detector (Laser 488 0.5%, Laser 552 0.2%) and PMT detector gain adjusted for appropriate brightfield image.

Live-imaging of aneuploid morula development

8-cell stage GSK923295 and DMSO treated embryos positive for H2B:RFP was transferred pre-equilibrated 2µL KSOM under oil in a 55mm glass-bottom dish and imaged on Leica SP8 confocal

microscope with a heated confocal chamber (37C, 5% CO2). Live imaging parameters were as follows: 5-minute time interval with z-stack consisting of 25 z-slices, z-step size 3.2µm, pinhole 1.6 AU, optical section 2.056µm, frame average 2, zoom 1.28 with acquired on 20x air objective. HyD detector (Laser 488 0.1%) and PMT detector gain adjusted for appropriate brightfield image.

Immunofluorescence imaging

Fixed and stained GSK923295 and DMSO-treated embryos were imaged on Leica SP8 confocal microscope to count chromosomes or cell numbers at the blastocyst. 63x oil objective (1.4 NA) was used. HyD detector was used with appropriate lasers (Laser 405 (UV), Laser 488 (Red), Laser 553 (Green)). Imaging parameters were as follows: z-step 1.00µm, pinhole 1 AU, optical section 2.057 all detected using a HyD detector.

Image Analysis

CyclinB1:GFP destruction

A region of interest (ROI) was taken through the widest z-slice of the cell including the nucleus and the majority of the cytoplasm. The mean intensity signal was taken from the ROI for each time frame. The mean intensity of an ROI over an uninjected embryo from the same z-slice was used as a measure of background variation and was subsequently subtracted from all raw values on each experimental day. Mean intensity was normalised to the highest and lowest raw value post nuclear envelope breakdown, to create a scale of CyclinB1:GFP destruction ranging from 0-100. During analysis, the mitotic cells were synchronised to NEBD and plotted as an average. The duration of M-phase was determined by the length of time from NEBD, visualised using H2B:RFP, to when the first frame of furrow ingression was observable. Anaphase was determined by the first frame in which there was a widening of the metaphase plate, followed by negative space between the two poleward moving chromosome clusters.

Calculation of CyclinB1:GFP half-life and destruction rate

Normalised Cyclin B1:GFP destruction curves synchronised to NEBD were individually fit to a Sigmoid-Boltzmann equation in MATLAB where y = f(x) = (A2+(100-A2))/(1+exp((x-T50)/dx)), an example shown in Figure 7. The value 100 was set as the upper asymptote, A2 was the lower asymptote, T50 is the half-life, and dx is the rate constant.

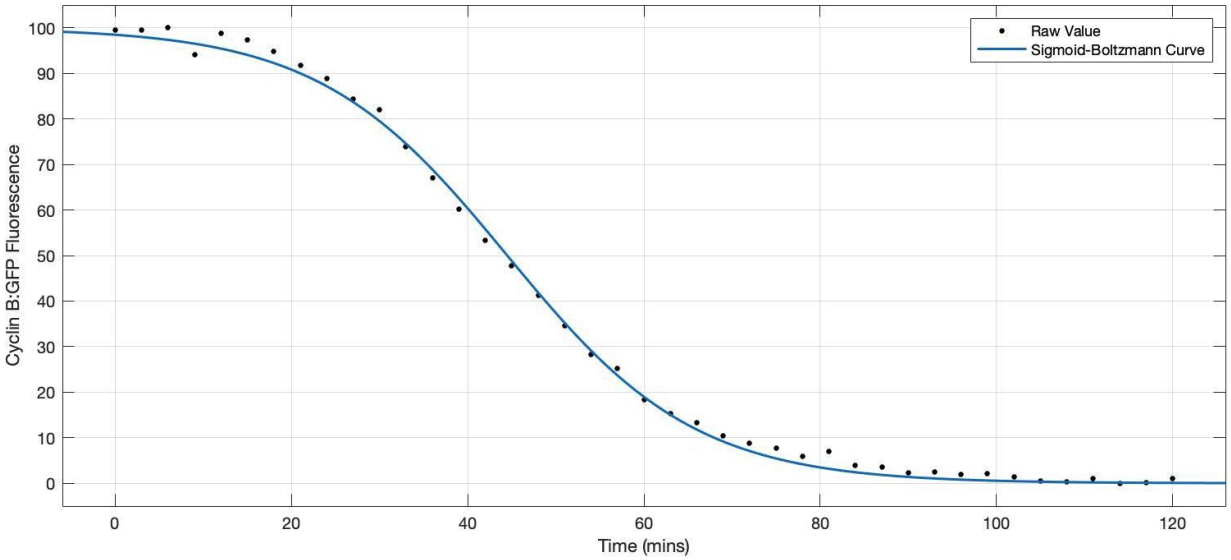

Figure 7 - Sigmoid-Boltzmann equation fit to CyclinB1:GFP destruction curve

Example of normalised and synchronised to NEBD CyclinB1:GFP destruction curves of individual cell fit to the equation f(x) = (A2+(100-A2))/(1+exp((x-T50)/dx)), coefficients with 95% confidence bounds: where A2 = lower asymptote, T50 = CyclinB1:GFP half-life, dx = rate constant Goodness of fit measured by adjusted R-squared value was always > 0.94.

Chromosome tracking

For tracking cell lineage, ImageJ plugin TrackMate was used (Ershov et al. 2022). LoG detector (Laplacian of Gaussian) filter was applied to the image filtered by an estimated objected diameter of 12 microns and quality threshold of 0.1. A lineage tree was generated and manually checked to ensure proper tracking of sister cells and interphase lengths of the 16-cell stage embryo were calculated.

Chromosome and cell number count

Z-slices analysed using ImageJ software, foci positive for both CENP-C and CREST were classified as a single kinetochore. Cell number count analysed using Hoechst signal displaying a single nuclei surrounded defined in a region of actin (Phalloidin) to define cell boundaries.

Statistical analysis

All statistical analysis was performed on GraphPad Prism 7 software (GraphPad Software, La Jolla, CA, USA, www.graphpad.com). Shapiro–Wilk normality tests were used to determine whether an unpaired two-tailed t-test or two-tailed Mann–Whitney test should be applied. For multiple comparisons, one-way ANOVA or Kruskal-Wallis tests were applied followed by Tukey's or Dunn's multiple comparisons test respectively to test statistical significance between groups. Statistical significance was considered when $P < 0.05$.

Results

Section 1 - Cell Cycle Control of Mitotic Exit

Cyclin B, Securin and Geminin are destroyed during M-phase

We explored the kinetics of several different cell cycle substrates destroyed throughout mitosis including Cyclin B, Securin and Geminin, shown in Figure 8 (Zhou et al. 2016). The aim being to identify how APC/C constructs were destroyed during mitosis in the early embryo, and if the constructs generated were viable for future experimentation. We found that these three substrates are all destroyed after NEBD at varying times and different rates (example of Cyclin B destruction Figure 8a). We found Securin:GFP mRNA microinjection to unreliably extend the duration of mitosis, which led us to exclude this construct from our analysis. Secondly, although the Geminin:Clover construct did not extend M-phase in the majority of injections, we suspect it is destroyed by an alternative APC/C form, known as APC/C-CDH1(Izawa and Pines 2011). APC/C-CDH1 becomes activated in late mitosis, hence we observed a slight delay in destruction onset in comparison with Securin and Cyclin B, which is well documented to be destroyed by the APC/C-CDC20 (Figure 8b) (Izawa and Pines 2011). Due to the difficulty in optimising Securin and Geminin probes, we continue the rest of the thesis with Cyclin B alone.

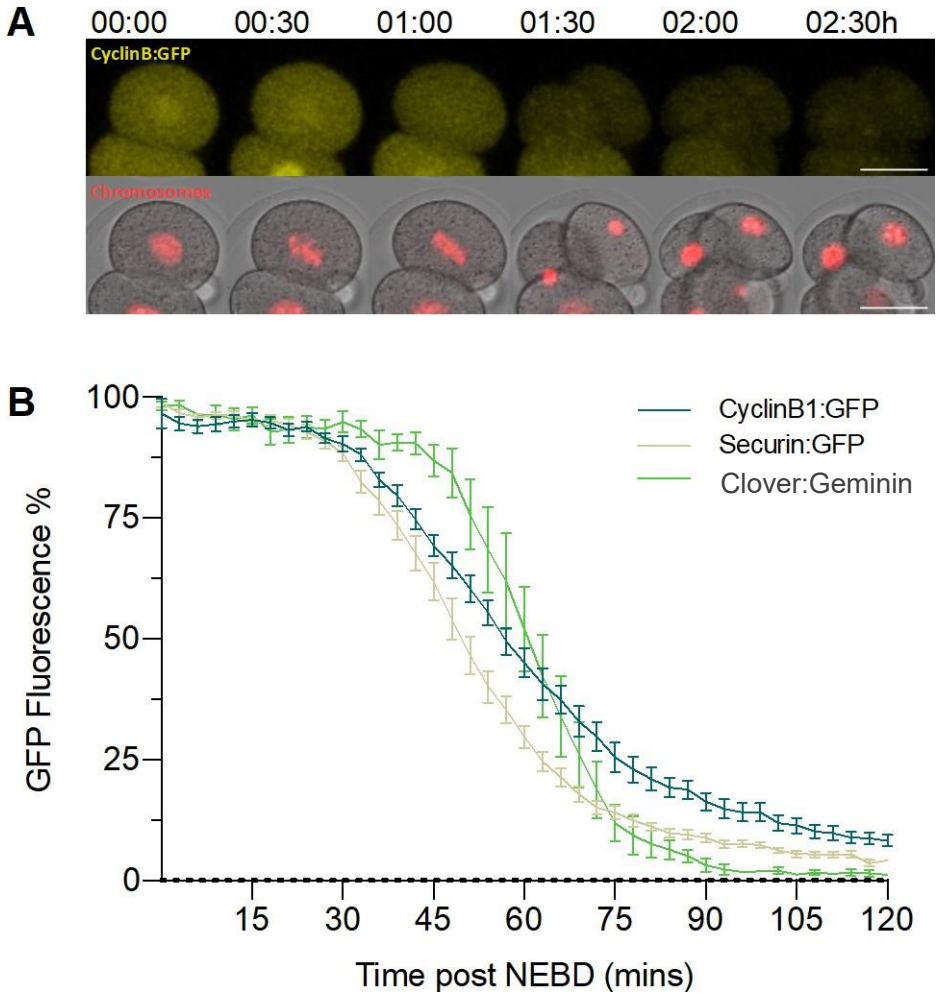

Figure 8 - Cyclin B, Geminin and Securin are all destroyed throughout mitosis

(a) Representative z-projection of 2-cell embryo microinjected with H2B:RFP (red) and CyclinB:GFP (yellow) which is destroyed during mitosis. Scale bar = 35µm. (b) 2-Cell stage embryos microinjected with CyclinB1:GFP, Clover:Geminin and Securin:GFP mRNA on 3 separate experimental days, normalised, synchronised (t0 = NEBD) and averaged destruction curves plotted together (n=12, 5, 15 respectively)

Cyclin B destruction dynamics in the 2-, 4- and 8-cell stage embryo

It was previously reported that the duration of M-phase becomes increasingly shorter throughout preimplantation development (Yamagata and FitzHarris 2013). To further assess the duration of M-phase in the preimplantation embryo we live-imaged unmanipulated zygote, 2-, 4- and 8-cell stage mouse embryos undergoing cell division. In this thesis, we define M-phase duration as the time interval between NEBD to furrow ingression. We found that the duration of M-phase becomes shorter at each developmental stage (Figure 9c; Zygote: 128min ± 3.50, 2-Cell: 54min ± 2.80, 4-cell: 48min ± 1.10, 8-Cell: 34min ± 0.90). The reason for a significantly prolonged specifically in the zygotic M-phase requires further exploration, however, recent studies have suggested a role of Plk1 specifically delaying APC/C activation in the 1st mitosis (Ajduk et al. 2017). We found that the developmental stage of the embryo determines the duration of M-phase (Figure 9c). To be able to determine how the cell cycle regulates the changing duration of M-phase, we used live- imaging to observe the key regulator of mitotic entry and exit, Cyclin B.

To observe the relationship between Cyclin B and the duration of M-phase, we microinjected the mRNA of fluorescently tagged Cyclin B (CyclinB1:GFP) and histone protein (H2B:RFP) in blastomeres at the zygote, 2-, 4- and 8-cell stage embryo (Figure 9a). This allowed the visualisation of Cyclin B destruction alongside chromosome segregation.

We first noticed that microinjection of high concentrations of Cyclin B mRNA caused an extension of mitosis (Figure S 1). Therefore we only injected blastomeres with mRNA concentration of [221] ng/ml and in addition, only included cells with a “normal” duration of M-phase. These criteria were defined by the M-phase duration of uninjected embryos, shown in Figure 9c. In cells with a normal duration of M-phase, chromosome organisation revealed the duration of both mitotic entry and mitotic exit were shorter (Figure S 2). The duration of mitotic entry, from NEBD to anaphase was reduced by 10 minutes at each mitosis (Figure S 2; 2-Cell: 51 mins ± 1.6, 4-Cell: 42 mins ± 1.5 8-Cell: 34 mins ± 1.3). This was also reflected in the duration of mitotic exit, the time from anaphase to furrow ingression (Figure S 2; 2-Cell: 16 mins ± 0.7, 4-Cell: 7 mins ± 0.4 8-Cell:

5 mins ± 0.6). In all, these data show that the duration of M-phase becomes shorter from the zygote to 8-cell mitosis.

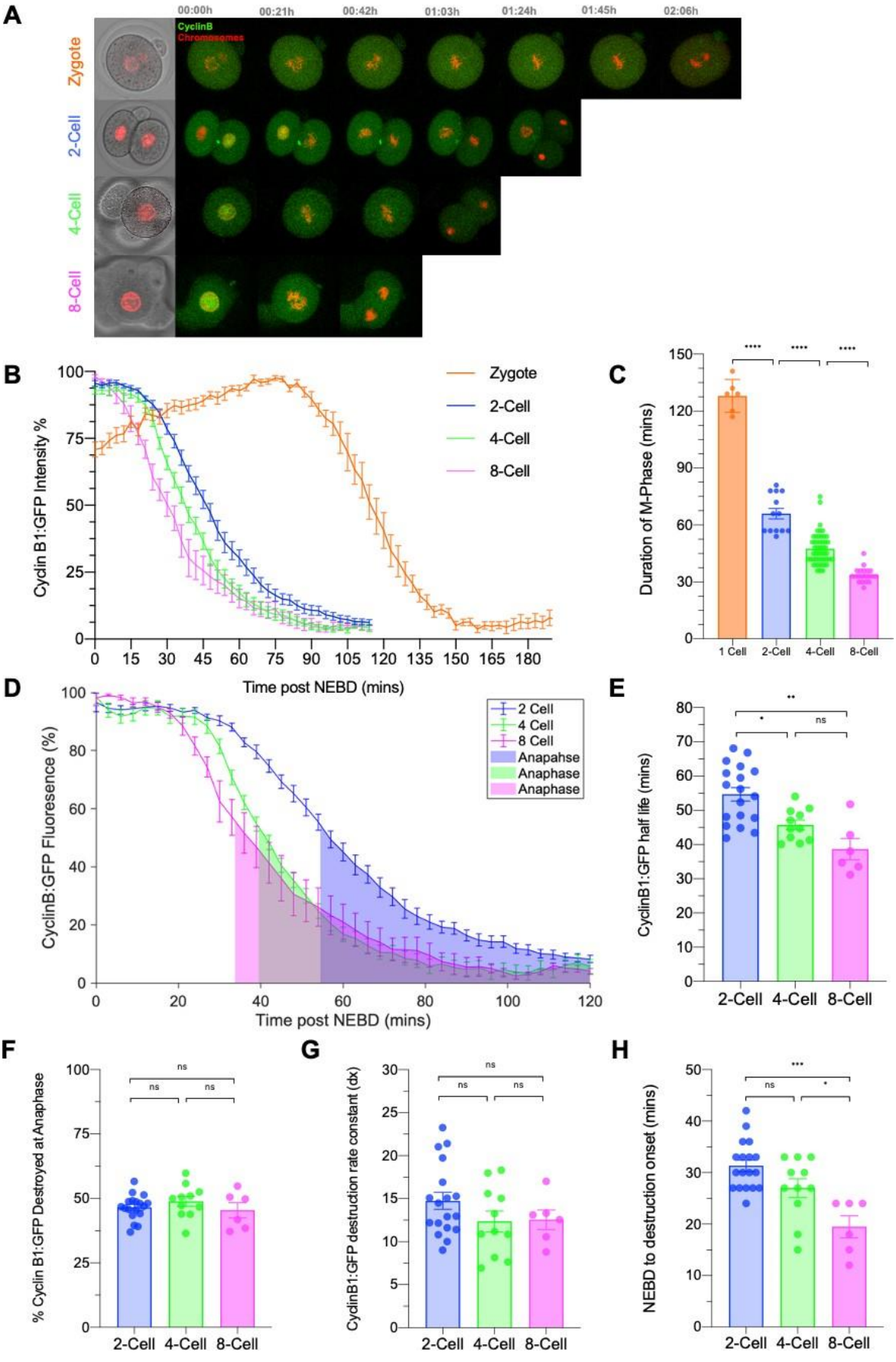
A
00:00h
00:21h
00:42h
01:03h
01:24h
01:45h
02:06h
CyclinB
Chromosomes
Zygote
2-Cell
4-Cell
8-Cell
B
Cyclin B1:GFP Intensity %
Zygote
2-Cell
4-Cell
8-Cell
Time post NEBD (mins)
C
Duration of M-Phase (mins)
1 Cell
2-Cell
4-Cell
8-Cell
D
CyclinB:GFP Fluoresence (%)
2 Cell
4 Cell
8 Cell
Anapahse
Anaphase
Anaphase
Time post NEBD (mins)
E
CyclinB1:GFP half life (mins)
2-Cell
4-Cell
8-Cell
F
% Cyclin B1:GFP Destroyed at Anaphase
2-Cell
4-Cell
8-Cell
G
CyclinB1:GFP destruction rate constant (dx)
2-Cell
4-Cell
8-Cell
H
NEBD to destruction onset (mins)
2-Cell
4-Cell
8-Cell

Figure 9 - Cyclin B destruction dynamics shortens throughout development

*(a) Representative z-projections from live-cell imaging of CyclinB:GFP destruction (green) and chromosome segregation (red) during the mitosis of the zygote, 2-cell, 4-cell and 8-cell stage mouse embryo. Both blastomeres of the 2-cell stage embryo were injected, whereas at the 4- and 8-cell stages only one blastomere was injected per embryo. Timepoint 00:00h is the first frame of NEBD, the montage ends at the point of chromosome segregation for each cell stage, shown in 21- minute intervals. (b) Normalised and synchronised to NEBD CyclinB1:GFP destruction in the Zygote, 2-, 4- and 8-cell stage embryo. (c) Time measured from NEBD to furrow ingression in uninjected zygote, 2-cell, 4-cell and 8-cell stage embryos using brightfield channel only (n=6, n=13, n=49, n=20 respectively). (d) Normalised average CyclinB1:GFP destruction synchronised to NEBD in 2-, 4- and 8-cell undergoing mitosis (n=18, n=11, n=6 respectively). The highlighted area under the curve represents the time post-mitotic exit (anaphase onset). (e) CyclinB1:GFP half-life becomes progressively shorter during preimplantation development (Kruskal-Wallis test **P<0.005 *P<0.05). (f) Percentage of CyclinB:GFP destroyed at the first timeframe of anaphase. (g) The rate constant of Cyclin B destruction, dx, remains unchanged. Values from (e and g) calculated by the Sigmoid-Boltzmann equation fit to individual Cyclin destruction curves. (h) Timing of Cyclin B destruction onset, calculated as minutes taken for 10% CyclinB:GFP destruction.*

Cyclin B destruction shortens throughout preimplantation development

We questioned how the cell cycle was regulating the observed changes in M-phase duration. Unsurprisingly, we found that there was a significant delay in the onset destruction of Cyclin B destruction in the zygote in comparison with the 2-, 4- and 8-cell stages, shown in Figure 9b (Ajduk et al. 2017). However, we also noticed a variation of Cyclin B destruction dynamics in the 2-, 4- and 8-cell. Therefore I wanted to investigate these less well-documented stages. Following previous studies, we also found the majority of Cyclin B to be destroyed within M-phase, from NEBD to furrow ingression (2-Cell: 67.8% ± 1.82 SEM), and continued to be destroyed after cytokinesis onset (Evans et al. 1983; Clute and Pines 1999; Ajduk et al. 2017; Afonso et al. 2019).

By fitting Cyclin B destruction curves to a Sigmoid-Boltzmann equation (described in Methods Figure 7), we were able to determine the half-life and rate of destruction in CyclinB:GFP positive cells. Concordant with the duration of M-phase, the half-life of Cyclin B became progressively shorter from the 2-cell to 8-cell stage (Figure 9e). We next explored what property of Cyclin B destruction dynamics changes in development to set a shorter half-life. We hypothesised three factors could be influencing Cyclin B dynamics to shorten M-phase; a faster rate of destruction, a change in the threshold of CDK1 activity for anaphase, or an earlier onset of Cyclin B destruction. We found Cyclin B to be destroyed at the same rate in all developmental stages (Figure 9g), suggesting that the APC/C reaches a maximal rate of destruction irrespective of cell stage. In addition, the proportion of Cyclin B destroyed before anaphase was consistently at 50% in all stages of preimplantation development (Figure 9f). This contributes to an existing hypothesis in somatic cells which suggests a certain threshold is met during destruction to initiate chromosome segregation (Potapova et al. 2006; Wolf, Sigl, and Geley 2007; Gavet and Pines 2010). Finally, we measured the timing of Cyclin B destruction onset, set by the time taken to reach 10% destruction. Destruction onset arrived progressively earlier after NEBD from the 2-cell, 4-cell and 8-cell stage embryo (Figure 9h), suggesting destruction onset is contributing to a shorter duration of M-phase.

The changing schedule of Cyclin B destruction is not governed by changes in cell size

In somatic cells the timing of cyclin B destruction onset is regulated by the SAC silencing. However, studies have shown that this checkpoint is not fully functional in the mouse embryo (Vázquez-Diez, Paim, and FitzHarris 2019), and chromosome segregation will occur in the presence of misaligned chromosomes. Interestingly the spindle assembly checkpoint does serve to extend mitosis as experiments have shown the use of a SAC inhibitor, AZ3146 which inhibits Mps1 kinase, and knockdown of SAC checkpoint protein Mad2 both shorten the length of mitosis. This shortened M-phase was also associated with a significant increase in the number of misaligned chromosomes at anaphase. However, SAC signalling in normally cultured embryos still failed to prevent anaphase onset in the presence of misaligned chromosomes. Suggesting the presence of

a SAC, but a lack of response to the presence of misaligned chromosomes. Therefore due to potential lack of a fully functional SAC, we hypothesised a different mechanism is dictating the onset of Cyclin B destruction. One idea we hypothesised was that changing cell size may have an influence on the timing of cyclin destruction. During preimplantation development the early embryo omits cellular growth between divisions, resulting in a series of reductive divisions where the cells halve in volume (Aiken et al. 2004; O'Farrell, Stumpff, and Su 2004; Tsichlaki and FitzHarris 2016). Therefore, we wanted to investigate whether cell size influences the timing of destruction onset.

To do this we used a cytoplasmic removal technique to aspirate 40% of the cytoplasm from a 2-cell embryo (Figure 10a and 10b). Thus creating an embryo that remains developmentally 2- cell but is the size of a 4-cell embryo. The duration of M-phase remained the unaffected in cytoplasm-reduced cells (sham controls: 64 mins ± 3; cytoplasm-removed: 60 ± 1). This was also reflected in the Cyclin B destruction curve which was indistinguishable between cytoplasm-reduced and unmanipulated controls (Figure 10c). The timing of destruction onset did not change significantly in cytoplasm-removed cells (sham controls: 28 mins ± 3; cytoplasm-removed: 33 mins ± 5), hence the timing of Cyclin B destruction is independent of cell size. Instead, the timing of Cyclin B destruction onset may be based on differences in transcription between developmental stages or remnant cytoplasmic content from the egg.

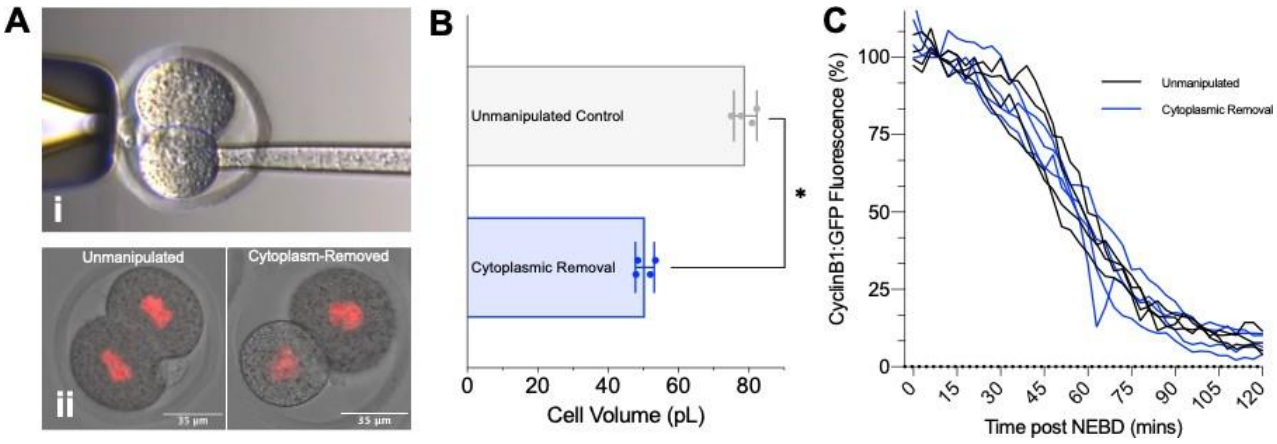

Figure 10 - The changing schedule of Cyclin B destruction is not governed by changes in cell size

*(ai) Cytoplasmic removal technique, using a glass needle to aspirate cytoplasm from a single blastomere, while the nucleus remains unperturbed. Cytoplasm removed from a single blastomere in a 2-cell stage embryo. (b) Amount of cytoplasm removed approximated by measuring the cell perimeter of the widest slice and calculating volume using equation: Volume (pL)=4/3 π[Perimeter/2π]^3 (n=4 sham control cells; n=4 cytoplasm-removed). (c) Cytoplasm-removed CyclinB1:GFP destruction profile (n=4 sham control cells, black; n=4 cytoplasm-removed, blue). Error bars represent SEM. NEBD=nuclear envelope breakdown. * P<0.05 two-tailed Mann- Whitney test. Scale Bar = 35 µm.*

Cyclin B destruction occurs in the presence of mis-segregating chromosomes

In somatic cells, the SAC delays the onset of Cyclin B destruction in the presence of misaligned chromosomes and improper kMT attachment. Recent studies have shown the spindle assembly checkpoint is not functional in the early mouse embryo, showing that anaphase progresses in the presence of Mad1-positive kinetochores (Vázquez-Diez, Paim, and FitzHarris 2019). In this study, it was not shown how Cyclin B destruction is influenced by the presence of mis-segregating chromosomes. We therefore compared Cyclin B destruction in 2-cell where we observed missegregated chromosomes (Figure 11a).

We found the rate of Cyclin B destruction (Figure 11b), and the proportion of Cyclin B destroyed before chromosome segregation was unaffected in erroneous divisions. Vázquez-Diez et al. showed that slowing the rate of Cyclin B destruction using APC inhibitors reduced the number of misaligned chromosomes at anaphase. However, we show the cell does not inherently possess such a rescue mechanism to slow the progression.

The types of erroneous chromosome segregations observed all resulted in lagging chromosomes (Figure 11b). Due to the resolution of the images, lack of kinetochore staining and orientation of the spindle it was difficult to visualise whether these chromosomes where misaligned along the metaphase plate. Importantly, we observed no change in the timing of destruction onset in erroneous divisions (Figure 11c). This suggests that either the SAC was satisfied and allowed progression into anaphase or that is not fully functional in detecting improperly attached microtubules in the preimplantation mouse embryo (Maciejewska et al. 2009; Vázquez- Diez, Paim, and FitzHarris 2019). This allows us to infer possibility of two models causing missegregation. Firstly, that the cell lacks a fully functional SAC, resulting in improper attachment to the spindle before anaphase onset and the missegregation of chromosomes. Secondly, the presence of undestroyed cyclin B at anaphase onset, as described in Figure 9, could be inducing lagging chromosomes. This is a possibility as previous studies in Drosophila have found that overexpression of cyclin B changes kinetochore behaviour during anaphase (Parry, Hickson & O'Farrell, 2003). This will be discussed further in the discussion.

Importantly, we observed no change in the timing of destruction onset in erroneous divisions (Figure 11c). Further suggesting that the SAC is not fully functional in the preimplantation mouse embryo (Maciejewska et al. 2009; Vázquez- Diez, Paim, and FitzHarris 2019).

Unchanged Cyclin B destruction onset in the presence of mis-segregating chromosomes also corresponds to our finding that erroneous divisions have a similar duration of M-phase (Figure

11d). Therefore, the duration of M-phase is not predictive of missegregations and morphokinetic movies would not be able to exclude these embryos for patient transfer.

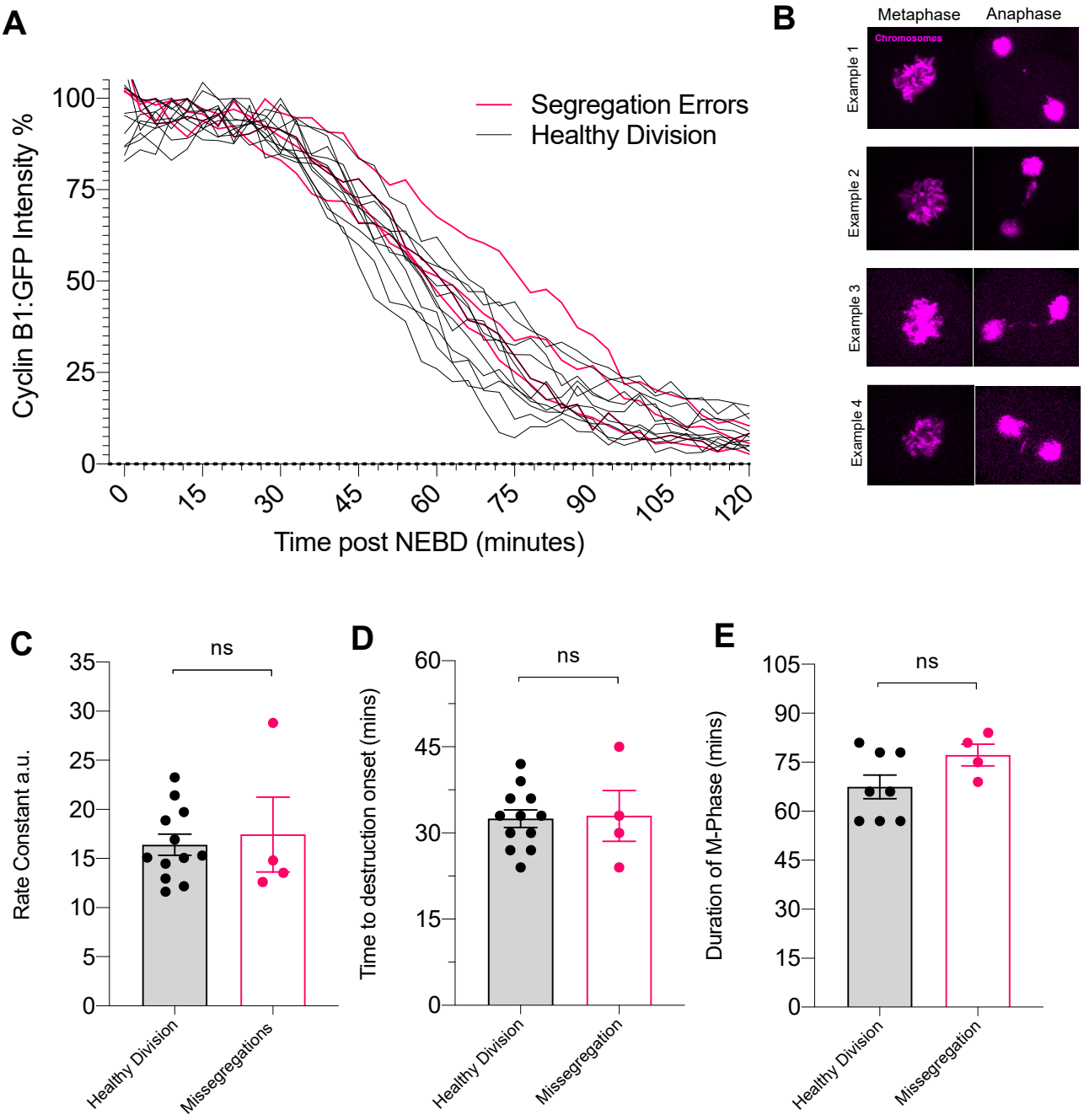

Figure 11 - Chromosome missegregations and Cyclin B destruction

(a) Normalised average CyclinB:GFP destruction in cells undergoing segregation errors shown in (n=4, red), compared to those with healthy divisions (n=12, black). (b) Images of chromosome (magenta) movements at the metaphase plate and during anaphase in all four examples of

missegregations. Each example shows snapshots before and after anaphase from single blastomeres where lagging chromosomes where observed. Cyclin B was measured in these examples (Fig 11B) and represented in Figures 11A, C, D and E. (c) Comparison of segregation error destruction rates using sigmoid-Boltzmann destruction rate constant (dx) (n=12 healthy; n=4 errors). (d) Time taken for 10% of CyclinB1:GFP destruction was classified as the timing of Cyclin B destruction onset (n=12 healthy; n=4 errors). (e) Duration of M-phase in 2-cell stage embryos undergoing segregation errors (n=12 healthy; n=4 errors). Two-tailed Mann- Whitney test ns = P>0.05. Error bars represent SEM. NEBD=nuclear envelope breakdown.

Section 2 - Impact of Aneuploidy on the Preimplantation Embryo

Aneuploidy does not alter the duration of mitosis or interphase in the morula

CENP-E is a motor protein localised to the kinetochore responsible for chromosome movement along the spindle (Bennett et al. 2015). CENP-E inhibition produces whole chromosome segregation errors during mitosis. To investigate how chromosome gains and losses may impact cell cycle timings we induced aneuploidy using a reversible CENP-E inhibitor (GSK923925). To be able to identify the impact of aneuploidy - we collected a homogenous group of embryos and induced aneuploidy by incubating 4-cell stage embryos in 500nM GSK923925 (Figure 12a).

This method, optimized in the lab by Dr. Lia Gomes Paim, generates heavily-aneuploid 8-cell stage embryos. Dr. Paim found this method to generate aneuploidy in 75% of all treated cells in the morula, in comparison to 13% in controls (Figure 12b). Treatment was also found to generate drastic gains and losses of chromosomes ranging from 1 to over 10. I used this same technique in my own experiments to understand if aneuploidy has an impact on the cell cycle and development.

Aneuploid embryos develop to blastocysts grossly normally

GSK923925 treated “aneuploid embryos” were live-imaged alongside DMSO-treated controls and to track chromosome movements during development (Figure 12c). Firstly, we found that aneuploid embryos, continued to undergo multiple rounds of divisions similarly to controls (Figure 12c). The lineage tree, shown in Figure 12d, illustrates a representative example of an aneuploid morula continuing to divide to at least the 32-cell stage. This shows aneuploid 8-cell developed to form blastocysts, illustrating that even when almost all the cells are aneuploid, the embryo divides and develops grossly normally. This is unlike most somatic cells, which have strict mechanisms to prevent the replication of aneuploid cells, through mechanisms like apoptosis or enter cell cycle arrest (M. Li et al. 2010; Santaguida and Amon 2015).

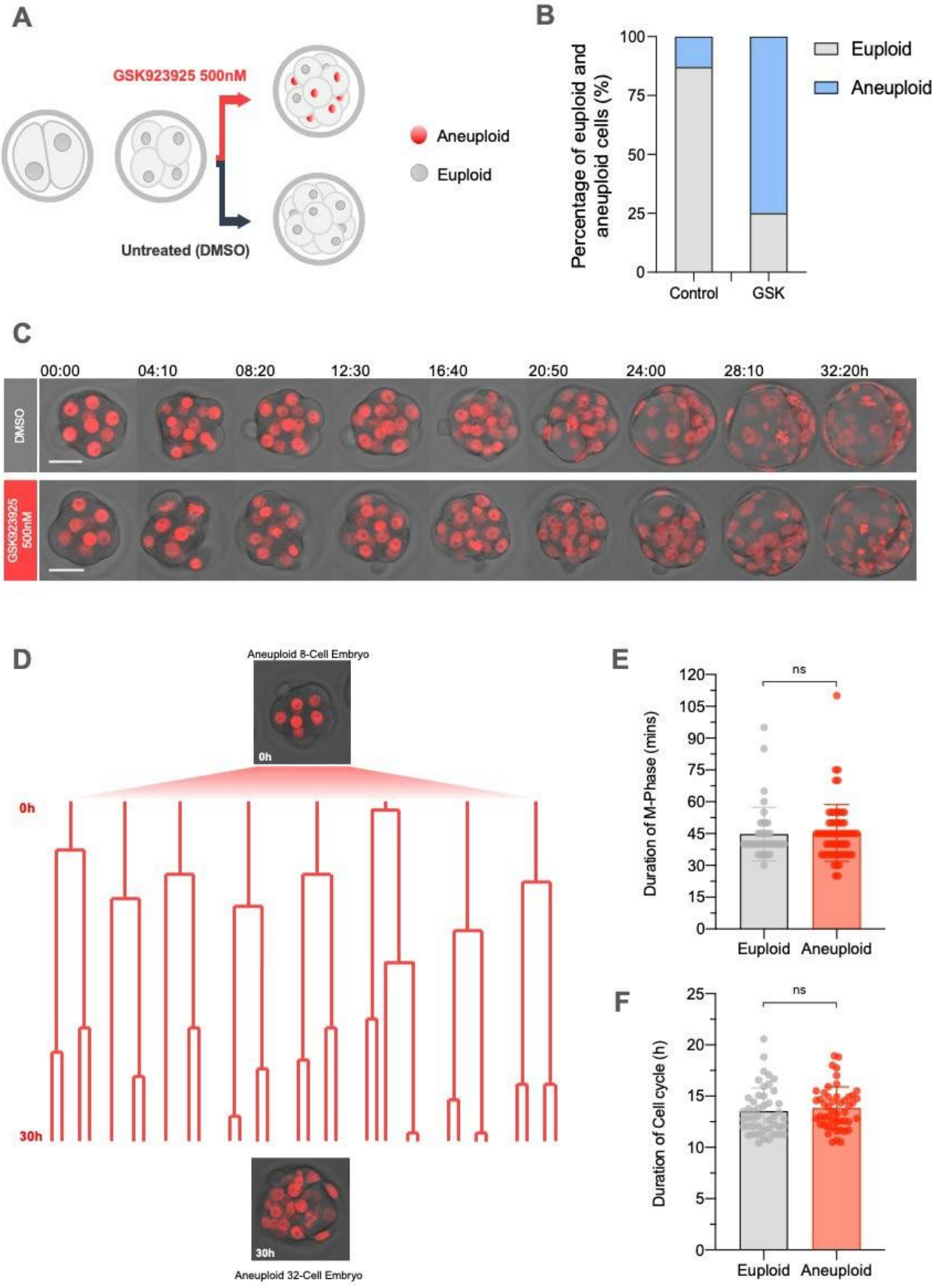
A
GSK923925 500nM
Untreated (DMSO)
Aneuploid
Euploid
B
Percentage of euploid and aneuploid cells (%)
100
75
50
25
0
Control
GSK
Euploid
Aneuploid
C
00:00
04:10
08:20
12:30
16:40
20:50
24:00
28:10
32:20h
DMSO
GSK923925 500nM
D
Aneuploid 8-Cell Embryo
0h
0h
30h
30h
Aneuploid 32-Cell Embryo
E
Duration of M-Phase (mins)
120
105
90
75
60
45
30
15
0
ns
Euploid
Aneuploid
F
Duration of Cell cycle (h)
25
20
15
10
5
0
ns
Euploid
Aneuploid

Figure 12 - Aneuploidy does not alter the duration of mitosis or interphase in the morula

(a) Schematic illustrating the experimental design for generating aneuploid morula, CENP-E inhibitor used GSK923925. (b) Data and analysis carried out by Dr. Lia Paim, treatment in (a) generates heavily-aneuploid 8-cell stage embryos with 75% of GSK923925 (n=9 aneuploid out of 12) treated cells to be aneuploid in comparison to 13% in DMSO controls (n=2 out of 15). (c) Representative z-projection of euploid and aneuploid embryo developing to blastocyst in morphokinetic movie, t0 = start of imaging. 2-cell embryos were microinjected with H2B:RFP to observe chromosomes (red) and aneuploidy was generated at the 8-cell stage. (d) Lineage tree generated through manual sister cell tracking illustrating each cell in a GSK923925 treated 8-cell embryo undergoing 2 rounds of cell division, accompanied by representative z-projection of H2B:RFP and single z slice of brightfield illustrating development to blastocyst. Cell cycle timings of morula remain unchanged in the presence of aneuploidy (e and f); (e) M-phase duration (DMSO n=40; GSK923925 n=63) and (f) interphase length (DMSO n=46; GSK923925 n=49). Two-tailed unpaired t-test ns=P>0.05. Error bars represent SEM. NEBD=nuclear envelope breakdown. Scale Bar = 35 microns.

Impact of aneuploidy on the cell cycle

In clinics, morphokinetics typically measure the duration of interphase, as a determinant of embryonic health, but it is unclear whether cell cycle timings are predictive of aneuploidy (Bamford et al. 2022; Campbell et al. 2013; Patel et al. 2016; Chavez et al. 2012). Here we found that aneuploidy alone had no impact on the duration of interphase in 16-cell stage embryos (Figure 12f). Therefore, this suggests that the mechanisms which detect aneuploidy and delay the cell cycle or induce hyperproliferation in somatic cells - appear not to be functional in the early embryo. Interestingly, other examples of known checkpoints preventing proliferation and slowing the cell cycle have been shown to not be in effect in the preimplantation embryo for example, the presence of tetraploidy, micronuclei and a long extension of m-phase known as the M-phase checkpoint (Paim and FitzHarris 2019; Vázquez-Diez et al. 2016; Allais and FitzHarris 2022). However, the data in this thesis data does not resolve whether other checkpoint mechanisms

which delay the cell cycle such as DNA damage may not be effective in the embryo and requires further investigation. Therefore, the mechanisms which respond to aneuploid to delay the cell cycle or induce hyperproliferation in somatic cells appear not to be functional in the early embryo.

Secondly, we questioned whether the presence of chromosome gains and losses would extend the duration of M-phase. However, we found the duration of an aneuploid M-phase at the 8-cell stage to be comparable with euploid cells (Figure 12e). These results together suggest that at this point in embryonic development morphokinetics is not a useful measure of detecting aneuploidy.

Impact of aneuploidy on the early embryo

The timings typically extracted from morphokinetic movies are timings between early cell divisions, such as the 2nd and 3rd mitosis. In addition, the 1st mitotic division in human zygotes is highly error-prone, frequently establishing an entirely aneuploid 2-cell stage embryo (Currie et al. 2022). Therefore, we decided to also investigate the impact of early aneuploidy. Zygotes were cultured in 500nM GSK923925 during the 1st mitosis to generate aneuploid 2-cell stage embryos (Figure 13a). During this experimental redesign, we also began culturing in GSK923925 without oil as we suspected that GSK923925 may be less effective under oil (see discussion and Figure S 3). To confirm we had generated aneuploidy, the treated 2-cell stage embryos were arrested in metaphase, fixed and stained for centromeres. Chromosome counts revealed 75% of blastomeres to have chromosomal gains and losses (Figure 13bii). Interestingly, this was only limited to single gains or losses of chromosomes (Figure 13c), unlike the diverse and heavy aneuploidy observed when 4-cell stage embryos were exposed to CENP-E inhibition. Importantly, creating aneuploidy at the 2-cell stage produces an entirely aneuploid embryo, with one daughter cell being hyperploid and one being hypoploid, eliminating the opportunity for euploid blastomeres to compensate for reduced aneuploid cell development.

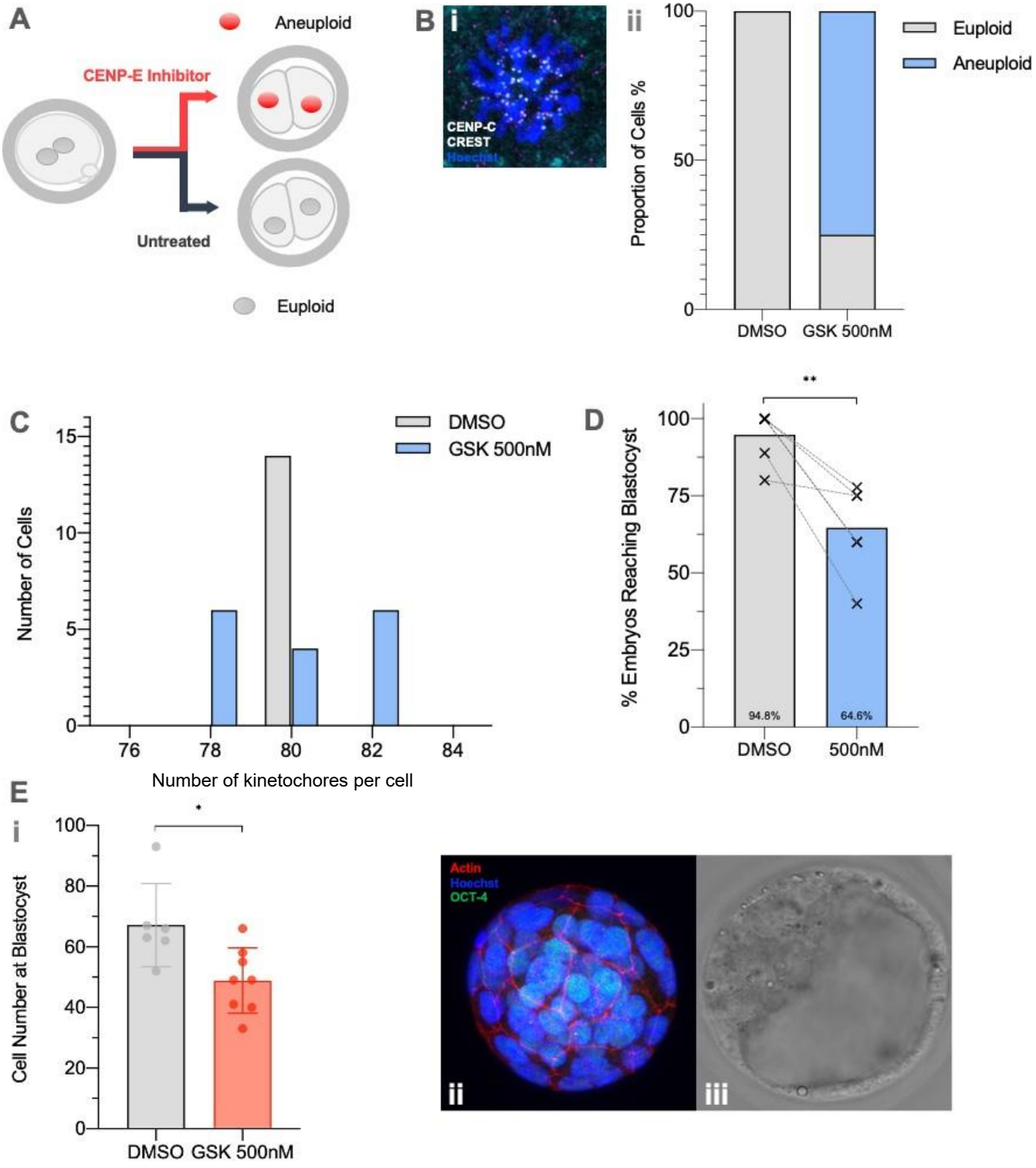
A
Aneuploid
CENP-E Inhibitor
Untreated
Euploid
B
i
CENP-C
CREST
Hoechst
ii
Proportion of Cells %
100
50
0
DMSO
GSK 500nM
Euploid
Aneuploid
C
DMSO
GSK 500nM
Number of Cells
15
10
5
0
76
78
80
82
84
Number of kinetochores per cell
D
**
% Embryos Reaching Blastocyst
100
75
50
25
0
94.8%
64.6%
DMSO
500nM
E
i
*
Cell Number at Blastocyst
100
80
60
40
20
0
DMSO
GSK 500nM
Actin
Hoechst
OCT-4
ii
iii

Figure 13 - Impact of aneuploidy induced early in embryonic development

*(a) Schematic illustrating the experimental design for generating aneuploid 2-cell stage embryo CENP-E inhibitor GSK923925. (b) Treated zygotes in GSK923925 as illustrated in (a) were fixed and co-stained for CENP-C, CREST and Hoechst to identify chromosome number representative z-projection shown in (b i). Treatment generated 75% of cells at the 2-cell stage to be aneuploid (b ii) (DMSO euploid n= 14, aneuploid n=0; GSK923925 euploid n=4, aneuploid n=12). (c) The extent of chromosome gains and losses were limited to gains of 1 chromosome only (Number of kinetochores per cell in DMSO 80 n=14. GSK923925; 78 n = 6, 80 n=4, 82 n=6). Kinetochore number 80 represents the error-free segregation of 80 kinetochores which was halved to 40 during segregation and then duplicated to 80 during the 2-cell stage S-phase. (d) The proportion of treated zygotes which developed to blastocyst (n=4 different experimental days), confirmed by presence of the blastocoel under the dissection microscope. (e ii) GSK923925 treated embryos that made blastocyst were fixed and stained with Hoechst (Blue), OCT-4 (Green), Phalloidin (Red), representative z-projection shown. (e iii) shows a brightfield image of blastocyst and presence of blastocoel. Cell number counted manually and shown in (e i) (DMSO Mean: n=6, GSK923925 Mean: n=8). Two-tailed Mann-Whitney test **P<0.005, *P<0.05. Error bars represent SEM. NEBD=nuclear envelope breakdown.*

Although we observed a slight detrimental impact on development, strikingly the majority of embryos continued developing to blastocyst (Figure 13d). In addition, of those aneuploid embryos which did reach blastocyst, we still observed cell numbers ranging from 33-66 cells per blastocyst (Figure 13e). This illustrates that entirely aneuploid 2-cell embryos still have the potential to undergo multiple rounds of cell division while evading cell cycle arrest and apoptotic mechanisms. We found that generating aneuploidy in the earlier cell stage of development still does not impact most cellular divisions occurring in the embryo (Figure 13). In summary, data from Figure 12 and Figure 13, show that aneuploid cells are still able to undergo multiple rounds of cell division at a similar rate that euploid ones do. Therefore, morphokinetic movies will have

trouble distinguishing an aneuploid from euploid embryo. However, this relies on the assumption that human embryos would behave the same as mouse embryos.

The mouse is commonly used as a model for mammalian embryonic development as it is a cheap and easily genetically manipulated mammalian model. In addition, both the human and mouse preimplantation embryo follow a similar pattern of events during development. They both undergo a series of reductive divisions after fertilisation which goes on to cavitate, form a blastocyst consisting of an epiblast, primitive endoderm and trophectoderm. This differentiation from totipotent to pluripotent stem cells utilises similar signalling pathways to those found in the human embryo. This blastocyst will then hatch from the zona pellucida to implant into the uterine lining (Taft 2008). In all, these similarities make using the mouse a useful model for inferring fundamental biological mechanisms to the human.

Other studies in mouse embryos have found little correlation between the duration of cell cycle and aneuploidy (Bolton et al. 2016; Vázquez-Diez et al. 2016; reviewed in Milewski and Ajduk 2017). Human studies also dispute the use of morphokinetics are a measure of predicting the ploidy status of the embryo. Several algorithms have been developed, all concluding different parameters as the most useful cell cycle timings for predicating ploidy, suggesting a lack of obvious measurements influenced by aneuploidy (Chavez et al. 2012; Basile et al. 2014; Del Carmen Nogales et al. 2017). Due to the discrepancies shown between clinics, international multicentre randomised trials are required to be able to improve conclusions about the influence of aneuploidy upon cell cycle timings (Milewski and Ajduk 2017).

One problem with the mouse model is that the cell cycle timings between divisions is much faster than that of the human embryo. However, one strong piece of evidence suggesting that human embryos also lack the cell cycle response to aneuploidy is that human mosaic and trisomic blastocysts are commonly found in IVF clinics (Su et al. 2016; Lin et al. 2020).

Another study supporting my suggestion that human embryos would continue to divide in the presence of aneuploidy used chemical induction of aneuploidy. Here, Human embryos exposed

to nocodazole a strong spindle poison to induce aneuploidy. They found that aneuploidy induced by Nocodazole was not able to activate apoptotic mechanisms until day 5 of development. When incubated before day 5, the human embryos were able to progress through the spindle assembly checkpoint and continue into a polyploid cell cycle. Further implying that these cell cycle arrest mechanisms may not be active in the first few divisions of the human embryo (Jacobs et al. 2017). This evidence suggests that human embryos are also able to continue to undergo several rounds of cell division, cavitate and form a blastocyst at a similar rate to those of their euploid counterparts. I think that this is strong evidence to support my findings that aneuploidy may also fail to mount a cell cycle arrest or delay response as detailed in somatic cells.

Discussion

This thesis set out to study the cell cycle control of mitotic exit in the preimplantation embryo and how mitotic exit may be influenced by atypical chromosome segregation. I then went on to assess the impact of aneuploidy on the embryo cell cycle and development. In Section 1, I demonstrate changing Cyclin B dynamics correlate with the duration of M-phase in a cell-size independent mechanism. Furthermore, we illustrate that the SAC, usually responsible for ensuring chromosome segregation fidelity, fails to inhibit Cyclin B destruction and anaphase in the presence of misaligned chromosomes. Section 2, demonstrates that after pharmacologically-inducing aneuploidy, embryos continue to undergo multiple rounds of cell division - developing grossly normally to euploid embryos. This suggests that cell cycle checkpoints maintaining genomic integrity in somatic cells, such as the SAC, senescence and apoptosis are not fully functional in the early embryo.

This discussion will explore the possible biological mechanisms that dictate developmentally changing Cyclin B dynamics, and I will propose some future directions of investigation to continue the work in this thesis. Secondly, I will discuss the clinical significance, caveats and future directions of our results that suggest embryos lack sufficient cell cycle responses to aneuploidy.

A role of Cyclin B destruction onset on mitotic errors

I chose to study Cyclin B and how its destruction changes throughout M-phase because it is well-documented to regulate CDK1 activity. The temporal regulation of M-phase is important as it encompasses the time available for chromosomes to correctly align before segregation (Therman et al. 1984). My first observation was that the duration of M-phase becomes shorter at each developmental stage, (Figure 9c).

It has been previously shown that micronucleus formation is rare in the early embryo, with 5% of cells at the 2-cell and 4-cell stage possessing micronuclei. Interestingly, the number of micronuclei per cell at the 8- and 16-cell stage rises to 13% and 25% respectively (Vázquez-Diez et al. 2016).

This suggests that during development the M-phase becomes increasingly less efficient in ensuring proper chromosome segregation. Vázquez-Diez et al. later showed that pharmacologically slowing the rate of Cyclin B destruction, thereby lengthening the duration of M-phase by ~10 minutes, significantly reduced the amount of misaligned chromosomes at anaphase and micronuclei formation (Vázquez-Diez, Paim, and FitzHarris 2019). They propose that the pharmacologically- induced longer M-phase allowed more time for the proper alignment of chromosomes. Perhaps one mechanism causing increased micronuclei during preimplantation development is related to Cyclin B destruction onset becoming earlier at the 2-, 4- and 8-cell stage (Figure 9h), generating a shorter M-phase and less time for proper alignment.

But why does Cyclin B destruction onset arrive earlier in an 8-cell stage embryo than in a 4-cell? Chromosomes align faster at each developmental stage (Tsichlaki and FitzHarris 2016), so intuitively one would assume that this results in earlier SAC silencing and subsequent Cyclin B destruction. However, I have shown that Cyclin B destruction is initiated in the presence of missegregating chromsomes, suggesting the potential of improper attachment and a weak SAC (Figure 11). Vázquez-Diez *et al.* also investigated the lack of a strong SAC in later stages of mouse preimplantation development, finding the SAC continues to be weak from the 4-cell stage embryo until the blastocyst (Vázquez-Diez, Paim, and FitzHarris 2019). Therefore, I do not expect the earlier onset of cyclin B destruction observed between the 4- and 8-cell stage embryo to be dependent on waiting for complete SAC satisfaction (Vázquez-Diez, Paim, and FitzHarris 2019). This study showed that SAC inhibitor, AZ3146, would shorten the duration of M-phase, suggesting partial functionality, so perhaps cyclin B destruction is held until the majority of connections to be made before initiating anaphase onset.

As the onset of Cyclin destruction is unlikely to be set by SAC satisfaction, I investigated other developmental idiosyncrasies during development. One being the possibility that cell size may change the timing of Cyclin B destruction onset. However, I found no difference between Cyclin B destruction between large and small cells of the same developmental stage (Figure 10), leaving the possibility that destruction onset could be a developmentally-regulated mechanism, although how this is regulated is unknown.

A meiotic hangover?

If Cyclin B destruction onset is SAC and cell-size independent; I hypothesise that remnant cytostatic factor (CSF) of the egg may influence Cyclin B destruction onset post-fertilisation. Emi2, a critical component of CSF, stabilises the Cyclin B-CDK1 complex to arrest eggs in metaphase II (Masui and Markert 1971). As a result, Emi2 delays Cyclin B destruction and anaphase until fertilisation, where it is then targeted for degradation by ubiquitin ligase βTrCP (Tunquist and Maller 2003; Shoji et al. 2006). One possibility is that remnant CSF may be at a lower but functional concentration in the zygote, which becomes less abundant with each cleavage. This could result in a gradual reduction in its ability to stabilise Cyclin B-CDK1, leading to a shorter time to destruction onset with each subsequent mitosis. It was previously suggested that Emi2 is unlikely to be involved in prolonging the first mitosis (Ajduk et al. 2017). However, this study only used mRNA-based (morpholino and siRNA) approaches to knockdown Emi2, without measuring protein content. These approaches do not exclude the possibility of Emi2 mRNA resynthesis and translation in the early zygote - or the possibility of incomplete destruction of Emi2 after egg activation (Madgwick et al. 2006). In summary, it remains to be fully addressed what dictates Cyclin B destruction onset.

My hypothesis is that although Emi2 is no longer translated in the embryo, residual protein from the oocyte could still remain in the cytosol. As the embryo develops from the zygote to morula, the concentration of residual Emi2 would gradually dimmish over time due to degradation or proteolysis. This would then fit the observed trend that cyclin B destruction becomes earlier and earlier from the zygote, 2-cell, 4-cell and 8-cell stage embryo – as the reduced residual pool of Emi2 become less effective in delaying cyclin B destruction.

To identify if residual Emi2 protein is the causative factor behind the observed shortening in the time from nuclear envelope breakdown to cyclin B destruction, future experiments could utilise Trim-Away. Trim-Away is a method using antibodies and TRIM21. TRIM21 is a naturally occurring human E3 ubiquitin ligase which recognises antibody bound pathogens in the cytoplasm (Clift et al. 2017). To employ this method, I would microinject mRNA of TRIM21 and the antibody specific

to Emi2 for complete proteolytic destruction of Emi2 in the zygote. Following this micromanipulation, I would then carry out CyclinB1:GFP destruction analysis to observe if cyclin B is still degraded sooner after nuclear envelop breakdown at each cell stage. If it is observed that at the 2-, 4- and 8-cell stage cyclin B destruction onset is now consistent at each cell stage, then I could conclude that residual Emi2 is playing a role in dictating the duration of cyclin B destruction onset in the early embryo. If no change in cyclin B destruction onset is observed, then I would begin to investigate other potential mechanisms dictating the onset of cyclin B destruction. One potential avenue would be to investigate the accumulation of spindle assembly checkpoint proteins on kinetochores and what threshold of SAC components is stripped from kinetochores for cyclin B destruction onset.

It is important to investigate the mechanisms which control the timing of destruction onset to understand why a greater frequency of micronuclei is observed during preimplantation development (Vázquez-Diez et al. 2016). It would be interesting for future study to investigate Cyclin B destruction onset beyond the 8-cell stage. Firstly, to identify if there is a limiting period of time that Cyclin B remains stable before destruction onset. Secondly, to identify when the SAC strength is re-instated and able to pause Cyclin B destruction in the presence of misaligned chromosomes.

Future experiments could also investigate how the embryonic developmental stage effects Cyclin destruction, by exploiting nuclear transfer techniques (Craven et al. 2010). This method would divorce the influence of the nucleus from its cytoplasmic content. Successfully transferring a 4-cell stage nucleus to an enucleated 2-cell stage embryo microinjected with CyclinB:GFP, could determine whether cytoplasm in a 2-cell stage embryo is contributing to delayed Cyclin destruction.

Cyclin B destruction: A job half-done

Another interesting observation made was that in all cell stages, anaphase seems to consistently take place at approximately 50% of CyclinB1:GFP destruction see Figure 9d. Although this is an

exogenous and GFP-tagged protein, which could impact destruction dynamics from endogenous cyclin B, our measurements show that certain threshold of cyclin B destruction is correlated with the metaphase-anaphase transition. Although we have found a correlation of anaphase to 50% of cyclin B destruction, we do not have the experiments to say that this is enough for required, as the decision to commit to anaphase could have happened at any point during the window from cyclin B destruction onset to anaphase. To identify if 50% of cyclin B destruction is required for anaphase, experiments utilising a stable cyclin B1 construct should be employed, such as those carried out in *Drosophila* and HeLa cells (Wolf, Sigl, and Geley 2007; Chang, Xu, and Luo 2003; Parry, Hickson, and O'Farrell 2003). After finding the concentration of stable cyclin B at which the metaphase-anaphase transition is inhibited, I would then use this at the 4-cell and 8-cell stage to observe if anaphase inhibition remains consistent with this concentration.

Many studies in somatic cells also point towards a threshold model of Cyclin B destruction during mitotic exit (Wolf et al. 2006; Xu and Chang 2007; Gavet and Pines 2010). A simple and elegant study of this idea by Wolf et al. shows stable Cyclin B1 construct produced a dosage-dependent response in the progression through mitosis. The highest levels of stable cyclin B expression produced a "pseudo-metaphase" like arrest phenotype where sister chromatids would separate and undergo anaphase but regressed to the metaphase plate in a prometaphase state. This was likely due to the kinetochore behaving in a prometaphase state, attempting to reform end-on attachments as they do when the anaphase wait signal is present in the spindle assembly checkpoint. Studies in *Drosophila* found that these sister chromatids would then form merotelic attachments (Parry, Hickson, and O'Farrell 2003). Moderate levels of expression would induce a "metaphase" arrest, where sister chromatids would separate and oscillate in and out of the metaphase plate. Finally, low levels of expression would generate a "telophase" like arrest, where a full anaphase occurs, but chromosomes remain condensed at the spindle poles and cytokinesis is initiated but incomplete (Wolf et al. 2006). However, we find that the potential Cyclin B destruction threshold leading to anaphase onset in embryos is much less than in somatic cells.

There is mixed literature suggesting how much Cyclin B is destroyed at anaphase. The majority of studies in somatic cells show anaphase to take place after the vast majority of Cyclin B has been destroyed (Clute and Pines 1999; Chang, Xu, and Luo 2003; Kamenz et al. 2015). Expression of non-degradable Cyclin B in HeLa cells found that at levels 30% of endogenous Cyclin B, stable Cyclin B was able to block the metaphase-anaphase transition, implying at least 70% of Cyclin B is degraded before anaphase onset (Chang, Xu, and Luo 2003). This is contrasting to our findings which show that in embryos, anaphase is taking place when only ~50% of Cyclin B destruction. In concordance with my findings, a recent study of Cyclin B dynamics in *Drosophila* S2 cells, HeLa cells and mouse oocytes also find a similar proportion of Cyclin B destruction at anaphase (Afonso et al. 2019).

Limitations of exogenous Cyclin B

One concern in this study was that we are introducing and exogenous cyclin B1 construct into the cell, introducing an increased abundance of cyclin B. Published studies suggest that the M/A transition is sensitive to levels of cyclin B1 (Sarafan-Vasseur et al. 2002), therefore we introduced criteria to carefully controlled for overexpression. The time from nuclear envelope breakdown to furrow ingression was recorded for all cells, uninjected and injected, visualised using brightfield microscopy. This created a range of "normal" duration of M-phase to then exclude any injected cells whose M-phase duration lay outside of this range. While optimising the concentration of CyclinB:GFP mRNA for microinjection, we did observe that when injecting at a concentration of [443]ng/mL 100% of blastomeres (n=10) were outside the M-phase duration range of control embryos. Suggesting that overexpression of cyclin B would have an impact on the cell cycle. However, after halving this concentration to [221]ng/mL, 80% of blastomeres (n=10) fell in the range of uninjected embryos. Confirming we were now using a concentration with a reduced impact on the cell cycle timing, making the assumption that we are not heavily impacting the cell cycle machinery valid. For all following experiments I used this concentration and strictly excluded any cells which had an M-phase extended beyond those of control uninjected embryos imaged simultaneously. Ideally, the use of an endogenously tagged CyclinB1:GFP mouse would

remove this limitation to our study, however this mouse model has not yet been developed for scientific use.

Anaphase onset in the presence of high Cyclin B could be one contributing factor to the increased frequency of chromosome missegregation in the mammalian embryo in comparison to somatic cells. Studies in the *Drosophila* embryo have shown that Cyclin B destruction causes changes in the kinetochore and spindle behaviour at anaphase which are required for appropriate segregation (Parry, Hickson, and O'Farrell 2003). Perhaps a higher CDK1 activity present at anaphase onset in mouse embryos is perturbing normal kinetochore and anaphase behaviour, increasing the frequency of missegregation. For this to be formally examined, utilising a CDK1 activity biosensor, using FRET dynamics, instead of Cyclin B as a secondary readout of CDK1 activity is essential (as used in Gavet and Pines 2010).

The other side of the balance: phosphatases

It is also important to remember the important role phosphatases play during mitotic exit. Phosphatases PP1 and PP2A also regulate major dephosphorylation events (Nasa and Kettenbach 2018), the timing of which would also be an important addition to determine the timing of chromosome segregation.

It is also important to remember the important role phosphatases play during mitotic exit. Phosphatases PP1 and PP2A also regulate major dephosphorylation events (Nasa and Kettenbach 2018). In particular, PP2A-B55 is a key player in removing the phosphorylation of cyclin B/Cdk1 substrates. Therefore, the timing of PP2A activation or the expression level of PP2A would also be important in determining the timing of mitotic exit. Analysing PP2A-B55 activity may reveal a different threshold of cell cycle component phosphorylation status which is required for the cell to commit to anaphase. One potential explanation for observing cyclin B destruction onset taking place sooner after metaphase in the 2-, 4- and 8-cell stage could be due to PP2A activity. If PP2A-B55 expression is greater by the time the cell reaches the 8-cell stage than the 2-cell stage, this

could explain why anaphase takes place sooner after NEBD, as CDK1 phosphorylation is reversed at a faster rate, facilitating chromosome segregation and mitotic exit to initiate earlier.

One way to investigate phosphatase activity in the live cell is to utilise fluorescent DiFMU, a small molecule which becomes fluorescent upon removal of its phosphate group (Welte et al. 2005). Although non-specific to PP2A, this could indicate a general idea of how much dephosphorylation occurs prior to anaphase onset. This may begin to identify a threshold of phosphatase activity is reached prior to the commitment to the metaphase/anaphase transition.

The embryo lacks functional cell cycle checkpoints

Somatic cells which undergo chromosome missegregations have three fates; continue the cell cycle, cell cycle arrest, or cell death. After becoming aneuploid, somatic cells typically activate tumour-suppressor mechanisms to prevent continued cell cycle (Ohashi et al. 2015; Thompson and Compton 2010; M. Li et al. 2010), and the cell will enter a senescence or apoptotic pathway. In Section 2 of this thesis, I performed experiments to investigate how aneuploidy impacts the cell cycle and development of the early embryo.

We found that the SAC failed to delay Cyclin B destruction in the presence of mis-segregating chromosomes (Figure 11). Vázquez-Diez et al. found 25% of cells at the morula stage, progress into anaphase in the presence of misaligned chromosomes. These misaligned chromosomes were able to recruit SAC components but failed to prolong M-phase and inhibit anaphase (Vázquez-Diez, Paim, and FitzHarris 2019). Interestingly, they found SAC inhibitor would shorten the SAC, suggesting partial functionality.

Vázquez-Diez et al. also found a strong SAC response, resulting in M-phase arrest, was only mounted in the presence of spindle challenge. In my thesis, examples of mis-segregating chromosomes (n=4), had no significant difference in the timing of Cyclin B destruction onset. However, in one example (n=1, not included in Figure 11), a prolongation of M-phase was observed when in the presence of extreme spindle defects and chaotic anaphase identified by a

distorted C-shaped direction of anaphase movement, which was rare and unrepresentative of most misaligned chromosomes observed. This was excluded from analysis to only observe the impact of misattachment to the spindle, without spindle defects. The fact that Vázquez-Diez et al. find spindle poison, nocodazole, to mount a strong SAC response potentially explains why spindle defects observed in this anomaly, lead to a prolonged M-phase and slowed Cyclin destruction. In all, these data still show that in the presence of mis-segregating chromosomes, the embryo fails to inhibit Cyclin B destruction and a failure of the first safety net in preventing the genesis of aneuploidy.

But why are these chromosomes missegregating? There are two, non-mutually exclusive models to explain the observed chromosome missegregations. Firstly, one explanation for cyclin B destruction and the observation of mis-segregating chromosomes is the presence of a weak SAC, which allows anaphase to progress in the presence of incompletely attached sister chromatids. Improperly attached kinetochores can result in the formation of lagging chromosomes, like those observed in Figure 11, due to opposing forces pulling from each pole of the spindle resulting in reduced chromatid velocity and a laggard. There is already evidence to suggest that the mouse embryo lacks a fully functional SAC, as Mad1 positive kinetochore still failed to prevent anaphase onset in the presence of misaligned chromosomes (Vázquez-Diez, Paim, and FitzHarris 2019). Secondly, incomplete destruction of cyclin B could be the causative factor to chromosome missegregations observed. Previous studies have shown that overexpression of cyclin B causes to stable kinetochore-microtubule attachments and chromosome missegregations (Wolf, Sigl, and Geley 2007; Parry, Hickson, and O'Farrell 2003). This would correlate with the observation in some of the missegregations in Figure 11, do not show severe chromosomes misalignment but chromosomes continue to lag during the anaphase. However, it is important to clarify that misalignment data was not able to be fully evaluated, due to a lack of kinetochore staining, resolution of images and orientation of the spindle. Therefore, a necessary future experiment to address whether the presence of the weak SAC is causing missegregations would be to also inject a live probe for Mad1 or kinetochore components e.g., CENP-C, to assess the alignment status and SAC activity prior to cyclin B destruction onset.

Another approach to distinguish these two potential models for chromosome missegregation could utilise the APC inhibitor, APCin, to slow rate of cyclin destruction. APCin is a specific inhibitor of the APC/C, blocking its interaction with Cdc20 (Gao et al. 2018). Slowing the rate of cyclin B destruction using mild APCin concentrations has been shown to previously rescue missegregation in the mouse embryo (Vázquez-Diez, Paim, and FitzHarris 2019). This study hypothesises that APC/C inhibition allows more time for chromosomes to correctly attach to the spindle before anaphase. APCin in conjunction with the microinjection of CyclinB1:GFP and H2B:RFP mRNA could be utilised to observe a slowed cyclin B1 destruction. If chromosomes continue to segregate when cyclin B1 destruction reaches 50% of destruction, this suggests that it is the presence of undestroyed cyclin B that may be inducing chromosome missegregations. However, if chromosomes segregate at a similar temporal time, instead of waiting for cyclin B1 reaching a certain threshold of destruction, this suggests that the missegregations observed in this study were as a result of a weak spindle assembly checkpoint.

The embryo lacks a functional response to aneuploidy

In this section, I will discuss how after we generate aneuploidy, the embryo continues to divide similarly to that of euploid embryos. This suggests a lack of cell cycle checkpoints that are present in somatic cells to prevent tumorigenesis.

GSK inactivation of oil

Firstly, I will discuss one caveat to our experimental design when generating aneuploidy. During our experimental redesign, we changed methodology from using GSK923925 drops of mineral oil to use without oil. This is due to the fact that I noticed a lack of aneuploidy when optimising the technique for use in zygotes. However I managed to generate aneuploidy when using 500nM GSK923925 without oil (see Figure 12bi). Figure S3, illustrates that GSK923925 is less effective when incubated in oil for different periods of time, suggesting that unexpectedly GSK923925 diffuses into the oil. Importantly, we do not expect this to change the results of experiments

where we did use oil (Figure 12), as dishes were set up exactly the same as Dr. Paim, who found that this still generated 75% aneuploidy (Figure 12b). However, we can no longer state that embryos were cultured in 500nM in this set of experiments, as we expect some but not all of the drug to diffuse into the oil. Although the use of culture media and drugs under oil is commonplace in the field, in the future we will avoid the use of drugs under oil, as our findings highlight that during incubation drugs can diffuse to oil.

G1 checkpoint failure

Here I demonstrate that after SAC failure, induced by CENP-E inhibition, aneuploid embryos continue to undergo multiple rounds of cell division and reach blastocyst, suggesting the failure of arrest and apoptosis pathways (Figure 12 and Figure 13). In addition to the SAC, somatic cells also possess G1 checkpoints, to block replication of aneuploid cells. In response to tetraploidy, tumour suppressor mechanisms will activate p53 via hippo pathway activation. Activation of p53 will promote the tetraploid cell to arrest in G1 which eventually transitions to a senescent phenotype (Ganem et al. 2014; Stukenberg 2004). Although we did not formally investigate DNA damage, the proportion of cells arresting in G1 or apoptotic markers, we can extrapolate that aneuploidy is unlikely to activate these pathways as we observe similar cell numbers in aneuploid and euploid controls (Figure 13, p58). This is not a surprise, as studies in the mouse embryo have directly shown the G1 tetraploidy checkpoint to be absent (Paim and FitzHarris 2019). Binucleated 4-cell stage embryos would develop to morula, indicating successful passage through the cell cycle and its checkpoints. Induced-tetraploidy failed to prevent anaphase in the presence of misaligned chromosomes but also caused extensive SAC-dependent M-phase lengthening.

Extensive M-phase can also activate G1 arrest mechanisms, through a mitotic clock mechanism. When undergoing a “stressful M-phase” somatic cells have a mitotic clock checkpoint (Dalton and Yang 2009; Lambrus and Holland 2017). Extension of the mitosis of RPE1 cells by over a threshold of 1.5 hours would activate a p38-p53 dependent G1 arrest (Uetake and Sluder 2010). The mitotic clock checkpoint was previously shown to induce widespread apoptosis in mouse embryos, but only after day E9.0 (Bazzi and Anderson 2014). Allais and FitzHarris show that in the

preimplantation embryo, a prolongation of M-phase of up to 6 hours in the 2nd mitosis was not able to initiate arrest (Allais and FitzHarris 2022). Although G2 arrest would occur when M-phases were prolonged for 14+ hours, within 6 hours of arrest mitotic errors such as premature sister chromatid separation were observed. In my own experiments, GSK923925 treatment during the 1st mitosis also significantly extended M-phase by 1.5 hours (Figure S3). However, zygotes were still able to develop to blastocyst, suggesting the mitotic clock checkpoint is not as effective as in somatic cells.

Bolton et al. generated chimeric mosaic embryos by combinining reversine-treated “aneuploid” blastomeres with euploid blastomeres. They found mosaic embryos develop almost identically to euploid controls, but with slightly different timings. Interestingly, they find that aneuploid cells become eliminated from the embryo only after the implantation stage (Bolton et al. 2016). Therefore, we conclude from our findings and current literature that both the SAC and interphase cell cycle checkpoints fail to prevent the genesis of aneuploidy and the continued replication of aneuploid cells in the preimplantation embryo (summarised below in Figure 14 - Failure of checkpoints in the preimplantation embryo facilitates mosaicism).

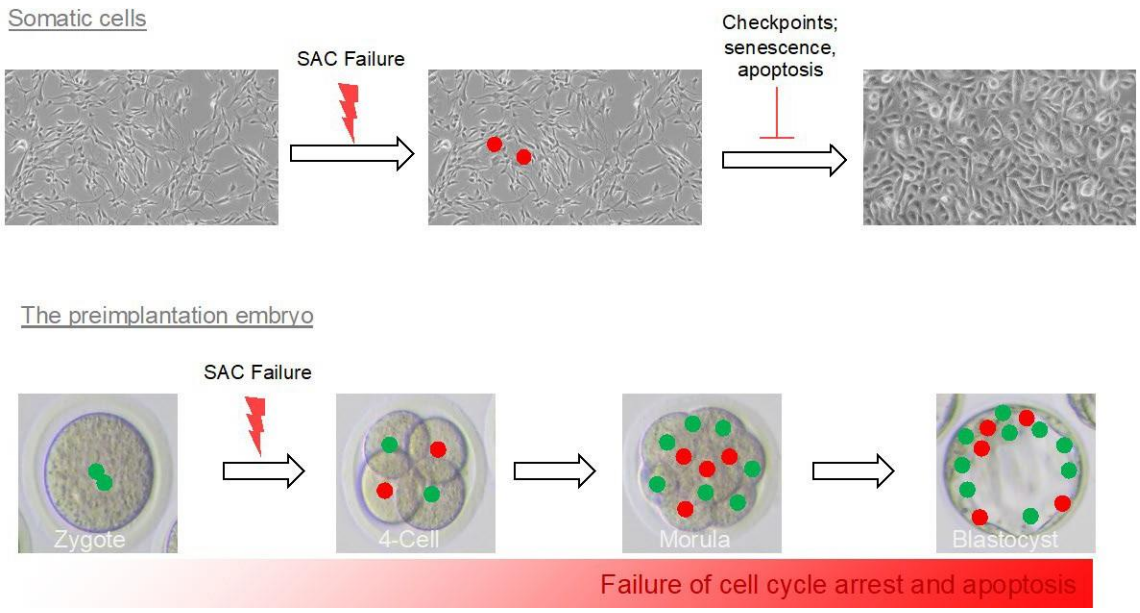

Figure 14 - Failure of checkpoints in the preimplantation embryo facilitates mosaicism

In the rare occurrence where somatic cells fail to segregate chromosomes faithfully leading to aneuploid cells. Functional checkpoints such as the mitotic clock checkpoint, tetraploidy checkpoint and DNA damage responses will lead to p53-activated senescence and apoptosis. However, neither of these exist in the mammalian embryo. We show that the SAC fails to inhibit anaphase in the presence of misaligned chromosomes, and the later cell cycle checkpoints fail to prevent continued replication of these aneuploid cells.

Morphokinetics may not be a viable tool to assess aneuploidy

We successfully generated aneuploid 2-cell stage embryos, the majority of which were able to develop to blastocyst (Figure 13). Analysis of cell cycle timings from aneuploidy generated at the 8-cell stage revealed similar cell cycle timings to euploid embryos (Figure 12). Although we were not able to determine if the live-imaged embryos were unquestionably aneuploid. Fixation of treated 2-cell stage embryos revealed 75% of blastomeres to have chromosome gains or losses. This is more robust than other studies which observed only a small increase in the incidence of aneuploidy after pharmacologically-induced aneuploidy (Bolton et al. 2016). From this we can

infer that the majority of embryos which made blastocyst were also aneuploid. Future experiments could utilise a live centromeric marker such as TALE- MajSat::Clover (Macaulay, Allais, and FitzHarris 2020) to count chromosomes in live cells and track their development to blastocyst.

We find that the duration of M-phase and interphase in aneuploid embryos was neither extended nor shortened, see Figure 12. This suggests that aneuploid embryos do not establish a hyper-proliferative or arrested state – as they continue development with similar cell cycle timings to euploid cells. Vázquez-Diez et al. confirm that micronucleus formation failed to prevent cells from dividing and did not affect cell cycle timings (Vázquez-Diez et al. 2016). DNA contained within these micronuclei displayed extreme DNA damage and loss of kinetochores entirely. Highlighting that DNA damage response mechanisms are also unable to detect micronuclei and aneuploidy to slow the cell cycle or arrest cells in interphase. We find embryos continue to divide with the same intervals (duration of interphase, Figure 12e) and speed (duration of M-phase, Figure 12d). Therefore, aneuploidy is unlikely to be identifiable via measurements of cell cycle timings. This study was not able to determine the impact on all phases of the cell cycle such as the length of G1, S and G2 which may highlight slight cell cycle differences in the G1 or S-phase in aneuploid cells. But regardless, brightfield movies used in morphokinetics would also be devoid of this ability.

One of the problems in human studies identifying cell cycle differences between aneuploid embryos is that embryos in IVF clinics are highly heterogenous, coming from a range of patient ages, exposures and types of infertility. Therefore, it is impossible to disentangle the cause and consequences of aneuploidy on embryo health. In this study, we were able to separate the sole impact of aneuploidy on cell cycle timings and found little distinguishable differences.

In summary, morphokinetics remains a controversial tool with mixed literature on its efficiency in predicting aneuploidy (Bamford et al. 2022; Campbell et al. 2013; Patel et al. 2016; Chavez et al. 2012). Predicting aneuploidy based on nuanced changes in cell cycle timings is likely to be

ineffective in identifying aneuploid cells or those undergoing erroneous chromosome segregation. However, morphokinetics may still serve a purpose in identifying extreme differences in cell cycle timing or cytokinesis failure. In addition, although cell cycle timings aren't affected by aneuploidy, this does not exclude other detrimental factors such as insufficient ATP production that may produce an observable phenotype in morphokinetic movies.

Bibliographic References

Afonso, Olga, Colleen M Castellani, Liam P Cheeseman, Jorge G Ferreira, Bernardo Orr, Luisa T Ferreira, James J Chambers, Eurico Morais-de-Sá, Thomas J Maresca, and Helder Maiato. 2019. 'Spatiotemporal Control of Mitotic Exit during Anaphase by an Aurora B- CDK1 Crosstalk'. Edited by Jon Pines and Anna Akhmanova. ELife 8 (August): e47646. https://doi.org/10.7554/eLife.47646.

Aiken, Catherine E. M., Peter P. L. Swoboda, Jeremy N. Skepper, and Martin H. Johnson. 2004. 'The Direct Measurement of Embryogenic Volume and Nucleo-Cytoplasmic Ratio during Mouse Pre-Implantation Development.' Reproduction (Cambridge, England) 128 (5): 527–35. https://doi.org/10.1530/rep.1.00281.

Ajduk, Anna, Bernhard Strauss, Jonathon Pines, and Magdalena Zernicka-Goetz. 2017. 'Delayed APC/C Activation Extends the First Mitosis of Mouse Embryos'. Scientific Reports 7 (1): 9682. https://doi.org/10.1038/s41598-017-09526-1.

Allais, Adélaïde, and Greg FitzHarris. 2022. 'Absence of a Robust Mitotic Timer Mechanism in Early Preimplantation Mouse Embryos Leads to Chromosome Instability'. Development (Cambridge, England) 149 (13): dev200391. https://doi.org/10.1242/dev.200391.

Anjur-Dietrich, Maya I., Colm P. Kelleher, and Daniel J. Needleman. 2021. 'Mechanical Mechanisms of Chromosome Segregation'. Cells 10 (2): 465. https://doi.org/10.3390/cells10020465.

Annual Review of Cell and Developmental Biology 28: 29–58. https://doi.org/10.1146/annurev-cellbio-101011-155718.

Aravamudhan, Pavithra, Alan A. Goldfarb, and Ajit P. Joglekar. 2015. 'The Kinetochore Encodes a Mechanical Switch to Disrupt Spindle Assembly Checkpoint Signalling'. Nature Cell Biology 17 (7): 868–79. https://doi.org/10.1038/ncb3179.

Auley, Alasdair Mac, Zena Werb, and Philip E. Mirkes. 1993. 'Characterization of the Unusually Rapid Cell Cycles during Rat Gastrulation'. Development 117 (3): 873–83. https://doi.org/10.1242/dev.117.3.873.

Baker, Darren J., Karthik B. Jeganathan, J. Douglas Cameron, Michael Thompson, Subhash Juneja, Alena Kopecka, Rajiv Kumar, et al. 2004. 'BubR1 Insufficiency Causes Early Onset of Aging-Associated Phenotypes and Infertility in Mice'. Nature Genetics 36 (7): 744–49. https://doi.org/10.1038/ng1382.

Bakhoum, Samuel F., Lilian Kabeche, John P. Murnane, Bassem I. Zaki, and Duane A. Compton. 2014. 'DNA-Damage Response during Mitosis Induces Whole-Chromosome Missegregation'. Cancer Discovery 4 (11): 1281–89. https://doi.org/10.1158/2159- 8290.CD-14-0403.

Balakier, H., N. J. MacLusky, and R. F. Casper. 1993. 'Characterization of the First Cell Cycle in Human Zygotes: Implications for Cryopreservation'. Fertility and Sterility 59 (2): 359–65. https://doi.org/10.1016/s0015-0282(16)55678-7.

Bamford, Thomas, Amy Barrie, Sue Montgomery, Rima Dhillon-Smith, Alison Campbell, Christina Easter, and Arri Coomarasamy. 2022. 'Morphological and Morphokinetic Associations with Aneuploidy: A Systematic Review and Meta-Analysis'. Human Reproduction Update 28 (5): 656–86. https://doi.org/10.1093/humupd/dmac022.

Basile, Natalia, Maria del Carmen Nogales, Fernando Bronet, Mireia Florensa, Marissa Riqueiros, Lorena Rodrigo, Juan García-Velasco, and Marcos Meseguer. 2014. 'Increasing the Probability of Selecting Chromosomally Normal Embryos by Time-Lapse Morphokinetics Analysis'. Fertility and Sterility 101 (3): 699-704.e1. https://doi.org/10.1016/j.fertnstert.2013.12.005.

Bazzi, Hisham, and Kathryn V. Anderson. 2014. 'Acentriolar Mitosis Activates a P53- Dependent Apoptosis Pathway in the Mouse Embryo'. Proceedings of the National Academy of Sciences of the United States of America 111 (15): E1491–1500. https://doi.org/10.1073/pnas.1400568111.

Ben-David, Uri, and Angelika Amon. 2020. 'Context Is Everything: Aneuploidy in Cancer'. Nature Reviews. Genetics 21 (1): 44–62. https://doi.org/10.1038/s41576-019-0171-x.

Bennett, Ailsa, Beatrice Bechi, Anthony Tighe, Sarah Thompson, David J. Procter, and Stephen S. Taylor. 2015. 'Cenp-E Inhibitor GSK923295: Novel Synthetic Route and Use as a Tool to Generate Aneuploidy.' Oncotarget 6 (25): 20921–32. https://doi.org/10.18632/oncotarget.4879.

Berntsen, Jørgen, Jens Rimestad, Jacob Theilgaard Lassen, Dang Tran, and Mikkel Fly Kragh. 2022. 'Robust and Generalizable Embryo Selection Based on Artificial Intelligence and Time-Lapse Image Sequences'. PLoS ONE 17 (2): e0262661. https://doi.org/10.1371/journal.pone.0262661.

Bolton, Helen, Sarah J. L. Graham, Niels Van der Aa, Parveen Kumar, Koen Theunis, Elia Fernandez Gallardo, Thierry Voet, and Magdalena Zernicka-Goetz. 2016. 'Mouse Model of Chromosome Mosaicism Reveals Lineage-Specific Depletion of Aneuploid Cells and Normal Developmental Potential'. Nature Communications 7 (March): 11165. https://doi.org/10.1038/ncomms11165.

Bouniol, C., E. Nguyen, and P. Debey. 1995. 'Endogenous Transcription Occurs at the 1-Cell Stage in the Mouse Embryo'. Experimental Cell Research 218 (1): 57–62. https://doi.org/10.1006/excr.1995.1130.

Brandeis, M., I. Rosewell, M. Carrington, T. Crompton, M. A. Jacobs, J. Kirk, J. Gannon, and T. Hunt. 1998. 'Cyclin B2-Null Mice Develop Normally and Are Fertile Whereas Cyclin B1-Null Mice Die in Utero'. Proceedings of the National Academy of Sciences of the United States of America 95 (8): 4344–49. https://doi.org/10.1073/pnas.95.8.4344.

Brooker, Amanda S., and Karen M. Berkowitz. 2014. 'The Roles of Cohesins in Mitosis, Meiosis, and Human Health and Disease'. Methods in Molecular Biology (Clifton, N.J.) 1170: 229–66. https://doi.org/10.1007/978-1-4939-0888-2_11.

Campbell, Alison, Simon Fishel, Natalie Bowman, Samantha Duffy, Mark Sedler, and Cristina Fontes Lindemann Hickman. 2013. 'Modelling a Risk Classification of Aneuploidy in Human Embryos Using Non-Invasive Morphokinetics'. Reproductive BioMedicine Online 26 (5): 477–85. https://doi.org/10.1016/j.rbmo.2013.02.006.

Castro, Ines J de, Raquel Sales Gil, Lorena Ligammari, Maria Laura Di Giacinto, and Paola Vagnarelli. 2017. 'CDK1 and PLK1 Coordinate the Disassembly and Reassembly of the Nuclear Envelope in Vertebrate Mitosis'. Oncotarget 9 (8): 7763–73. https://doi.org/10.18632/oncotarget.23666.

Chan, Chii Jou, Maria Costanzo, Teresa Ruiz-Herrero, Gregor Mönke, Ryan J. Petrie, Martin Bergert, Alba Diz-Muñoz, L. Mahadevan, and Takashi Hiiragi. 2019. 'Hydraulic Control of Mammalian Embryo Size and Cell Fate'. Nature 571 (7763): 112–16. https://doi.org/10.1038/s41586-019-1309-x.

Chang, Donald C., Naihan Xu, and Kathy Q. Luo. 2003. 'Degradation of Cyclin B Is Required for the Onset of Anaphase in Mammalian Cells *'. Journal of Biological Chemistry 278 (39): 37865–73. https://doi.org/10.1074/jbc.M306376200.

Chavez, Shawn L., Kevin E. Loewke, Jinnuo Han, Farshid Moussavi, Pere Colls, Santiago Munne, Barry Behr, and Renee A. Reijo Pera, dirs. 2012. Dynamic Blastomere Behaviour Reflects Human Embryo Ploidy by the Four-Cell Stage. Vol. 3. England. https://doi.org/10.1038/ncomms2249.

Chunduri, Narendra Kumar, and Zuzana Storchová. 2019. 'The Diverse Consequences of Aneuploidy'. Nature Cell Biology 21 (1): 54–62. https://doi.org/10.1038/s41556-018-0243-8.

Ciemerych, Maria A., and Peter Sicinski. 2005. 'Cell Cycle in Mouse Development'. Oncogene 24 (17): 2877–98. https://doi.org/10.1038/sj.onc.1208608.

Cimini, D., B. Howell, P. Maddox, A. Khodjakov, F. Degrassi, and E. D. Salmon. 2001. 'Merotelic Kinetochore Orientation Is a Major Mechanism of Aneuploidy in Mitotic Mammalian Tissue Cells'. The Journal of Cell Biology 153 (3): 517–27. https://doi.org/10.1083/jcb.153.3.517.

Cimini, Daniela, Lisa A. Cameron, and E. D. Salmon. 2004. 'Anaphase Spindle Mechanics Prevent Mis-Segregation of Merotelically Oriented Chromosomes'. Current Biology: CB 14 (23): 2149–55. https://doi.org/10.1016/j.cub.2004.11.029.

Cimini, Daniela. 2008. 'Merotelic Kinetochore Orientation, Aneuploidy, and Cancer'. Biochimica Et Biophysica Acta 1786 (1): 32–40. https://doi.org/10.1016/j.bbcan.2008.05.003.

Clarke, Duncan J., Marisa Segal, Sanne Jensen, and Steven I. Reed. 2001. 'Mec1p Regulates Pds1p Levels in S Phase: Complex Coordination of DNA Replication and Mitosis'. Nature Cell Biology 3 (7): 619–27. https://doi.org/10.1038/35083009.

Clift, Dean, William A. McEwan, Larisa I. Labzin, Vera Konieczny, Binyam Mogessie, Leo C. James, and Melina Schuh. 2017. 'A Method for the Acute and Rapid Degradation of Endogenous Proteins'. Cell 171 (7): 1692-1706.e18. https://doi.org/10.1016/j.cell.2017.10.033.

Clute, Paul, and Jonathon Pines. 1999. 'Temporal and Spatial Control of Cyclin B1 Destruction in Metaphase'. Nature Cell Biology 1 (2): 82–87. https://doi.org/10.1038/10049.

Collin, Philippe, Oxana Nashchekina, Rachael Walker, and Jonathon Pines. 2013. 'The Spindle Assembly Checkpoint Works like a Rheostat Not a Toggle-Switch'. Nature Cell Biology 15 (11): 10.1038/ncb2855. https://doi.org/10.1038/ncb2855.

Compton, Duane A. 2011. 'Mechanisms of Aneuploidy'. Current Opinion in Cell Biology 23 (1): 109–13. https://doi.org/10.1016/j.ceb.2010.08.007.

Copp, A. J. 1978. 'Interaction between Inner Cell Mass and Trophectoderm of the Mouse Blastocyst. I. A Study of Cellular Proliferation.' Journal of Embryology and Experimental Morphology 48 (December): 109–25.

Courtois, Aurélien, Melina Schuh, Jan Ellenberg, and Takashi Hiiragi. 2012. 'The Transition from Meiotic to Mitotic Spindle Assembly Is Gradual during Early Mammalian Development'. The Journal of Cell Biology 198 (3): 357–70. https://doi.org/10.1083/jcb.201202135.

Crasta, Karen, Neil J. Ganem, Regina Dagher, Alexandra B. Lantermann, Elena V. Ivanova, Yunfeng Pan, Luigi Nezi, Alexei Protopopov, Dipanjan Chowdhury, and David Pellman. 2012. 'DNA Breaks and Chromosome Pulverization from Errors in Mitosis'. Nature 482 (7383): 53–58. https://doi.org/10.1038/nature10802.

Craven, Lyndsey, Helen A. Tuppen, Gareth D. Greggains, Stephen J. Harbottle, Julie L. Murphy, Lynsey M. Cree, Alison P. Murdoch, et al. 2010. 'Pronuclear Transfer in Human Embryos to Prevent Transmission of Mitochondrial DNA Disease'. Nature 465 (7294): 82–85. https://doi.org/10.1038/nature08958.

Cundell, Michael J., Ricardo Nunes Bastos, Tongli Zhang, James Holder, Ulrike Gruneberg, Bela Novak, and Francis A. Barr. 2013. 'The BEG (PP2A-B55/ENSA/Greatwall) Pathway Ensures Cytokinesis Follows Chromosome Separation'. Molecular Cell 52 (3): 393–405. https://doi.org/10.1016/j.molcel.2013.09.005.

Currie, Cerys E., Emma Ford, Lucy Benham Whyte, Deborah M. Taylor, Bettina P. Mihalas, Muriel Erent, Adele L. Marston, Geraldine M. Hartshorne, and Andrew D. McAinsh. 2022. 'The First Mitotic Division of Human Embryos Is Highly Error Prone'. Nature Communications 13 (1): 6755. https://doi.org/10.1038/s41467-022-34294-6.

Dalton, W. Brian, and Vincent W. Yang. 2009. 'THE ROLE OF PROLONGED MITOTIC CHECKPOINT ACTIVATION IN THE FORMATION AND TREATMENT OF CANCER'. Future Oncology (London, England) 5 (9): 1363–70. https://doi.org/10.2217/fon.09.118.

Del Carmen Nogales, Maria, Fernando Bronet, Natalia Basile, Eva María Martínez, Alberto Liñán, Lorena Rodrigo, and Marcos Meseguer. 2017. 'Type of Chromosome Abnormality Affects Embryo Morphology Dynamics'. Fertility and Sterility 107 (1): 229-235.e2. https://doi.org/10.1016/j.fertnstert.2016.09.019.

Dick, Amalie E., and Daniel W. Gerlich. 2013. 'Kinetic Framework of Spindle Assembly Checkpoint Signaling'. Nature Cell Biology 15 (11): 1370–77. https://doi.org/10.1038/ncb2842.

Donnelly, Neysan, Verena Passerini, Milena Dürrbaum, Silvia Stingele, and Zuzana Storchová. 2014. 'HSF1 Deficiency and Impaired HSP90-Dependent Protein Folding Are Hallmarks of Aneuploid Human Cells'. The EMBO Journal 33 (20): 2374–87. https://doi.org/10.15252/embj.201488648.

Enserink, Jorrit M., and Richard D. Kolodner. 2010. 'An Overview of CDK1-Controlled Targets and Processes'. Cell Division 5 (1): 11. https://doi.org/10.1186/1747-1028-5-11.

Ershov, Dmitry, Minh-Son Phan, Joanna W. Pylvänäinen, Stéphane U. Rigaud, Laure Le Blanc, Arthur Charles-Orszag, James R. W. Conway, et al. 2022. 'TrackMate 7: Integrating State-of-the-Art Segmentation Algorithms into Tracking Pipelines'. Nature Methods 19 (7): 829–32. https://doi.org/10.1038/s41592-022-01507-1.

Evans, Tom, Eric T. Rosenthal, Jim Youngblom, Dan Distel, and Tim Hunt. 1983. 'Cyclin: A Protein Specified by Maternal MRNA in Sea Urchin Eggs That Is Destroyed at Each Cleavage Division'. Cell 33 (2): 389–96. https://doi.org/10.1016/0092-8674(83)90420-8.

Fededa, Juan Pablo, and Daniel W. Gerlich. 2012. 'Molecular Control of Animal Cell Cytokinesis'. Nature Cell Biology 14 (5): 440–47. https://doi.org/10.1038/ncb2482.

FitzHarris, Greg, John Carroll, and Karl Swann. 2018. 'Chapter 19 - Electrical-Assisted Microinjection for Analysis of Fertilization and Cell Division in Mammalian Oocytes and Early Embryos'. In Mitosis and Meiosis Part A, edited by Helder Maiato and Melina Schuh, 144:431–40. Methods in Cell Biology. Academic Press. https://doi.org/10.1016/bs.mcb.2018.03.036.

Fleming, T. P., P. D. Warren, J. C. Chisholm, and M. H. Johnson. 1984. 'Trophectodermal Processes Regulate the Expression of Totipotency within the Inner Cell Mass of the Mouse Expanding Blastocyst'. Journal of Embryology and Experimental Morphology 84 (December): 63–90.

Frouin, Isabelle, Magali Toueille, Elena Ferrari, Igor Shevelev, and Ulrich Hübscher. 2005. 'Phosphorylation of Human DNA Polymerase λ by the Cyclin-Dependent Kinase Cdk2/Cyclin A Complex Is Modulated by Its Association with Proliferating Cell Nuclear Antigen'. Nucleic Acids Research 33 (16): 5354–61. https://doi.org/10.1093/nar/gki845.

Ganem, Neil J., Hauke Cornils, Shang-Yi Chiu, Kevin P. O'Rourke, Jonathan Arnaud, Dean Yimlamai, Manuel Théry, Fernando D. Camargo, and David Pellman. 2014. 'Cytokinesis Failure

Triggers Hippo Tumor Suppressor Pathway Activation'. Cell 158 (4): 833–48. https://doi.org/10.1016/j.cell.2014.06.029.

Gao, Yuan, Benyuan Zhang, Yuming Wang, and Guanning Shang. 2018. 'Cdc20 Inhibitor Apcin Inhibits the Growth and Invasion of Osteosarcoma Cells'. Oncology Reports 40 (2): 841–48. https://doi.org/10.3892/or.2018.6467.

Gautier, Jean, Jeremy Minshull, Manfred Lohka, Michael Glotzer, Tim Hunt, and James L. Maller. 1990. 'Cyclin Is a Component of Maturation-Promoting Factor from Xenopus'. Cell 60 (3): 487–94. https://doi.org/10.1016/0092-8674(90)90599-A.

Gavet, Olivier, and Jonathon Pines. 2010. 'Progressive Activation of CyclinB1-CDK1 Coordinates Entry to Mitosis'. Developmental Cell 18 (4): 533–43. https://doi.org/10.1016/j.devcel.2010.02.013.

Georgadaki, Katerina, Nikolas Khoury, Demetrios A. Spandidos, and Vasilis Zoumpourlis. 2016. 'The Molecular Basis of Fertilization (Review)'. International Journal of Molecular Medicine 38 (4): 979–86. https://doi.org/10.3892/ijmm.2016.2723.

Gershony, Ofir, Tal Pe'er, Meirav Noach-Hirsh, Natalie Elia, and Amit Tzur. 2014. 'Cytokinetic Abscission Is an Acute G1 Event'. Cell Cycle 13 (21): 3436–41. https://doi.org/10.4161/15384101.2014.956486.

Girard, F., U. Strausfeld, A. Fernandez, and N. J. Lamb. 1991. 'Cyclin A Is Required for the Onset of DNA Replication in Mammalian Fibroblasts'. Cell 67 (6): 1169–79. https://doi.org/10.1016/0092-8674(91)90293-8.

Gomes, Ana Margarida, Bernardo Orr, Marco Novais-Cruz, Filipe De Sousa, Joana Macário-Monteiro, Carolina Lemos, Cristina Ferrás, and Helder Maiato. 2022. 'Micronuclei from Misaligned Chromosomes That Satisfy the Spindle Assembly Checkpoint in Cancer Cells'. Current Biology 32 (19): 4240-4254.e5. https://doi.org/10.1016/j.cub.2022.08.026.

Greco, Ermanno, Maria Giulia Minasi, and Francesco Fiorentino. 2015. 'Healthy Babies after Intrauterine Transfer of Mosaic Aneuploid Blastocysts'. New England Journal of Medicine 373 (21): 2089–90. https://doi.org/10.1056/NEJMc1500421.

Green, Rebecca A., Ewa Paluch, and Karen Oegema. 2012. 'Cytokinesis in Animal Cells'. Annual Review of Cell and Developmental Biology 28: 29–58. https://doi.org/10.1146/annurev-cellbio-101011-155718.

Hagting, Anja, Nicole Den Elzen, Hartmut C. Vodermaier, Irene C. Waizenegger, Jan-Michael Peters, and Jonathon Pines. 2002. 'Human Securin Proteolysis Is Controlled by the Spindle Checkpoint and Reveals When the APC/C Switches from Activation by Cdc20 to Cdh1'. The Journal of Cell Biology 157 (7): 1125–37. https://doi.org/10.1083/jcb.200111001.

Haigis, Kevin M., and Alejandro Sweet-Cordero. 2011. 'New Insights into Oncogenic Stress'. Nature Genetics 43 (3): 177–78. https://doi.org/10.1038/ng0311-177.

Hassold, T., and P. Hunt. 2001. 'To Err (Meiotically) Is Human: The Genesis of Human Aneuploidy'. Nature Reviews. Genetics 2 (4): 280–91. https://doi.org/10.1038/35066065.

Hauf, Silke, Richard W. Cole, Sabrina LaTerra, Christine Zimmer, Gisela Schnapp, Rainer Walter, Armin Heckel, Jacques van Meel, Conly L. Rieder, and Jan-Michael Peters. 2003. 'The Small Molecule Hesperadin Reveals a Role for Aurora B in Correcting Kinetochore-Microtubule Attachment and in Maintaining the Spindle Assembly Checkpoint'. The Journal of Cell Biology 161 (2): 281–94. https://doi.org/10.1083/jcb.200208092.

Heim, Andreas, Anja Konietzny, and Thomas U. Mayer. 2015. 'Protein Phosphatase 1 Is Essential for Greatwall Inactivation at Mitotic Exit'. EMBO Reports 16 (11): 1501–10. https://doi.org/10.15252/embr.201540876.

Hook, ErnestB. 1981. 'PREVALENCE OF CHROMOSOME ABNORMALITIES DURING HUMAN GESTATION AND IMPLICATIONS FOR STUDIES OF ENVIRONMENTAL MUTAGENS'. The Lancet, Originally published as Volume 2, Issue 8239, 318 (8239): 169–72. https://doi.org/10.1016/S0140-6736(81)90356-1.

Howe, Katie, and Greg FitzHarris. 2013. 'A Non-Canonical Mode of Microtubule Organization Operates throughout Pre-Implantation Development in Mouse'. Cell Cycle 12 (10): 1616–24. https://doi.org/10.4161/cc.24755.

Izawa, Daisuke, and Jonathon Pines. 2011. 'How APC/C-CDC20 Changes Its Substrate Specificity in Mitosis'. Nature Cell Biology 13 (3): 223–33. https://doi.org/10.1038/ncb2165.

Jackman, M., M. Firth, and J. Pines. 1995. 'Human Cyclins B1 and B2 Are Localized to Strikingly Different Structures: B1 to Microtubules, B2 Primarily to the Golgi Apparatus.' The EMBO Journal 14 (8): 1646–54. https://doi.org/10.1002/j.1460-2075.1995.tb07153.x.

Jacobs, K., H. Van de Velde, C. De Paepe, K. Sermon, and C. Spits. 2017. 'Mitotic Spindle Disruption in Human Preimplantation Embryos Activates the Spindle Assembly Checkpoint but Not Apoptosis until Day 5 of Development'. Molecular Human Reproduction 23 (5): 321–29. https://doi.org/10.1093/molehr/gax007.

Johnson, M. H., and C. A. Ziomek. 1981. 'The Foundation of Two Distinct Cell Lineages within the Mouse Morula'. Cell 24 (1): 71–80. https://doi.org/10.1016/0092-8674(81)90502-x.

Jones, Keith T. 2010. 'Cohesin and CDK1: An Anaphase Barricade'. Nature Cell Biology 12 (2): 106–8. https://doi.org/10.1038/ncb0210-106.

Kabeche, Lilian, and Duane A. Compton. 2013. 'Cyclin A Regulates Kinetochore Microtubules to Promote Faithful Chromosome Segregation'. Nature 502 (7469): 110–13. https://doi.org/10.1038/nature12507.

Kabeche, Lilian, Hai Dang Nguyen, Rémi Buisson, and Lee Zou. 2018. 'A Mitosis-Specific and R Loop-Driven ATR Pathway Promotes Faithful Chromosome Segregation'. Science (New York, N.Y.) 359 (6371): 108–14. https://doi.org/10.1126/science.aan6490.

Kallio, Marko J., Mark L. McCleland, P. Todd Stukenberg, and Gary J. Gorbsky. 2002. 'Inhibition of Aurora B Kinase Blocks Chromosome Segregation, Overrides the Spindle Checkpoint, and

Perturbs Microtubule Dynamics in Mitosis'. Current Biology: CB 12 (11): 900–905. https://doi.org/10.1016/s0960-9822(02)00887-4.

Kamenz, Julia, Tamara Mihaljev, Armin Kubis, Stefan Legewie, and Silke Hauf. 2015. 'Robust Ordering of Anaphase Events by Adaptive Thresholds and Competing Degradation Pathways'. Molecular Cell 60 (3): 446–59. https://doi.org/10.1016/j.molcel.2015.09.022.

Karasu, Mehmet E., Nora Bouftas, Scott Keeney, and Katja Wassmann. 2019. 'Cyclin B3 Promotes Anaphase I Onset in Oocyte Meiosis'. The Journal of Cell Biology 218 (4): 1265–81. https://doi.org/10.1083/jcb.201808091.

Katsuno, Yuko, Ayumi Suzuki, Kazuto Sugimura, Katsuzumi Okumura, Doaa H. Zineldeen, Midori Shimada, Hiroyuki Niida, Takeshi Mizuno, Fumio Hanaoka, and Makoto Nakanishi. 2009. 'Cyclin A-Cdk1 Regulates the Origin Firing Program in Mammalian Cells'. Proceedings of the National Academy of Sciences of the United States of America 106 (9): 3184–89. https://doi.org/10.1073/pnas.0809350106.

Keshri, Riya, Ashwathi Rajeevan, and Sachin Kotak. 2020. 'PP2A--B55γ Counteracts Cdk1 and Regulates Proper Spindle Orientation through the Cortical Dynein Adaptor NuMA'. Journal of Cell Science 133 (14): jcs243857. https://doi.org/10.1242/jcs.243857.

Kimura, K., M. Hirano, R. Kobayashi, and T. Hirano. 1998. 'Phosphorylation and Activation of 13S Condensin by CDC2 in Vitro'. Science (New York, N.Y.) 282 (5388): 487–90. https://doi.org/10.1126/science.282.5388.487.

Korotkevich, Ekaterina, Ritsuya Niwayama, Aurélien Courtois, Stefanie Friese, Nicolas Berger, Frank Buchholz, and Takashi Hiiragi. 2017. 'The Apical Domain Is Required and Sufficient for the First Lineage Segregation in the Mouse Embryo'. Developmental Cell 40 (3): 235-247.e7. https://doi.org/10.1016/j.devcel.2017.01.006.

Kubiak, Jacek Z., Franck Chesnel, Laurent Richard-Parpaillon, Franck Bazile, Aude Pascal, Zbigniew Polanski, Marta Sikora-Polaczek, Zuzanna Maciejewska, and Maria A. Ciemerych. 2008. 'Temporal Regulation of the First Mitosis in Xenopus and Mouse Embryos'. Molecular and Cellular Endocrinology 282 (1–2): 63–69. https://doi.org/10.1016/j.mce.2007.11.023.

Kuhn, Jonathan, and Sophie Dumont. 2017. 'Spindle Assembly Checkpoint Satisfaction Occurs via End-on but Not Lateral Attachments under Tension'. Journal of Cell Biology 216 (6): 1533–42. https://doi.org/10.1083/jcb.201611104.

Kwon, Mijung, Mitchell L. Leibowitz, and Jae-Ho Lee. 2020. 'Small but Mighty: The Causes and Consequences of Micronucleus Rupture'. Experimental & Molecular Medicine 52 (11): 1777–86. https://doi.org/10.1038/s12276-020-00529-z.

Lambrus, Bramwell G., and Andrew J. Holland. 2017. 'A New Mode of Mitotic Surveillance'.

Lampson, Michael A., and Ekaterina L. Grishchuk. 2017. 'Mechanisms to Avoid and Correct Erroneous Kinetochore-Microtubule Attachments'. Biology 6 (1): 1. https://doi.org/10.3390/biology6010001.

Lara-Gonzalez, Pablo, Jonathon Pines, and Arshad Desai. 2021. 'Spindle Assembly Checkpoint Activation and Silencing at Kinetochores'. Seminars in Cell & Developmental Biology 117 (September): 86–98. https://doi.org/10.1016/j.semcdb.2021.06.009.

Lee, Miler T., Ashley R. Bonneau, and Antonio J. Giraldez. 2014. 'Zygotic Genome Activation during the Maternal-to-Zygotic Transition'. Annual Review of Cell and Developmental Biology 30: 581–613. https://doi.org/10.1146/annurev-cellbio-100913-013027.

Li, Min, and Pumin Zhang. 2009. 'The Function of APC/CCdh1 in Cell Cycle and Beyond'. Cell Division 4 (1): 1–7. https://doi.org/10.1186/1747-1028-4-2.

Li, Min, Xiao Fang, Darren J. Baker, Linjie Guo, Xue Gao, Zhubo Wei, Shuhua Han, Jan M. van Deursen, and Pumin Zhang. 2010. 'The ATM–P53 Pathway Suppresses Aneuploidy- Induced

Tumorigenesis'. Proceedings of the National Academy of Sciences 107 (32): 14188–93. https://doi.org/10.1073/pnas.1005960107.

Li, Rong, and Jin Zhu. 2022. 'Effects of Aneuploidy on Cell Behaviour and Function'. Nature Reviews Molecular Cell Biology 23 (4): 250–65. https://doi.org/10.1038/s41580-021-00436-9.

Lin, Pin-Yao, Chun-I Lee, En-Hui Cheng, Chun-Chia Huang, Tsung-Hsien Lee, Hui-Hsin Shih, Yi-Ping Pai, Yi-Chun Chen, and Maw-Sheng Lee. 2020. 'Clinical Outcomes of Single Mosaic Embryo Transfer: High-Level or Low-Level Mosaic Embryo, Does It Matter?' Journal of Clinical Medicine 9 (6): 1695. https://doi.org/10.3390/jcm9061695.

Lindqvist, Arne, Helena Källström, Andreas Lundgren, Emad Barsoum, and Christina Karlsson Rosenthal. 2005. 'Cdc25B Cooperates with Cdc25A to Induce Mitosis but Has a Unique Role in Activating Cyclin B1-Cdk1 at the Centrosome.' The Journal of Cell Biology 171 (1): 35–45. https://doi.org/10.1083/jcb.200503066.

Liu, D., M. M. Matzuk, W. K. Sung, Q. Guo, P. Wang, and D. J. Wolgemuth. 1998. 'Cyclin A1 Is Required for Meiosis in the Male Mouse'. Nature Genetics 20 (4): 377–80. https://doi.org/10.1038/3855.

Lorca, T., and A. Castro. 2013. 'The Greatwall Kinase: A New Pathway in the Control of the Cell Cycle'. Oncogene 32 (5): 537–43. https://doi.org/10.1038/onc.2012.79.

Macaulay, Angus D., Adélaïde Allais, and Greg FitzHarris. 2020. 'Chromosome Dynamics and Spindle Microtubule Establishment in Mouse Embryos'. The FASEB Journal 34 (6): 8057–67. https://doi.org/10.1096/fj.201902947R.

Maciejewska, Zuzanna, Zbigniew Polanski, Katarzyna Kisiel, Jacek Z. Kubiak, and Maria A. Ciemerych. 2009. 'Spindle Assembly Checkpoint-Related Failure Perturbs Early Embryonic Divisions and Reduces Reproductive Performance of LT/Sv Mice'. REPRODUCTION 137 (6): 931–42. https://doi.org/10.1530/REP-09-0011.

Maciejowski, John, Yilong Li, Nazario Bosco, Peter J. Campbell, and Titia de Lange. 2015. 'Chromothripsis and Kataegis Induced by Telomere Crisis.' Cell 163 (7): 1641–54. https://doi.org/10.1016/j.cell.2015.11.054.

MacQueen, H. A., and M. H. Johnson. 1983. 'The Fifth Cell Cycle of the Mouse Embryo Is Longer for Smaller Cells than for Larger Cells'. Journal of Embryology and Experimental Morphology 77 (October): 297–308.

Madgwick, Suzanne, David V. Hansen, Mark Levasseur, Peter K. Jackson, and Keith T. Jones. 2006. 'Mouse Emi2 Is Required to Enter Meiosis II by Reestablishing Cyclin B1 during Interkinesis'. Journal of Cell Biology 174 (6): 791–801. https://doi.org/10.1083/jcb.200604140.

Masui, Y., and C. L. Markert. 1971. 'Cytoplasmic Control of Nuclear Behavior during Meiotic Maturation of Frog Oocytes'. The Journal of Experimental Zoology 177 (2): 129–45. https://doi.org/10.1002/jez.1401770202.

Meena, Jitendra K, Aurora Cerutti, Christine Beichler, Yohei Morita, Christopher Bruhn, Mukesh Kumar, Johann M Kraus, et al. 2015. 'Telomerase Abrogates Aneuploidy- Induced Telomere Replication Stress, Senescence and Cell Depletion'. The EMBO Journal 34 (10): 1371–84. https://doi.org/10.15252/embj.201490070.

Merrick, Karl A., Stéphane Larochelle, Chao Zhang, Jasmina J. Allen, Kevan M. Shokat, and Robert P. Fisher. 2008. 'Distinct Activation Pathways Confer Cyclin Binding Specificity on Cdk1 and Cdk2 in Human Cells'. Molecular Cell 32 (5): 662–72. https://doi.org/10.1016/j.molcel.2008.10.022.

Milewski, Robert, and Anna Ajduk. 2017. 'Time-Lapse Imaging of Cleavage Divisions in Embryo Quality Assessment'. Reproduction 154 (2): R37–53. https://doi.org/10.1530/REP-17-0004.

Mitchison, T., L. Evans, E. Schulze, and M. Kirschner. 1986. 'Sites of Microtubule Assembly and Disassembly in the Mitotic Spindle'. Cell 45 (4): 515–27. https://doi.org/10.1016/0092-8674(86)90283-7.

Mitra, Jayashree, and Greg H Enders. 2004. 'Cyclin A/Cdk2 Complexes Regulate Activation of Cdk1 and Cdc25 Phosphatases in Human Cells'. Oncogene 23 (19): 3361–67. https://doi.org/10.1038/sj.onc.1207446.

Molinari, M., C. Mercurio, J. Dominguez, F. Goubin, and G. F. Draetta. 2000. 'Human Cdc25 A Inactivation in Response to S Phase Inhibition and Its Role in Preventing Premature Mitosis'. EMBO Reports 1 (1): 71–79. https://doi.org/10.1093/embo-reports/kvd018.

Moura, Margarida, and Carlos Conde. 2019. 'Phosphatases in Mitosis: Roles and Regulation'. Biomolecules 9 (2): 55. https://doi.org/10.3390/biom9020055.

Murphy, M., M. G. Stinnakre, C. Senamaud-Beaufort, N. J. Winston, C. Sweeney, M. Kubelka, M. Carrington, C. Bréchot, and J. Sobczak-Thépot. 1997. 'Delayed Early Embryonic Lethality Following Disruption of the Murine Cyclin A2 Gene'. Nature Genetics 15 (1): 83–86. https://doi.org/10.1038/ng0197-83.

Nasa, Isha, and Arminja N. Kettenbach. 2018. 'Coordination of Protein Kinase and Phosphoprotein Phosphatase Activities in Mitosis'. Frontiers in Cell and Developmental Biology 6 (March): 30. https://doi.org/10.3389/fcell.2018.00030.

Nguyen, Thomas B., Katia Manova, Paola Capodieci, Catherine Lindon, Steve Bottega, Xiang-Yuan Wang, Jale Refik-Rogers, Jonathon Pines, Debra J. Wolgemuth, and Andrew Koff. 2002. 'Characterization and Expression of Mammalian Cyclin B3, a Prepachytene Meiotic Cyclin *'. Journal of Biological Chemistry 277 (44): 41960–69. https://doi.org/10.1074/jbc.M203951200.

Nicklas, R. B. 1997. 'How Cells Get the Right Chromosomes'. Science (New York, N.Y.) 275 (5300): 632–37. https://doi.org/10.1126/science.275.5300.632.

Nurse, Paul. 1975. 'Genetic Control of Cell Size at Cell Division in Yeast'. Nature 256 (5518): 547–51. https://doi.org/10.1038/256547a0.

O'Farrell, Patrick H. 2001. 'Triggering the All-or-Nothing Switch into Mitosis'. Trends in Cell Biology 11 (12): 512–19.

O'Farrell, Patrick H., Jason Stumpff, and Tin Tin Su. 2004. 'Embryonic Cleavage Cycles: How Is a Mouse like a Fly?' Current Biology: CB 14 (1): R35-45. https://doi.org/10.1016/j.cub.2003.12.022.

Ohashi, Akihiro, Momoko Ohori, Kenichi Iwai, Yusuke Nakayama, Tadahiro Nambu, Daisuke Morishita, Tomohiro Kawamoto, et al. 2015. 'Aneuploidy Generates Proteotoxic Stress and DNA Damage Concurrently with P53-Mediated Post-Mitotic Apoptosis in SAC-Impaired Cells'. Nature Communications 6 (1): 7668. https://doi.org/10.1038/ncomms8668.

Pagano, M., R. Pepperkok, F. Verde, W. Ansorge, and G. Draetta. 1992. 'Cyclin A Is Required at Two Points in the Human Cell Cycle'. The EMBO Journal 11 (3): 961–71. https://doi.org/10.1002/j.1460-2075.1992.tb05135.x.

Paim, Lia Mara Gomes, and Greg FitzHarris. 2019. 'Tetraploidy Causes Chromosomal Instability in Acentriolar Mouse Embryos'. Nature Communications 10 (1): 4834. https://doi.org/10.1038/s41467-019-12772-8.

Parry, Devin H., Gilles R. X. Hickson, and Patrick H. O'Farrell. 2003. 'Cyclin B Destruction Triggers Changes in Kinetochore Behavior Essential for Successful Anaphase'. Current Biology: CB 13 (8): 647–53. https://doi.org/10.1016/s0960-9822(03)00242-2.

Passerini, Verena, Efrat Ozeri-Galai, Mirjam S. de Pagter, Neysan Donnelly, Sarah Schmalbrock, Wigard P. Kloosterman, Batsheva Kerem, and Zuzana Storchová. 2016. 'The Presence of Extra Chromosomes Leads to Genomic Instability'. Nature Communications 7 (February): 10754. https://doi.org/10.1038/ncomms10754.

Patel, Deven V., Preeti B. Shah, Aditi P. Kotdawala, Javier Herrero, Irene Rubio, and Manish R. Banker. 2016. 'Morphokinetic Behavior of Euploid and Aneuploid Embryos Analyzed by Time-Lapse in Embryoscope'. Journal of Human Reproductive Sciences 9 (2): 112–18. https://doi.org/10.4103/0974-1208.183511.

Petersen, B. O., J. Lukas, C. S. Sørensen, J. Bartek, and K. Helin. 1999. 'Phosphorylation of Mammalian CDC6 by Cyclin A/CDK2 Regulates Its Subcellular Localization'. The EMBO Journal 18 (2): 396–410. https://doi.org/10.1093/emboj/18.2.396.

Pfister, Katherine, Justyna L. Pipka, Colby Chiang, Yunxian Liu, Royden A. Clark, Ray Keller, Paul Skoglund, Michael J. Guertin, Ira M. Hall, and P. Todd Stukenberg. 2018. 'Identification of Drivers of Aneuploidy in Breast Tumors.' Cell Reports 23 (9): 2758–69. https://doi.org/10.1016/j.celrep.2018.04.102.

Pines, Jonathon. 2006. 'Mitosis: A Matter of Getting Rid of the Right Protein at the Right Time'. Trends in Cell Biology 16 (1): 55–63. https://doi.org/10.1016/j.tcb.2005.11.006.

Potapova, Tamara A, John R Daum, Bradley D Pittman, Joanna R Hudson, Tara N Jones, David L Satinover, P Todd Stukenberg, and Gary J Gorbsky. 2006. 'The Reversibility of Mitotic Exit in Vertebrate Cells'. Nature 440 (7086): 954–58. https://doi.org/10.1038/nature04652.

Rappaport, R. 1996. Cytokinesis in Animal Cells. Developmental and Cell Biology Series. Cambridge: Cambridge University Press. https://doi.org/10.1017/CBO9780511529764.

Reignier, Arnaud, Jenna Lammers, Paul Barriere, and Thomas Freour. 2018. 'Can Time-Lapse Parameters Predict Embryo Ploidy? A Systematic Review'. Reproductive Biomedicine Online 36 (4): 380–87. https://doi.org/10.1016/j.rbmo.2018.01.001.

Rieder, C. L., A. Schultz, R. Cole, and G. Sluder. 1994. 'Anaphase Onset in Vertebrate Somatic Cells Is Controlled by a Checkpoint That Monitors Sister Kinetochore Attachment to the Spindle'. The Journal of Cell Biology 127 (5): 1301–10. https://doi.org/10.1083/jcb.127.5.1301.

Santaguida, Stefano, and Angelika Amon. 2015. 'Short- and Long-Term Effects of Chromosome Mis-Segregation and Aneuploidy'. Nature Reviews. Molecular Cell Biology 16 (8): 473–85. https://doi.org/10.1038/nrm4025.

Sarafan-Vasseur, Nasrin, Aude Lamy, Jeannette Bourguignon, Florence Le Pessot, Philip Hieter, Richard Sesboüé, Christian Bastard, Thierry Frébourg, and Jean-Michel Flaman. 2002.

‘Overexpression of B-Type Cyclins Alters Chromosomal Segregation’. Oncogene 21 (13): 2051–57. https://doi.org/10.1038/sj.onc.1205257.

Segal, David J., and Ernest E. McCoy. 1974. ‘Studies on Down’s Syndrome in Tissue Culture. I. Growth Rates Protein Contents of Fibroblast Cultures’. Journal of Cellular Physiology 83(1): 85–90. https://doi.org/10.1002/jcp.1040830112.

Shi, Qinghua, and Randall W. King. 2005. ‘Chromosome Nondisjunction Yields Tetraploid Rather than Aneuploid Cells in Human Cell Lines’. Nature 437 (7061): 1038–42. https://doi.org/10.1038/nature03958.

Shoji, Shisako, Naoko Yoshida, Manami Amanai, Maki Ohgishi, Tomoyuki Fukui, Satoko Fujimoto, Yoshikazu Nakano, Eriko Kajikawa, and Anthony C. F. Perry. 2006. ‘Mammalian Emi2 Mediates Cytostatic Arrest and Transduces the Signal for Meiotic Exit via CDC20’. The EMBO Journal 25 (4): 834. https://doi.org/10.1038/sj.emboj.7600953.

Sikora-Polaczek, Marta, Anna Hupalowska, Zbigniew Polanski, Jacek Z. Kubiak, and Maria A. Ciemerych. 2006a. ‘The First Mitosis of the Mouse Embryo Is Prolonged by Transitional Metaphase Arrest1’. Biology of Reproduction 74 (4): 734–43. https://doi.org/10.1095/biolreprod.105.047092. ———. 2006b. ‘The First Mitosis of the Mouse Embryo Is Prolonged by Transitional Metaphase Arrest1’. Biology of Reproduction 74 (4): 734–43. https://doi.org/10.1095/biolreprod.105.047092.

Silkworth, William T., Isaac K. Nardi, Lindsey M. Scholl, and Daniela Cimini. 2009. ‘Multipolar Spindle Pole Coalescence Is a Major Source of Kinetochore Mis-Attachment and Chromosome Mis-Segregation in Cancer Cells’. PLoS ONE 4 (8): e6564. https://doi.org/10.1371/journal.pone.0006564.

Smith, R K, and M H Johnson. 1986. ‘Analysis of the Third and Fourth Cell Cycles of Mouse Early Development’. Journal of Reproduction and Fertility 76 (1): 393–99. https://doi.org/10.1530/jrf.0.0760393.

Strauss, Bernhard, Andrew Harrison, Paula Almeida Coelho, Keiko Yata, Magdalena Zernicka-Goetz, and Jonathon Pines. 2018. 'Cyclin B1 Is Essential for Mitosis in Mouse Embryos, and Its Nuclear Export Sets the Time for Mitosis'. The Journal of Cell Biology 217 (1): 179–93. https://doi.org/10.1083/jcb.201612147.

Stukenberg, P. Todd. 2004. 'Triggering P53 after Cytokinesis Failure'. The Journal of Cell Biology 165 (5): 607–8. https://doi.org/10.1083/jcb.200405089.

Su, Yu, Jian-Jun Li, Cassie Wang, Ghassan Haddad, and Wei-Hua Wang. 2016. 'Aneuploidy Analysis in Day 7 Human Blastocysts Produced by in Vitro Fertilization'. Reproductive Biology and Endocrinology 14 (1): 20. https://doi.org/10.1186/s12958-016-0157-x.

Taft, Robert A. 2008. 'Virtues and Limitations of the Preimplantation Mouse Embryo as a Model System'. Theriogenology 69 (1): 10–16. https://doi.org/10.1016/j.theriogenology.2007.09.032.

Takahashi, Akiko, Naoko Ohtani, Kimi Yamakoshi, Shin-ichi Iida, Hidetoshi Tahara, Keiko Nakayama, Keiichi I. Nakayama, Toshinori Ide, Hideyuki Saya, and Eiji Hara. 2006. 'Mitogenic Signalling and the P16INK4a–Rb Pathway Cooperate to Enforce Irreversible Cellular Senescence'. Nature Cell Biology 8 (11): 1291–97. https://doi.org/10.1038/ncb1491.

Taylor, Tyl H., Susan A. Gitlin, Jennifer L. Patrick, Jack L. Crain, J. Michael Wilson, and Darren K. Griffin. 2014. 'The Origin, Mechanisms, Incidence and Clinical Consequences of Chromosomal Mosaicism in Humans'. Human Reproduction Update 20 (4): 571–81. https://doi.org/10.1093/humupd/dmu016.

Therman, Eeva, Dolores A. Buchler, Usko Nieminen, and Sakari Timonen. 1984. 'Mitotic Modifications and Aberrations in Human Cervical Cancer'. Cancer Genetics and Cytogenetics 11 (2): 185–97. https://doi.org/10.1016/0165-4608(84)90113-4.

Thompson, Larry J., Mathieu Bollen, and Alan P. Fields. 1997. 'Identification of Protein Phosphatase 1 as a Mitotic Lamin Phosphatase*'. Journal of Biological Chemistry 272 (47): 29693–97. https://doi.org/10.1074/jbc.272.47.29693.

Thompson, Sarah L., and Duane A. Compton. 2010. ‘Proliferation of Aneuploid Human Cells Is Limited by a P53-Dependent Mechanism’. The Journal of Cell Biology 188 (3): 369–81. https://doi.org/10.1083/jcb.200905057.

Torres, Eduardo M., Tanya Sokolsky, Cheryl M. Tucker, Leon Y. Chan, Monica Boselli, Maitreya J. Dunham, and Angelika Amon. 2007. ‘Effects of Aneuploidy on Cellular Physiology and Cell Division in Haploid Yeast’. Science 317 (5840): 916–24. https://doi.org/10.1126/science.1142210.

Trends in Cell Biology 27 (5): 314–21. https://doi.org/10.1016/j.tcb.2017.01.004.

Tsai, Tony Y.-C., Julie A. Theriot, and James E. Ferrell Jr. 2014. ‘Changes in Oscillatory Dynamics in the Cell Cycle of Early Xenopus Laevis Embryos’. PLOS Biology 12 (2): e1001788. https://doi.org/10.1371/journal.pbio.1001788.

Tsichlaki, Elina, and Greg FitzHarris. 2016. ‘Nucleus Downscaling in Mouse Embryos Is Regulated by Cooperative Developmental and Geometric Programs’. Scientific Reports 6(1): 28040. https://doi.org/10.1038/srep28040.

Tunquist, Brian J., and James L. Maller. 2003. ‘Under Arrest: Cytostatic Factor (CSF)-Mediated Metaphase Arrest in Vertebrate Eggs.’ Genes & Development 17 (6): 683–710. https://doi.org/10.1101/gad.1071303.

Uetake, Yumi, and Greenfield Sluder. 2010. ‘Prolonged Prometaphase Blocks Daughter Cell Proliferation despite Normal Completion of Mitosis’. Current Biology : CB 20 (18): 1666. https://doi.org/10.1016/j.cub.2010.08.018.

Vázquez-Diez, Cayetana, and Greg FitzHarris. 2018. ‘Causes and Consequences of Chromosome Segregation Error in Preimplantation Embryos’. Reproduction 155 (1): R63–76. https://doi.org/10.1530/REP-17-0569.

Vázquez-Diez, Cayetana, Kazuo Yamagata, Shardul Trivedi, Jenna Haverfield, and Greg FitzHarris. 2016. ‘Micronucleus Formation Causes Perpetual Unilateral Chromosome Inheritance in Mouse

Embryos'. Proceedings of the National Academy of Sciences of the United States of America 113 (3): 626–31. https://doi.org/10.1073/pnas.1517628112.

Vázquez-Diez, Cayetana, Lia Mara Gomes Paim, and Greg FitzHarris. 2019. 'Cell-Size-Independent Spindle Checkpoint Failure Underlies Chromosome Segregation Error in Mouse Embryos'. Current Biology: CB 29 (5): 865-873.e3. https://doi.org/10.1016/j.cub.2018.12.042.

Vermeulen, Katrien, Dirk R. Van Bockstaele, and Zwi N. Berneman. 2003. 'The Cell Cycle: A Review of Regulation, Deregulation and Therapeutic Targets in Cancer'. Cell Proliferation 36 (3): 131–49. https://doi.org/10.1046/j.1365-2184.2003.00266.x.

Vigneron, Suzanne, Estelle Brioudes, Andrew Burgess, Jean-Claude Labbé, Thierry Lorca, and Anna Castro. 2009. 'Greatwall Maintains Mitosis through Regulation of PP2A'. The EMBO Journal 28 (18): 2786–93. https://doi.org/10.1038/emboj.2009.228.

Wagner, Elizabeth, and Michael Glotzer. 2016. 'Local RhoA Activation Induces Cytokinetic Furrows Independent of Spindle Position and Cell Cycle Stage'. The Journal of Cell Biology 213 (6): 641–49. https://doi.org/10.1083/jcb.201603025.

Wang, Guang-Fei, Qincai Dong, Yuanyuan Bai, Jing Yuan, Quanbin Xu, Cheng Cao, and Xuan Liu. 2017. 'Oxidative Stress Induces Mitotic Arrest by Inhibiting Aurora A-Involved Mitotic Spindle Formation'. Free Radical Biology & Medicine 103 (February): 177–87. https://doi.org/10.1016/j.freeradbiomed.2016.12.031.

Welte, Stefan, Karl-Heinz Baringhaus, Wolfgang Schmider, Günter Müller, Stefan Petry, and Norbert Tennagels. 2005. '6,8-Difluoro-4-Methylumbiliferyl Phosphate: A Fluorogenic Substrate for Protein Tyrosine Phosphatases.' Analytical Biochemistry 338 (1): 32–38. https://doi.org/10.1016/j.ab.2004.11.047.

Wheatley, Sally P., Edward H. Hinchcliffe, Michael Glotzer, Anthony A. Hyman, Greenfield Sluder, and Yu-li Wang. 1997. 'CDK1 Inactivation Regulates Anaphase Spindle Dynamics and Cytokinesis In Vivo'. The Journal of Cell Biology 138 (2): 385–93.

Williams, Bret R., Vineet R. Prabhu, Karen E. Hunter, Christina M. Glazier, Charles A. Whittaker, David E. Housman, and Angelika Amon. 2008. 'Aneuploidy Affects Proliferation and Spontaneous Immortalization in Mammalian Cells'. Science 322 (5902): 703–9. https://doi.org/10.1126/science.1160058.

Wolf, Frank, Cornelia Wandke, Nina Isenberg, and Stephan Geley. 2006. 'Dose-Dependent Effects of Stable Cyclin B1 on Progression through Mitosis in Human Cells'. The EMBO Journal 25 (12): 2802. https://doi.org/10.1038/sj.emboj.7601163.

Wolf, Frank, Reinhard Sigl, and Stephan Geley. 2007. '"... The End of the Beginning": CDK1 Thresholds and Exit from Mitosis.' Cell Cycle (Georgetown, Tex.) 6 (12): 1408–11.

Xu, Naihan, and Donald C. Chang. 2007. 'Different Thresholds of MPF Inactivation Are Responsible for Controlling Different Mitotic Events in Mammalian Cell Division'. Cell Cycle (Georgetown, Tex.) 6 (13): 1639–45. https://doi.org/10.4161/cc.6.13.4385.

Yamagata, Kazuo, and Greg FitzHarris. 2013. '4D Imaging Reveals a Shift in Chromosome Segregation Dynamics during Mouse Pre-Implantation Development'. Cell Cycle 12 (1): 157–65. https://doi.org/10.4161/cc.23052.

Yamano, Hiroyuki, Julian Gannon, Hiro Mahbubani, and Tim Hunt. 2004. 'Cell Cycle-Regulated Recognition of the Destruction Box of Cyclin B by the APC/C in Xenopus Egg Extracts'. Molecular Cell 13 (1): 137–47. https://doi.org/10.1016/s1097-2765(03)00480-5.

Yuan, Kai, and Patrick H. O'Farrell. 2015. 'Cyclin B3 Is a Mitotic Cyclin That Promotes the Metaphase-Anaphase Transition'. Current Biology : CB 25 (6): 811–16. https://doi.org/10.1016/j.cub.2015.01.053.

Yüce, Özlem, Alisa Piekny, and Michael Glotzer. 2005. 'An ECT2–Centralspindlin Complex Regulates the Localization and Function of RhoA'. The Journal of Cell Biology 170 (4): 571–82. https://doi.org/10.1083/jcb.200501097.

Zhang, Cheng-Zhong, Alexander Spektor, Hauke Cornils, Joshua M. Francis, Emily K. Jackson, Shiwei Liu, Matthew Meyerson, and David Pellman. 2015. 'Chromothripsis from DNA Damage in Micronuclei'. Nature 522 (7555): 179–84. https://doi.org/10.1038/nature14493.

Zhang, Lei, Daimin Wei, Yueting Zhu, Yuan Gao, Junhao Yan, and Zi-Jiang Chen. 2019. 'Rates of Live Birth after Mosaic Embryo Transfer Compared with Euploid Embryo Transfer'. Journal of Assisted Reproduction and Genetics 36 (1): 165–72. https://doi.org/10.1007/s10815-018-1322-2.

Zhang, Suyang, Leifu Chang, Claudio Alfieri, Ziguo Zhang, Jing Yang, Sarah Maslen, Mark Skehel, and David Barford. 2016. 'Molecular Mechanism of APC/C Activation by Mitotic Phosphorylation'. Nature 533 (7602): 260–64. https://doi.org/10.1038/nature17973.

Zhou, Chunshui, Andrew E. H. Elia, Maria L. Naylor, Noah Dephoure, Bryan A. Ballif, Gautam Goel, Qikai Xu, et al. 2016. 'Profiling DNA Damage-Induced Phosphorylation in Budding Yeast Reveals Diverse Signaling Networks'. Proceedings of the National Academy of Sciences of the United States of America 113 (26): E3667–75. https://doi.org/10.1073/pnas.1602827113.

Zhou, Zhuan, Mingjing He, Anil A. Shah, and Yong Wan. 2016. 'Insights into APC/C: From Cellular Function to Diseases and Therapeutics'. Cell Division 11 (1): 9. https://doi.org/10.1186/s13008-016-0021-6.

Zhu, Changjun, Eric Lau, Robert Schwarzenbacher, Ella Bossy-Wetzel, and Wei Jiang. 2006. 'Spatiotemporal Control of Spindle Midzone Formation by PRC1 in Human Cells'. Proceedings of the National Academy of Sciences of the United States of America 103 (16): 6196–6201. https://doi.org/10.1073/pnas.0506926103.

Supplementary Figures

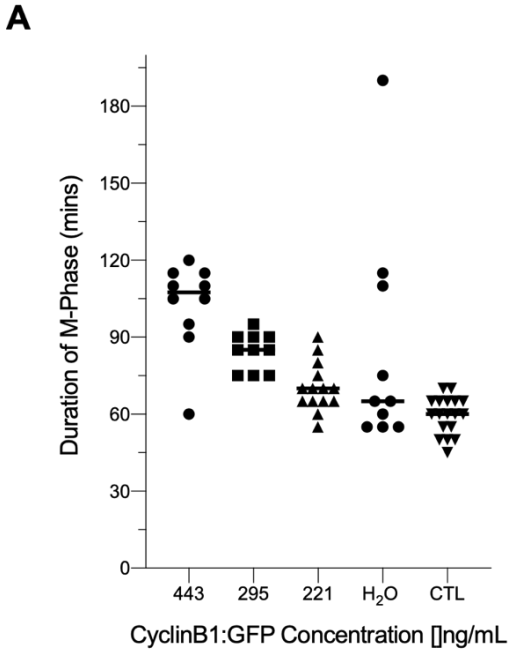

Figure S 1 - Overexpression of CyclinB:GFP extends M-phase.

(a) Microinjection of high concentrations of CyclinB1:GFP mRNA causes extension of M-phase. CyclinB1:GFP was injected at several different titrations to find the injection concentration at which M-phase was not pertrubed. Microinjection with H2O generally had no impact on the duration of M-phase in comparison to completely uninjected controls (CTL). For all future experiments we only used the concentration (221ng/mL) and only analysed cells which fell in same M-phase duration range as uninjected cells.

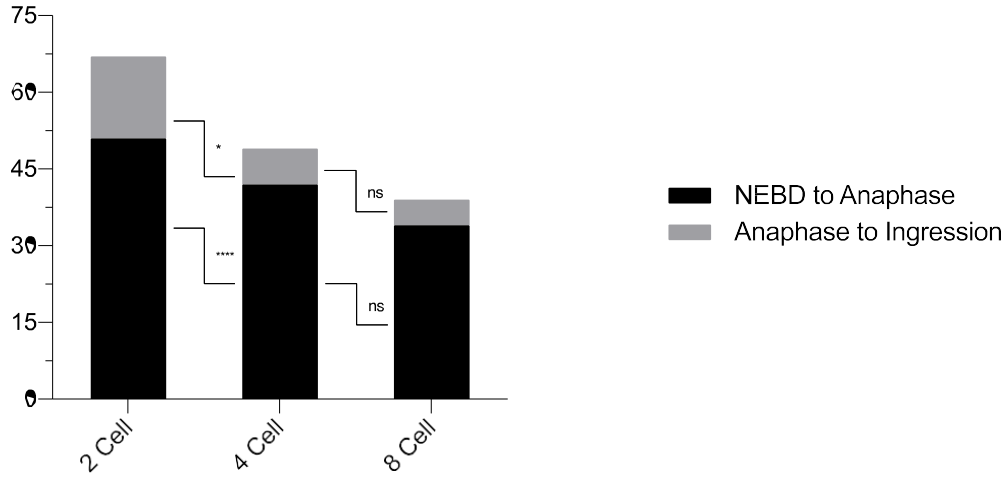

Figure S 2 - Mitotic entry and exit duration at different cell stages.

*Time from NEBD to anaphase (mitotic entry) and anaphase to furrow ingression (mitotic exit) was measured using H2B:RFP signal in the 2-cell 4-cell and 8-cell stage mouse embryo. Imaged using live-cell confocal imaging with 3 minute intervals. (Kruskal-Wallis test *P<0.05, ****P<0.0001; n=18, n=11, n=6 respectively)*

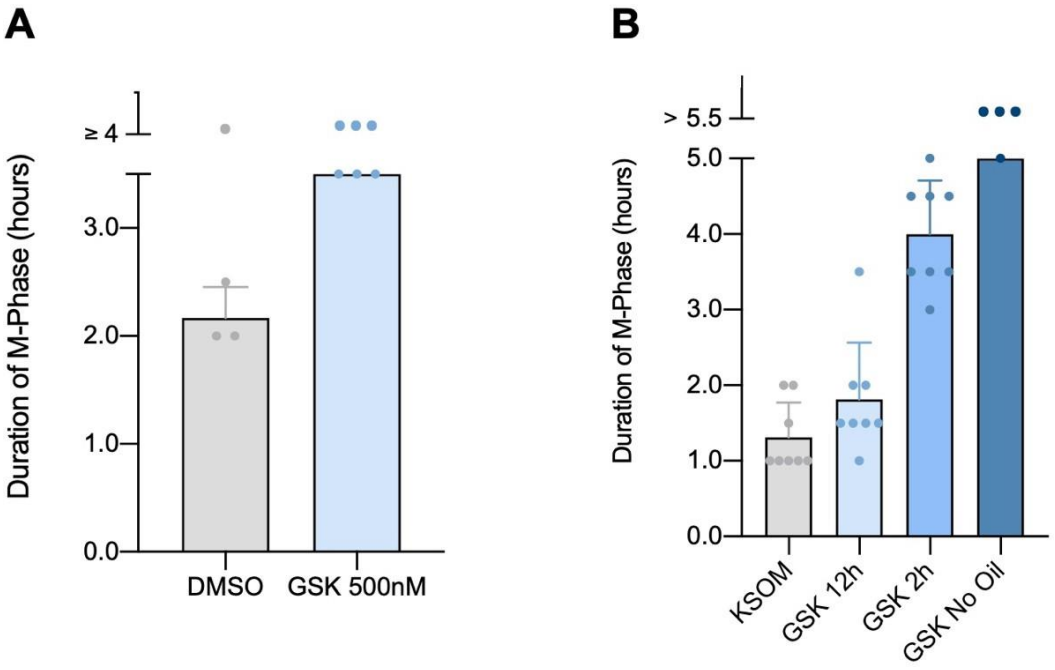

Figure S 3 - GSK923925 extends M-phase duration in zygotes and is less effective under oil.

(a) Zygotes treated in GSK923925 have a significantly prolonged M-phase. M-phase duration measured from time from NEBD to furrow ingression in 500nM GSK923925 (500nM GSK) or 1:1000 DMSO as a control. Zygotes manually checked for NEBD and furrow ingression every 30 minutes. Embryos which took >4h were observed to have undergone NEBD 4 hours before experiment stopped without undergoing furrow ingression. Experiment stopped after 4.5 hours of observation, however the next day all zygotes were 2-cell stage (n=1 DMSO; n=3 GSK 923925). This suggests GSK923925 is working and extended M-phase through inhibiting metaphase. (b) GSK923925 is less effective under oil. GSK923925 was equilibrated under oil, for 12 hours, 2 hours and under no oil at all. 2-cell stage embryos were introduced to the respective media at the same time and the duration of M-phase was measured. GSK923925 had a slight extension of M- phase suggesting CENP-E was not fully inhibited, however an extended M-phase response became more pronounced with reduced amount of time spent under oil. M-phase was most extended in GSK without the presence of oil. 2-cell stage embryos which took >5h were observed to have undergone NEBD 5 hours before experiment stopped without undergoing furrow ingression (n=3 GSK923925 no oil). Experiment stopped after 5 hours of observation, however the next day all 2-cell embryos were 4-cell stage